

Microfluidic Devices for Investigation of Zebrafish Larvae's Electrotaxis and their Applications to Dopamine System Studies

Amir Reza Peimani

A THESIS SUBMITTED TO THE FACULTY OF GRADUATE
STUDIES IN PARTIAL FULFILMENT OF THE REQUIREMENT FOR
THE DEGREE OF MASTER OF APPLIED SCIENCE

Graduate Program in Mechanical Engineering

York University

Toronto, Ontario

December 2017

© Amir Reza Peimani, 2017

Abstract

Zebrafish (*Danio rerio*) have been used as a model organism for genetic, neural, and behavioral screening assays due to their high genetic homology with humans. The zebrafish larvae behavior, such as movement and orientation, in response to various stimulations including chemical and optical stimuli, have been widely investigated. However, unlike other organisms such as *Caenorhabditis elegans*, research on zebrafish sensory-motor responses to electrical stimuli, called electrotaxis, has been overlooked. We took advantage of microfluidics technology and developed two novel devices to investigate zebrafish larvae's electrotaxis quantitatively for the first time.

The first device was used to demonstrate general zebrafish electrotaxis in a range of 3-9 μA electric currents by confining the larva to move and orient only in the longitudinal direction. We found that electrotaxis is dependent on the strength, direction, and time of electrical signal application. The larvae could orient and swim towards the anode and increasing the electrical strength resulted in a stronger electrotaxis (a higher anode-directed orientation rate). Also, the zebrafish tended to exhibit a lower electrotaxis during the night than the daytime. Thus, by administration of several dopamine agonists with various doses in the zebrafish at night, we showed that electrotaxis is modulated by their D2-like dopamine receptors.

The second device was designed to partially immobilize the larva's head while the tail was freed to move so that subtle electrotaxis motor behaviors such as J- and C-bend could be investigated. We examined the tail-beat frequency (TBF) and response duration of zebrafish electrotaxis in a range of 1-9 μA currents. We observed that the

highest TBF occurs at the lowest current while the response duration revealed a reverse U-shaped effect with the longest response happening at the intermediate currents. We also explored the role of Pannexin1 protein membrane (Panx1) in the zebrafish by experimenting electrotaxis of the Panx1 knockout larvae. It was shown that Panx1 might play an effective role in modulating electrotaxis at lower currents. Our devices can be employed for chemical screening and further examination of biological and neurological pathways involved in zebrafish electrotaxis. By experimenting different gene mutants inside our devices, the genetic pathways and functions in electrotaxis can also be examined. Electrotaxis movement assay can also be used as a tool for chemical screening in toxicological and pharmaceutical applications.

Acknowledgement

I would like to express my gratitude to my supervisor Dr. Pouya Rezai for his non-stop assistance, support, and patient guidance during my research. I will never forget his generous offer which granted me to come to Canada and conduct research under his supervision. His constant advices have truly helped me to develop my professional presenting, writing, and researching skills. I have been lucky to have had a supervisor who cared more than enough to spend his holidays and family times helping us to flourish in our careers. I wish him the best in his academic and personal lives.

I am also grateful for all the helps that I received from Dr. Zoidl who has been generously collaborating in this thesis. I also want to thank my committee member, Dr. Ghafar-Zadeh for his commitment during my studies at York University. I wish them all the best in their future careers.

I want to express my deepest gratitude to the persons who are the only reasons that I breathe, live, and survive all of the difficult situations, *my Maman (Mum), Baba (Dad), Aji (Sister), and my Madar & Nane (Grandmams)*. Without them, I can no longer exist, let alone to be successful in any stage of my life.

Lastly, I would like to thank all of my old friends, Mohammad, Amir, Ehsan, Javad, and Sajad and the friends I made at York, Amin, Ramtin, Laya, Mehdi, Ahmad, Amin, Mohsen, Nima, Pardis, Khaled, Hossein, Vikas, Mahdi, Sina, Elnaz, and Maryam.

Table of Contents

Abstract	ii
Acknowledgement	iv
List of Figures	viii
Glossary of Terms	xix
Chapter 1 Introduction and Literature Review	1
1.1 Zebrafish Larva as a Model Organism for Behavioral Studies	1
1.2 Conventional Methods to Study Zebrafish Larvae Behaviors.....	6
1.3 Microfluidic Technologies for Zebrafish Behavioral Studies	8
1.4 Biological and Technological Gaps: Zebrafish LARVA Electrotaxis	15
1.5 Research Goals and Objectives.....	19
1.6 Thesis Structure	21
1.7 Contributions	21
1.7.1 Journal Papers.....	22
1.7.2 Book Chapters	23
1.7.3 Conference Papers.....	23
Chapter 2 Materials and Methods	24
2.1 Zebrafish Larvae Generation and Maintenance	24
2.2 Chemical Preparation and Larvae Exposure.....	25
2.3 Microfluidic Device Fabrication	26
2.4 Viability Test.....	26
2.5 Statistical Analysis	27
Chapter 3 A Microfluidic Device to Study Electrotaxis and Dopaminergic System of Zebrafish Larvae	28
3.1 Introduction	28
3.2 Experimental Section	29
3.2.1 Design of the Microfluidics Device	29
3.2.2 Experimental Setup and Procedure.....	31
3.2.3 Data Analysis.....	33
3.3 Results and Discussions	34
3.3.1 Electrotaxis of Zebrafish Larva in a Channel	34

3.3.2 Viability and Morphological State of Zebrafish Larvae after Electrotaxis in the Device.....	39
3.3.3 Time-of-Day Dependency of Electrotactic Behavior in Zebrafish Larvae.....	41
3.3.4 Microfluidic Electrotaxis as a Tool for Screening Dopaminergic Compounds	44
3.3.5 Electrotactic Speed, Place Preference, and Swimming Pattern of Zebrafish Larvae.....	47
3.3.6 Role of D1- and D2-Dopamine Receptors in Zebrafish Larvae’s Electrotaxis	49
3.4 Conclusion	50
Chapter 4 A Microfluidic Device to Study Subtle Phenotypes of Zebrafish Larvae Electrotaxis Using Wild-Type and Knockout Models.....	53
4.1 Introduction	53
4.2 Experimental Section	55
4.2.1 Design and Fabrication of the Microfluidic Device	55
4.2.2 Experimental Setup	57
4.2.3 Experimental Procedure	58
4.2.4 Video and Image Analysis	60
4.2.5 Behavioral Phenotyping and Motor Pattern Characterization	61
4.3 Results and Discussions.....	62
4.3.1 Electrotaxis of Semi-Immobilized Zebrafish Larvae	62
4.3.2 Electrotactic Tail-Beat Frequency (TBF) of Zebrafish Larvae	64
4.3.3 Electrotactic Response Duration of KO and WT Zebrafish Larvae	66
4.3.4 Electrotactic Motor Patterns of Semi-Immobilized Zebrafish Larvae.....	68
4.4 Conclusions	72
Chapter 5 Thesis Summary and Prospects	75
5.1 Thesis Summary	75
5.2 Thesis Prospects	78
5.2.1 Future Technological Research Direction.....	79
5.2.2 Future Biological Research Directions.....	80
References	81
Appendix. A.....A Microfluidic Device for Quantitative Investigation of Zebrafish Larvae’s Rheotaxis.....	99
A.1. Introduction.....	99
A.2. Microfluidic Device.....	101
A.3. Experimental Procedure and Rheotaxis Quantification	103

A.4. Results and Discussions..... 103
 A.4.1 Rheotaxis of Zebrafish Larva in a Channel..... 104
 A.4.2 Effect of Flow Velocity on Rheotaxis of Zebrafish Larva in a Channel 106
 A.4.3 Effect of Flow Velocity on Rheotaxis Location in the Channel 108
 A.4.4 Viability of Zebrafish Larvae after Rheotaxis Assay in the Channel 110
A.5. Conclusions 110

List of Figures

<i>Figure 1-1. Photographs of the zebrafish at different embryonic and larval developmental stages from 12 minutes to 3 dpf [23]. Reproduced and reprinted with permissions from the publishers of Ref 23.</i>	<i>2</i>
<i>Figure 1-2 Discrete captured frames of a 17 dpf free-swimming zebrafish larva moving backward inside a petri dish. Overlay is the frame-on-frame photo of movement [29]. Reprinted with permissions from the publishers of Ref 29.</i>	<i>2</i>
<i>Figure 1-3. Distinct behavioral motor patterns of a 17 dpf semi-immobilized zebrafish larva, such as J-turn (J-bend), C-bend, forward/routine, and escape/struggling swimming patterns, with the larva's head embedded and fixed in agarose while the tail is free to move. Red and black lines represent the resting position and tail angle (with respect to the resting position) versus time, respectively [29]. Reprinted with permissions from the publishers of Ref 29.</i>	<i>4</i>
<i>Figure 1-4. Microfluidic device for a chemical screening assay on the zebrafish larvae [70]. (a) Schematic design of the microfluidic device where the larva is immobilized by agarose and its mouth and tail are free to be exposed to the drug and recorded, respectively. (b) Side-view of the larva's head embedded and fixed in agarose with its mouth being exposed for the chemical delivery. (c) Schematic images of the zebrafish larva under exposure to two chemicals. (d) Real images of the larva immobilized in agarose under different chemical exposure states. Reprinted with permissions from the publishers of Ref 70.</i>	<i>10</i>
<i>Figure 1-5. Microfluidic device made from PDMS for oxygen-deprivation studies [67]. (a) Real image of a zebrafish larva trapped and fixed by a barrier and hydrodynamic force</i>	

of the flow streaming from the left to right. Scale bar: 0.35 mm. (b) Real image of the device. Scale bar: 4 mm. (c) Schematic design of the channels in which various types of gases could be utilized to decrease or increase the level of oxygen in the environment, benefiting from permeability of PDMS. Reprinted with permissions from the publishers of Ref 67..... 11

Figure 1-6. Microfluidic device for neural and behavioral screening of the zebrafish larvae activities [71]. (a) Scheme of the chip with real images of the immobilized fish in end-tapered channels of the (i) Motion, (ii) Lateral, and (iii) Dorsal chips. The larva is exposed to the chemical through the horizontal channel which is perpendicular to the trapping channel. Scale bar: 0.2 mm. (b) Behavioral responses of the larva trapped in the “Motion” chip for neural and movement monitoring. By maintaining a slow flow rate inside the channel, larva’s head was gently immobilized (top right) for florescence imaging (top left). Ethanol and E3 water switched at the specific periods to apply or release the stimulus (top left). Movement responses were classified into the fin beats, eye saccades, overall body movements, and eye nystagmus (bottom). Scale bar: 200 μm (top right). (c) Images of the larva trapped in the “Lateral” chip (left) where its cardiac physiology can be monitored and analyzed (right). Scale bar, 200 μm (left), 25 μm (right). (d) Brain function and neural imaging of the zebrafish larva trapped in the “Dorsal” chip. Scale bars: 200 μm (left image), 100 μm (top right image), 50 μm (bottom right image). Reprinted with permissions from the publishers of Ref 71..... 13

Figure 1-7 Real picture of multiple trapped zebrafish larvae in the electrophysiology microfluidic device [75]. Reprinted with permissions from the publishers of Ref 75. 14

Figure 1-8. Microfluidic device for zebrafish larvae imaging. (a) Photograph of the microfluidic device in which the zebrafish larva can be immobilized for ESEM imaging [76]. (b) Cross-sectional side-view of the ESEM device illustrating its various features [76]. Reprinted with permissions from the publishers of Ref 76. 15

Figure 1-9. (a) Electrotaxis of *C. elegans* shown by the movement of a worm towards the cathode (at the right of the picture) under application of a 4 V.cm^{-1} electric field (E) inside a microchannel. (b) Schematic of the microchannel device used to study *C. elegans* electrotaxis [56]. Reprinted with permissions from the publishers of Ref 56.... 16

Figure 1-10. Schematics of different electric microfluidic devices for *C. elegans* sorting (a,b) [58], [82] and *S.prombe* electrotaxis (c) [89]. Reprinted with permissions from the publishers of Ref 58, 82 and 89. 17

Figure 3-1. The microfluidic device consisted of inlet and outlet tubes, U-shaped channel, main channel and two side channels with tubes at the ends instrumented with two electrode wires. The length, width and height of the main channel were 63.3, 1.6 and 0.55 mm, respectively. 30

Figure 3-2. The experimental set-up consisted of the microfluidic device, two syringe pumps, direct current sourcemeter, microscope and two cameras, one on the microscope for close-up imaging and another on a stand for movement recording of the zebrafish larvae..... 32

Figure 3-3. Bright-field images of a 7 dpf zebrafish larva being loaded into the device through the tilted inlet, shown in sequential images from a bottom view of the inlet reservoir under a microscope. Once the larva was loaded into the inlet reservoir, the flows in the side and main channels (from left to right) ensured smooth loading of the

larva from the reservoir into the channel by keeping the zebrafish straight and clear from the channel walls. Scale bar: 1 mm..... 33

Figure 3-4. Electrotaxis of the 5-7 dpf zebrafish larvae in a microfluidic channel. (a)

Electrotactic response of a 7 dpf zebrafish larva to a 3 μA electric current stimulus (i and ii) and its subsequent movement in the channel towards the anode (iii and iv) with a speed of 37.5 $\text{mm}\cdot\text{s}^{-1}$. (b) Electrotactic orientation of the 5-7 dpf zebrafish larvae (N=30

in three independent trials) stimulated with the electric currents of 3 μA and 15 μA .

Results are compared to a control group of 30 animals, not exposed to any electric current, which shows statistically significant differences for both groups (**: two-tailed t-test, $p\text{-value}<0.01$). The control group preferred staying in their original orientation, and less than 10% of the larvae demonstrated a rotation in the channel. Once the zebrafish were exposed to the electric current of 3 μA and 15 μA , more than 80% of them responded to the stimuli within 15 s by re-orientation towards the anode. Higher electric current resulted in a more robust electrotactic orientation (e.g., 100% for 15 μA) suggesting that the zebrafish larvae were sensitive to current magnitude, but there was no significant difference in the response between the two electrically-stimulated groups (two-tailed t-test: $p\text{-value}>0.05$). (c) Electrotactic speed of the 5-7 dpf zebrafish larvae (N=15 in three independent trials) in response to electric currents in the channel. Larvae responded to the 3 μA and 15 μA electric currents with movement speeds of $58.5\pm 19.0 \text{ mm}\cdot\text{s}^{-1}$ and $41.5\pm 13.1 \text{ mm}\cdot\text{s}^{-1}$ towards the anode, respectively. An increase in the electric current resulted in a significant (**: two-tailed t-test, $p\text{-value}<0.01$) decrease in the electrotactic speed. This observation can be attributed to a partial paralysis caused by the high electric current. 35

Figure 3-5. Survival and morphological abnormality of the 5-7 dpf zebrafish larvae tested in the microfluidic electrotaxis screening device, then monitored off-chip for 30 days (N=10 per condition). (a) Off-chip survival of zebrafish larvae, after exposure to 3 μ A and 15 μ A electric current (EC) in the device, compared to that of the fish not exposed to any EC in the device as Device Control group and the fish that were not exposed to the device or EC as Reference Control group. The Device Control zebrafish and the ones exposed to 3 μ A EC showed similar survival to the Reference Control group. The zebrafish exposed to 15 μ A EC were severely affected by the stimulus and demonstrated a significant fatality during the assay period. (b) Survival of 5-7 dpf zebrafish larvae during the first four days after the experiments (N=20 per condition). The larvae tested inside the device without any electrical exposure (Device Control) and the ones exposed to the 3 μ A electric current (EC) survived analogously to the Reference Control (two-tailed t-test: p -value>0.05). However, the 15 μ A EC application resulted in a larger number of fish deaths which was significantly different from the Reference Control (two-tailed t-test: p -value<0.05). This shows that the low EC of 3 μ A can be employed for further applications whereas the higher EC of 15 μ A is not viable for the larvae and brings about severe mortality. (c) Morphological abnormality of the above-mentioned zebrafish larvae during 4 weeks of observation after the experiments. The zebrafish exposed to the device and 3 μ A EC showed a small morphological abnormality effect (<25%) and were mostly observed to be intact as the Reference Control fish (c-i). However, 60% of the larvae exposed to 15 μ A EC could not recover from the exposure and lost their normal morphology mostly with a spinal bending (c-ii)

which was significantly different from the Reference Control (**: two-tailed t-test: p-value<0.01). 40

Figure 3-6. Zebrafish larvae's electrotaxis (N=20 fish in three independent trials) stimulated by an electric current of 3 μ A during day (11am-4 pm) and night (8-11 pm) along with the control group of zebrafish not exposed to the current. The control groups showed an arbitrary movement with less than 10% reorientation or no movement at all at day and night, respectively. Exposure to electric current resulted in significant electrotaxis responses at different times, but there was a significant drop in the larvae's response at night (**: two-tailed t-test, p-value<0.01), revealing that the larvae are not amply sensitive to the electric current of 3 μ A at night. 42

Figure 3-7. Effect of the time (i.e. early and late day and night) on electrotaxis of the zebrafish larvae (N=15 fish in three independent trials). Data shows that there is no difference between zebrafish electrotaxis within the early and late hours of the day or night (two-tailed t-test, p-value>0.05). 44

Figure 3-8. Effect of apomorphine at different concentrations on electrotaxis of 5-7 dpf zebrafish larvae at night. The larvae were treated with three apomorphine concentrations of 0.2, 1.8 and 50 μ M, then tested in the microfluidic device at three electric current levels in three independent trials. Each drug concentration involved N=30 fish for 3 μ A and 6 μ A and N=15 fish for 9 μ A electric currents. Results show that the low-dose apomorphine exposure of 0.2 μ M significantly increases zebrafish's electrotaxis at nighttime (two-tailed t-test, *: p-value<0.05, **: p-value<0.01), but this effect can only be detected if a low electric current (e.g. 3 μ A) is used. Increased dosage of apomorphine beyond 0.2 μ M resulted in no electrotaxis difference from the

control group, although statistically lower electrotaxis than 0.2 μM treatment was assessed. At the medium current, although there was a reducing trend in electrotaxis upon increase of apomorphine concentration, only the medium-dose exposure resulted in a significantly reduced response (two-tailed t-test, **: $p\text{-value} < 0.01$). At the high-level current, effect of apomorphine on electrotaxis was benign because the electrotaxis response was fully saturated with the strong electric current. 45

Figure 3-9. Absolute lateral distance of larvae's center of mass from the centerline of the channel (dashed-line in the insert graph) during electrotaxis of the 5-7 dpf zebrafish larvae. Using a current of 3 μA , $N=18$ zebrafish were tested at daytime while $N=21$ larvae were exposed to a 0.2 μM dose of apomorphine and tested at night. The results were statistically different from each other (two-tailed t-test, **: $p\text{-value} < 0.01$). This revealed that the apomorphine-treated zebrafish demonstrate preference to move closer to the channel wall by displaying stronger body strikes with more struggling swimming behavior, while the control zebrafish preferred to swim closer to the centerline of the channel with dominant forward swimming patterns. 48

Figure 3-10. Electrotaxis of the zebrafish larvae treated with 50 μM of SKF-38393 (D1-like receptors) and 16.7 μM of Quinpirole (D2-like receptors) at night ($N=15$ in three independent trials for each condition). The results show no statistical difference between control and SKF-38393 treated larvae's electrotaxis (two-tailed t-test, $p\text{-value} > 0.05$), while Quinpirole proves to significantly increase electrotaxis (two-tailed t-test, *: $p\text{-value} < 0.05$). 50

Figure 4-1. A microfluidic device for electrotaxis screening of the semi-immobilized zebrafish larva. The device (top image) consisted of three layers. Main (top) layer

consisted of a tilted-inlet, side channel, loading channel, trapping region (TR), screening pool, outlet, and two electrode spots. The valve (bottom) layer consisted of a trapping valve channel and two tubes at the ends. The PDMS membrane (middle) layer was sandwiched between the other two layers. The region of interest (ROI) is magnified (bottom left) to show more details about the TR, pool, and crescent-like pillar, which aided fabricating and de-bubbling the device. The TR is also magnified (bottom right) to display how the larva is partially immobilized. Inside the TR, the tail tip-point is shown by a black circle which was tracked by a software. The main channel centerline and two lower and upper thresholds are also drawn manually which helped with calculating the TBF. 57

Figure 4-2. The experimental setup consisted of the microfluidic device, microscope, camera, two syringe pumps, sourcemeter, and computer to collect videos. The screen is showing a 7 dpf zebrafish larva trapped inside the TR..... 58

Figure 4-3. Electrotaxis of the semi-immobilized zebrafish larvae. (a) Microscope-based sequential images of a 7 dpf zebrafish larva exhibiting electrotaxis inside the microfluidic device. Once exposed to a 1 μ A electric current (i), the zebrafish larva displayed different motor patterns such as C-bend (ii), no movement (iii), and struggling swimming (iv). (b) Different motor patterns were graphically recognized and characterized using the plot of tail tip position versus time during electrotaxis. The TBF and response duration were also determined using the data of this plot. 63

Figure 4-4. Electrotactic TBF of the WT and KO zebrafish larvae (N = 20 and 15, respectively, per current in three independent trials) at different electric currents. The highest TBF was observed at the lowest electric current for both larvae types. Also, at

the low currents of 1 and 3 μ A, the TBF of the WT larvae was statistically lower than the KO larvae (p-value<0.01)...... 65

Figure 4-5. Electrotaxis response duration of the WT and KO zebrafish larvae (N = 20 and 15, respectively, per current in three independent trials) at different electric currents. Shortest electrotaxis took place at the lowest and highest electric currents. At the low currents of 1 and 3 μ A, the Panx1 loss seemed to have a regulating influence on larvae electrotaxis by statistically demonstrating a lower response duration in the KO larvae than the WT ones (p-value<0.01)...... 67

Figure 4-6. Quantitative analysis of the fractional duration of various electrotactic motor patterns of the WT and KO zebrafish larvae (N = 20 and 15, respectively, per current in three independent trials). C-bend or C (a), J-bend or J (b), flick or fl (c), routine swimming or rs (d), no movement or nm (e), and struggling or st (f) are among the observed electrotactic motor patterns of the larvae..... 69

Figure A. 1. The microfluidic device used to study the rheotaxis of 5-7 days post fertilization (dpf) zebrafish larvae. It consisted of a tilted inlet tube for loading the larva, a U-shaped expanding channel for retaining the larva in the device, and a main channel for rheotaxis studies. Water flow in the side channel helped conveniently loading the zebrafish larva into the main channel with length, width, and height of 63.3 mm, 1.6 mm, and 0.55 mm, respectively. The main channel was divided into three sections 1, 2, and 3, representing the spatial locations at which the larvae responded to the flow at different flow velocities. The setup included two syringe pumps, a microscope connected to a camera, and the microfluidic device..... 102

Figure A. 2. Bright field images of a 7 dpf zebrafish larva (a) before, (b-c) during, and (d) after rheotactic orientation upon stimulation by a water flow velocity of 19 mm.sec⁻¹ in section 1 of the device. The direction of the flow is from right to the left of the pictures (tail-to-head). It is observed that the larva tends to display rheotaxis by swimming against the flow within 1.3 seconds..... 105

*Figure A. 3. Positive rheotaxis of zebrafish larvae (N=34 larvae per condition) inside an enclosed channel in response to average flow velocities of 9.5, 19, and 38 mm.sec⁻¹. The control group was not exposed to any flow in the device and the reported response is for any arbitrary re-orientation. The results show no desire in the larvae for rotation and their preference to remain in the initially loaded orientation without any flow in the channel; however, once the flow velocities of 9.5 and 19 mm.sec⁻¹ were applied, the rheotactic behavior increased significantly (***: two-tailed t-test, p-value<0.001). At 38 mm.sec⁻¹, the zebrafish larvae demonstrated a low rheotactic response which was not different from the random movement of control larvae (two-tailed t-test, p-value>0.05). 107*

Figure A. 4. Spatial distribution of rheotactic response of zebrafish larvae (N=14 larvae per condition) along the three sections of the main channel (1: initial anterior, 2: mid-channel, and 3: posterior location). The control larvae tended to randomly reorient mostly within section 1 of the device where they were initially loaded. At the lowest flow velocity of 9.5 mm.sec⁻¹, the spatial distribution of response was uniform across the three sections, whereas at 19 mm.sec⁻¹, a large portion of responses took place at section 1 immediately upon exposure to flow. This contends that the larvae become more sensitive to the flow once exposed to a medium flow velocity of 19 mm.sec⁻¹

compared to 9.5 mm.sec⁻¹. The response to 38 mm.sec⁻¹ mostly occurred in section 3, which implies that the larvae failed to overcome the flow strength and were carried out of the device before they could appropriately respond..... 109

Glossary of Terms:

Agarose – A gelling agent which is used in various biological applications such as nucleic acid separation, cells culturing platform, and fixation of different organisms such as the zebrafish larvae.

Apomorphine- A non-selective dopamine agonist that activates the D1- and D2-like dopamine receptors and is used in treatment of the Parkinson's disease.

Behavioral Screening – Standardized and systematic evaluation of the behaviors in humans and various organisms to, for example, cure the behavioral diseases.

Bilateral Tail Turn – Lateral oscillation of the zebrafish tail to both sides of its body.

Biological Pathway – Interactions inside a cell which leads to an alteration or outcome involved in metabolism, signal transmission, etc.

Caenorhabditis elegans (C. elegans) – A transparent worm which is extensively studied as a model organism in various biological applications such as human disease modelling due to their genetic homology with humans.

Cognitive Function – The brain activities that result in gaining knowledge and information which includes learning, memory, attention, etc.

Confocal Imaging – An optical imaging technique using the confocal microscopes for the visual and quantitative assessment of various biological samples with a high resolution. The technique provides the user with capturing a sequence of 2D images in different depths in order to reproduce a 3D structure. It is widely used in life science and the optics.

Danio rerio – Binomial name of the zebrafish, which is a model organism for various biological studies such as drug discovery and human disease modelling.

Days Post Fertilization (dpf) – An established term to show the zebrafish developmental stage by reporting the number of days after the zebrafish fertilization, i.e. the union of the fish's sperm and egg.

Disease Pathology – General study of disease treatment and diagnosis.

Dopamine Agonist and Antagonist – The chemical compounds that either activate (agonist) or block (antagonist) the dopamine receptors. They are widely used in treatment of various neurological disorders such as schizophrenia.

Dopamine Receptors – A class of G protein-coupled receptors in the central nervous system (CNS) of the vertebrates which are involved in different neurological states such as pleasure, motivation, learning, etc.

D1- and D2-like Dopamine Receptor Groups – Subfamilies of the dopamine receptors which form almost the whole dopamine receptors.

Drosophila melanogaster – A type of fly, commonly called fruit fly, which are widely used as model organisms in developmental biology due to their advantageous features such as high genome similarity to humans.

Drug Discovery – Discovery of a new medication in the fields of medicine and biology.

E3 Water – Fish medium which is produced with a mixture of the distilled water and salt used for raising the fish embryos and larvae.

Electroencephalography (EEG) Activity – Electrical activities of the brain which is recorded by noninvasively placing the electrodes along the sculp.

Electrokinetics – Study of the mechanical motion of particles in the fluids which are electrically induced.

Electrophysiology – Examination of the electrical activities of biological cells, tissues, and organs such as neurons, heart, etc, which can inform the examiner about any abnormality in the targeted object.

Electrotaxis – Response of biological cells and organisms, such as the zebrafish, to an electrical stimulus.

Embryonic Development – Process of growing a living organism, such as the zebrafish, from the egg fertilization stage until the embryonic/larval stage (i.e. early stages of a fish development).

Environmental Scanning Electron Microscope (ESEM) – A scanning electron microscope (SEM) which is applicable for a gaseous environment monitoring.

Gene Mutation – Permanent alteration of a gene in terms of the DNA sequences which retains various biological influences on the activities of the targeted gene.

Genetic Screening – Monitoring the activities and changes in a gene or protein for different biological applications such as curing the genetic disorders.

GCaMP – Genetically encoded calcium indicator, which is a composite of the green fluorescent protein (GFP), calmodulin (CaM, i.e. a protein), and M13 (i.e. a synthetic

peptide), that can act as a sensor to determine any neural activities of the living organisms such as the zebrafish.

Hydrodynamic Force – Executed force on an object immersed in a fluid due to the motions of surrounding fluid.

Environmental Hypoxia – Oxygen deprivation of the air or water which is detrimental to the living organisms.

ImageJ – An open source, Java-based program which is used for image processing and analysis developed by the National Institutes of Health.

Kinovea – An open source software for a semi-automated video analysis used in various applications such as targeted point tracking on a trajectory.

Knockout – Genetic modification or disruption of a living organism, such as the zebrafish, to alter their behaviors in response to a particular environmental cue.

Larvae – Developmental stage of the zebrafish when they become 3 days post fertilization (dpf) until 30 dpf.

Lateral-line – A system of organs in the living aquatic organisms which senses and detects the movements of their surrounding water.

Model Organism – Laboratorial non-human species including the zebrafish that retain many advantageous characteristics such as easy handling and high genetic similarity to humans which make them appealing models for various biological applications such as drug discovery and human disease modelling.

Mutant – New organism produced from an alteration in a gene of the normal organism.

Neural Circuits – Functional entities of the nervous system which are formed and organized from the communicating neurons to process various types of information.

Neural Screening – Monitoring the activities of neurons in response to any environmental cues using various electrical or imaging techniques.

Pannexin – A vertebrate protein family, consisting of the Panx1, Panx2, and Panx3, which are widely expressed in the brain and have different functions such as sensory processing in the nervous system.

Pectoral Fin – Anatomical features of a fish made of the bony spines and covered by the skin which are located on the sides of the fish helping them with swimming.

Phenotype – Integration of an organism's detectable characteristics, such as the behaviors and morphological features, which can be revealed due to various environmental factors.

Polydimethylsiloxane (PDMS) – A transparent and permeable elastomeric polymer which is commonly used in the microfluidic devices fabrication.

Quinpirole – A selective dopamine agonist which mostly acts on the D2-like dopamine receptor group.

Rheotaxis – A common behavior exhibited by the aquatic species which is defined as turning, holding position and swimming against an approaching flow.

Schizosaccharomyces pombe (S.pombe) – A yeast which is used as a model organism in cell biology.

Sensory-Motor System – The biological system whose role is to combine information from the sensory and motor systems in order to control the bodily movements.

SKF 38393 – A selective dopamine agonist which mostly acts on the D1-like dopamine receptor group.

Unilateral Tail Turn – The lateral oscillation of the zebrafish tail to its either sides.

Visual System – Part of the central nervous system (CNS) of the organisms enabling them to process and respond to the visual cues properly.

Wilde Type (WT) – The most common zebrafish strain which is represented as a normal (non-mutated) strain in the zebrafish population.

Yeasts – Single-cell microorganisms which are used in biotechnology.

Chapter 1

Introduction and Literature Review

Small organisms have been used as popular models for disease investigations due to their molecular mechanisms, cellular processes, and genetic pathways which are highly conserved in humans [1]–[3]. The most widely-used small-scale groups of the model organisms for various biological applications [4]–[6] are *Caenorhabditis elegans* (worm) [7], *Drosophila melanogaster* (fruit fly) [8] and *Danio rerio* (zebrafish) [9] due to their characteristics such as cellular simplicity and high genetic homology with humans [10]. However, zebrafish have recently garnered more interest since, unlike worms and fruit flies, they are vertebrates which are more similar to humans in terms of the genetic, physiological, anatomical, and behavioral characteristics [11].

1.1 ZEBRAFISH LARVA AS A MODEL ORGANISM FOR BEHAVIORAL STUDIES

The *Danio rerio* or zebrafish are the simplest vertebrate model organisms that are widely used in drug discovery [12], brain mapping [13], disease modeling [14], [15], neural assays [16], [17], and behavioral screening [18]–[20] applications due to their high genetic homology with humans [21] and quick embryonic and larval development (Fig. 1-1) [22], [23]. Starting at 4-5 days post fertilization (dpf), the zebrafish larvae fully develop many sensory-motor functions to independently swim in the aqueous environments (Fig. 1-2) [22], [23]. The larvae also offer several unique advantages including optical transparency [13] and small dimension [24] that suit them well for various *in-vivo* behavioral and neural investigations. However, the neuronal pathways

and genetic developments involved in various zebrafish larvae behaviors in response to the environmental cues are not fully understood yet [13], [15], [25]–[28].

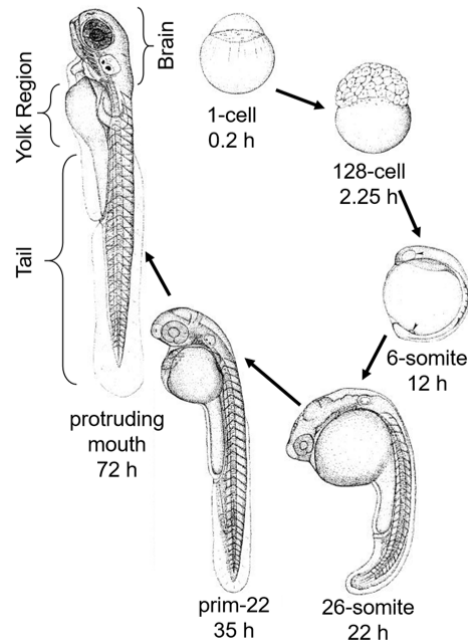


Figure 1-1. Photographs of the zebrafish at different embryonic and larval developmental stages from 12 minutes to 3 dpf [23]. Reproduced and reprinted with permissions from the publishers of Ref 23.

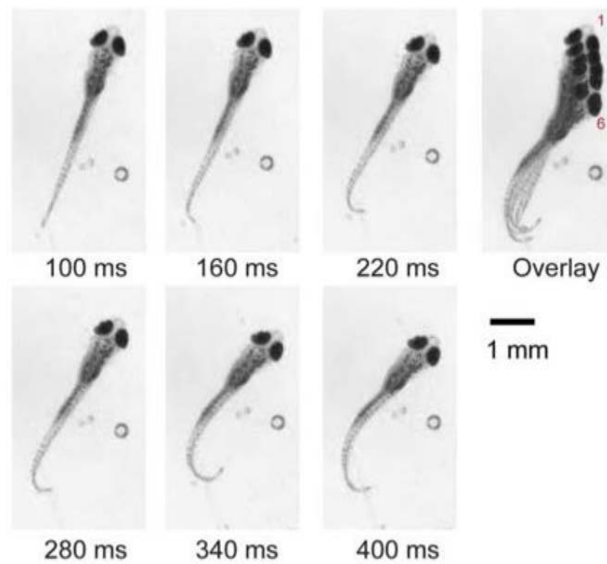


Figure 1-2 Discrete captured frames of a 17 dpf free-swimming zebrafish larva moving backward inside a petri dish. Overlay is the frame-on-frame photo of movement [29]. Reprinted with permissions from the publishers of Ref 29.

The most widely-studied zebrafish larvae behaviors are prey-capturing [30], escape [27], and orientation [31]–[34]. Prey-capturing behavior is generally exhibited when the larva is seeking food. Escape behavior is defined as avoiding an approaching predator or a similar simulated situation. Orientation behavior is reflection of the larvae to a variety of the environmental cues by turning their bodies towards or away from the original stimulus.

The abovementioned behaviors are displayed by the zebrafish larvae in the form of specific motor patterns such as O-bend [35], J-bend [30], [36], C-bend [37]–[39], forward/routine [40] and escape/struggling [29] swimming, flick [41], and backward motion [29] patterns. Overlaid images related to some of these motor patterns and their corresponding tail movement graphs are shown in Fig. 1-3. O-bend pattern is defined as the thorough tail turn which mimics the letter “O”. J-bend pattern is defined as the small unilateral tail motion which mimics the letter “J”. C-bend pattern is defined as the large and fast unilateral tail turn which mimics the letter “C”. Forward/routine and struggling swimming patterns are defined as the small and large bilateral tail turns, respectively. Flick pattern is defined as the tail motion with very small tail turns which could not be classified into any of the mentioned patterns. Backward motion takes place when the larva is swimming backward (Fig 1-2). The advantages of analyzing different locomotion and motor patterns are discussed later in this chapter.

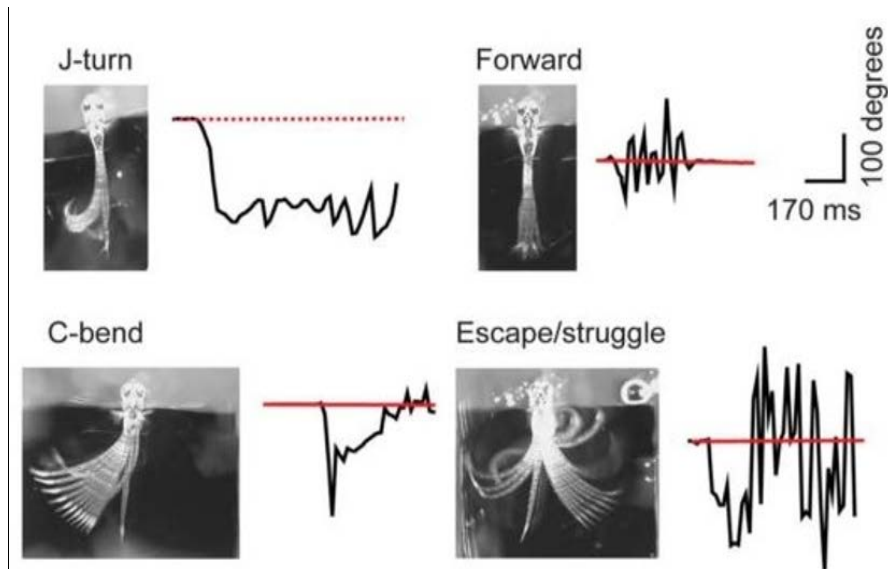


Figure 1-3. Distinct behavioral motor patterns of a 17 dpf semi-immobilized zebrafish larva, such as J-turn (J-bend), C-bend, forward/routine, and escape/struggling swimming patterns, with the larva's head embedded and fixed in agarose while the tail is free to move. Red and black lines represent the resting position and tail angle (with respect to the resting position) versus time, respectively [29]. Reprinted with permissions from the publishers of Ref 29.

The zebrafish movement behavior can also be quantified in terms of the response duration, latency, speed [31], travelled distance [20], pectoral fin beats frequency [40], eye saccades and nystagmus movements [18], and tail beat frequency (TBF) [29]. Latency is defined as the time duration from the stimulus application onset until the response initiation. Response duration is measured from the beginning to the end of movement. The travelled distance is measured as the distance that the fish travel during the response duration. For the freely moving zebrafish, speed is defined as the ratio of travelled distance over the response duration due to application of a stimulus. The oscillation frequency of pectoral fin during the movement is called pectoral fin beats frequency. Eye saccades and nystagmus movements are defined as any fast rotational and convergent or divergent movements of the zebrafish eyes, respectively. TBF is

defined as the ratio of tail motion cycles over its corresponding time (the methods to calculate tail motion cycles may differ for different applications).

It has been shown that none of the abovementioned motor patterns occur arbitrarily [29]; thus, one can examine various zebrafish behaviors in more detail by analyzing their corresponding motor patterns. This is truly beneficial for a variety of biological applications aimed at understanding how neural circuits, sensory-motor systems, and genes are involved in evoking a specific behavior and executing the corresponding pattern. For instance, it is believed that zebrafish cognitive functions are involved in the prey-capturing behavior [30], [36] during which the larva exhibits J-bend pattern with a slow swimming predominantly. Another example relates to the Mauthner cells which are expressed in the zebrafish hindbrain segments [42]. These cells are engaged in the escape behavior during which the zebrafish mostly display C-bend and struggling swimming patterns. It has also been shown that the zebrafish lateral-line and visual systems are engaged in the rheotaxis behavior [31], i.e. turning and orienting against the flow once exposed to a streaming water [31], [43].

Motor patterns have a broad application in genetic studies as well. O. Fajardo et al. [29] demonstrated a significant difference in J-bend pattern between the wild type, which did not display any J-bend, and a particular mutant strain, which showed an increased J-bend pattern rate in response to the light stimuli. They concluded that specific neurons (rather than a visual input or non-specific neuron induction) can repeatedly trigger J-bend pattern and should then be involved in the prey-capturing behavior accordingly [36].

Overall, screening and quantifying the zebrafish motor behaviors have been a demanded but challenging task. We will discuss a variety of techniques and platforms that the researchers have employed to study the zebrafish behaviors in next sections.

1.2 CONVENTIONAL METHODS TO STUDY ZEBRAFISH LARVAE BEHAVIORS

The common requirements in zebrafish-based behavioral studies are application of an external stimulus to evoke the response, followed by investigation of the consequent body movements and patterns. The most popular conventional platforms to study the zebrafish movement phenotypes are petri dishes [29], multi-well plates [20], [44] and agarose gel substrates [45], [46]. These platforms are used to fully or partially immobilize the larvae for exposure to various stimuli such as chemical [20], sound [47], [48] and light [30], [49], followed by quantification of their corresponding activities. Each of the mentioned platforms will be elaborated with an example below.

O. Fajardo et al. [29] performed a behavioral analysis of the zebrafish larvae inside a petri dish under no physical restrictions so that the larvae could freely swim in all directions (Fig. 1-2). They studied the responses of the wild type and a mutant (i.e. HuC:itTA/Ptet:ChR2YFP, abbreviated as ChR2) larva to the light stimulus. It was concluded that the backward motion, as a specific movement, is executed by activation of ChR2 protein which is widely expressed in zebrafish cells. They also examined the activities of the semi-immobile zebrafish larvae, where the larva's head was embedded inside agarose gel leaving the tail and pectoral fins free to move. By fixing the larva's head, subtle behaviors and motor patterns could be observed, quantified, and characterized, while the brain activities could be fluorescently imaged. This was not

easily achievable with a freely moving larva. The behaviors were classified into several motor patterns such as J-turn (J-bend), forward and struggling swimming, C-bend and no movements (as shown in Fig. 1-3). The results revealed involvement of a group of neurons in the zebrafish midbrain in triggering J-bend pattern.

T. Iron et al. [20] investigated the effect of various dopaminergic drugs, which are used to target the dopaminergic receptors in zebrafish brain, on the larvae movement inside a 96-well plate. They showed that all dopaminergic drugs can dose-dependently alter the larva movements in a way that dopamine agonists and antagonists increase and decrease the movement, respectively.

I. Bionco et al. [30] developed an assay in which the larvae were partially restrained in a petri dish using agarose gel, for behavioral investigation. The larvae responded to a moving optical stimulus by exhibiting J-bend pattern and eye convergence movements. Thus, they proposed that, since J-bend pattern is involved in the zebrafish prey-capturing behavior, the eye convergence might also help the larva to spot the prey.

Despite the advantages of conventional behavioural screening techniques via using petri dishes, well-plates, and agarose gel, these platforms suffer from several shortcomings. Using agarose to partially immobilize the larvae can be time-consuming, irreversible, and intricate due to the agar heating-cooling processes. It was also shown that covering the larva's head with agarose might bring about the possibility of oxygen deprivation and morphological damages, making agarose unsuitable for post-exposure assays [50]. The disadvantages associated with petri dishes and well-plates are difficult

manipulation of the fluids and cumbersome processes for accurate stimuli control due to the 3D environment of the plate. Furthermore, quantitative analysis of the larvae behaviors is challenging due to the difficulties and complications associated with imaging, accessibility to the organ-of-interest, and assessment of the subtle movement phenotypes [50]–[52].

There is a high demand for accurate, repeatable, and simple experimental tools to quantitatively monitor the zebrafish larvae activities, such as movement behavior, under controllable conditions. Microfluidics is one of the powerful technologies extensively explored for zebrafish behavior screening.

1.3 MICROFLUIDIC TECHNOLOGIES FOR ZEBRAFISH BEHAVIORAL STUDIES*

Microfluidics is the science and technology of handling fluids at the micrometer to millimeter scale using microfabricated components such as channels, chambers, valves and pumps. This technological field has been extensively advanced and developed over the last two decades [53]. Due to micro-scale dimension of the structures, microfluidics can offer several useful advantages such as low fluid and energy consumption in analytical investigations. Moreover, due to the small and compatible channel sizes, one can readily investigate the small biological objects such as cells, tissues, organs, and organisms with microfluidics for various biomedical applications [53].

* This section with slight changes was published as a book chapter: K. Youssef, P. Bayat, A.R. Peimani, S. Dibaji, and P. Rezai, “Miniaturized Sensors and Actuators for Biological Studies on Small Model Organisms of Disease”, in *Environmental, Chemical and Medical Sensors*, S. Bhattacharya, Editor, Springer, 2017.

Microfluidic devices can be made of various materials including polymers, silicon, glass, paper, and thread [54]. Polymers, particularly Polydimethylsiloxane (PDMS), have proven to be more useful and applicable for rapid prototyping of the microchips used in biological applications. For example, PDMS has several advantageous characteristics such as cost- and time-effective fabrication process, biocompatibility, gas permeability, and flexibility (as opposed to the fragility of glass and silicon) [54]. PDMS-based microfluidic devices have been utilized for neural and behavioral investigation of the small model organisms such as *C. elegans* [55]–[62], *D. melanogaster* [63]–[66] and *D. rerio* [67]–[71]. Precise manipulation of the organisms and chemicals, assay automation, throughput enhancement, lower biochemical consumption, and simpler experimentation for the end users are among the merits offered by microfluidics in organism-based studies [72]–[74].

Various microfluidic devices and techniques have been proposed for monitoring the behavior of zebrafish larvae [69]–[71]. R. Candelier et al. [70] developed a microfluidic device made of the transparent acrylic slabs, i.e. Polymethylmethacrylate (PMMA), to partially immobilize and expose the zebrafish larvae to different chemicals. The device (Fig. 1-4a) included an open pool where the larva was partially immobilized with agar while its head was positioned in front of a chemical infusion channel (Fig. 1-4b) and its tail was free to move for behavioral screening (Fig. 1-4a). In this study, different flavors of citric acid (CA), as a sour aversive chemical, and L-proline (LP), as an appetitive tastant, were delivered (Fig. 1-4c) in a step-pulse mode (Fig. 1-4d) to examine the gustatory neuronal responses and tail movement behavior of the larva. It was shown that majority of the dorsal, medial and ventral neurons respond to either CA

or LP, while a few reacted to both. Furthermore, the monitored tail motions proved that whenever there was a behavioral response, neuronal reactions induced by the chemicals were also significant. By comparing the neuronal responses with and without the association of tail motions, the authors showed that the sensory and gustatory-induced responses were related to specific regions of the brain.

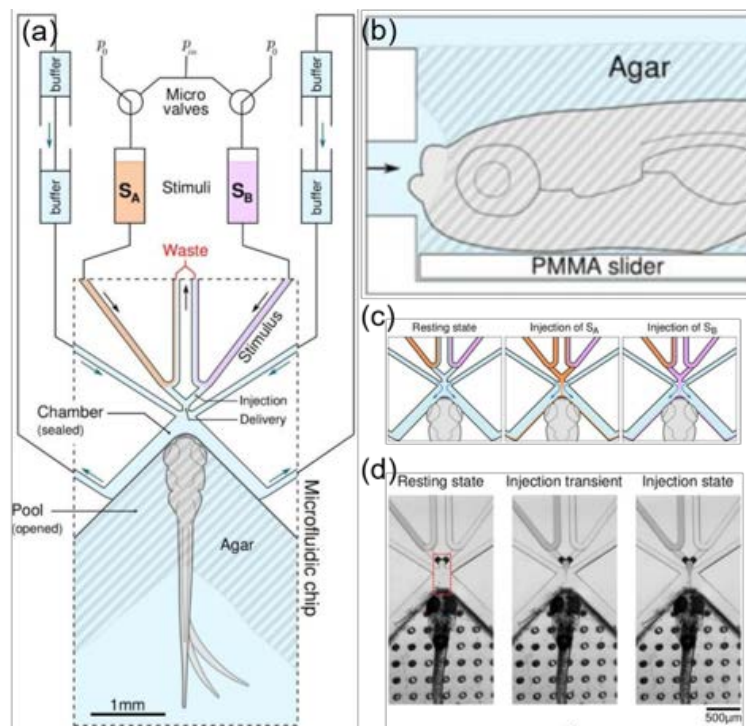


Figure 1-4. Microfluidic device for a chemical screening assay on the zebrafish larvae [70]. (a) Schematic design of the microfluidic device where the larva is immobilized by agarose and its mouth and tail are free to be exposed to the drug and recorded, respectively. (b) Side-view of the larva's head embedded and fixed in agarose with its mouth being exposed for the chemical delivery. (c) Schematic images of the zebrafish larva under exposure to two chemicals. (d) Real images of the larva immobilized in agarose under different chemical exposure states. Reprinted with permissions from the publishers of Ref 70.

In order to study the zebrafish behavior under exposure to oxygen deprivation (i.e. hypoxia), M. Erickstad et al. [67] developed a microfluidic device which allowed the users to manipulate different oxygen concentrations in the zebrafish medium. Their PDMS device contained a zebrafish channel in which a larva was loaded and trapped

by utilizing the microfabricated obstacle and hydrodynamic force (Fig. 1-5a). Two sets of zigzag microchannels were designed to integrate two different gases A and B with two medium streams (Fig. 1-5b,c). Permeability of the PDMS channel walls to the gases made it possible to manipulate the oxygen level in the exposure media. The results suggested that the body movement rate and pectoral fin beats significantly increase with the strongest hypoxia treatment (i.e. $[O_2] = 1.8\%$), in comparison with the control group.

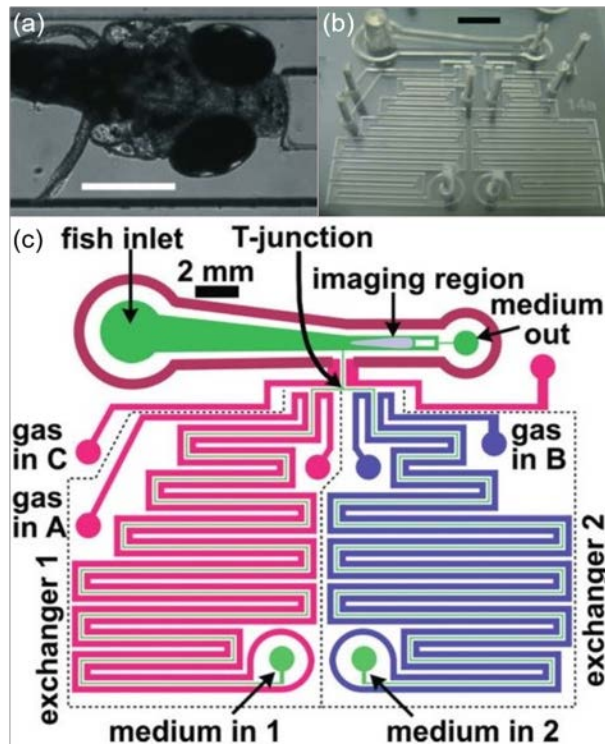


Figure 1-5. Microfluidic device made from PDMS for oxygen-deprivation studies [67]. (a) Real image of a zebrafish larva trapped and fixed by a barrier and hydrodynamic force of the flow streaming from the left to right. Scale bar: 0.35 mm. (b) Real image of the device. Scale bar: 4 mm. (c) Schematic design of the channels in which various types of gases could be utilized to decrease or increase the level of oxygen in the environment, benefiting from permeability of PDMS. Reprinted with permissions from the publishers of Ref 67.

X. Lin et al. [71] designed a microfluidic system (Fig. 1-6a) which included three different devices called “Motion” (Fig. 1-6 a-i), “Lateral” (Fig. 1-6 a-ii), and “Dorsal” (Fig. 1-6 a-iii) microchips in which the zebrafish larvae were trapped in different positions and

orientations. In the Motion chip, the larva was partially free to display motor behaviors (Fig. 1-6b). Different responses to various doses of ethanol were characterized via quantification of the fin beats, eye saccades, overall body movements, and eye nystagmus (Fig. 1-6b). In the Lateral chip, the larva was laterally immobilized for cardiac screening in a way that the whole physiology of heart was monitored (Fig. 1-6c). In the Dorsal chip, the larva was dorsally immobilized for brain function monitoring and fluorescence imaging (Fig. 1-6d). In each microchip, the larvae were loaded through a channel into the device and immobilized one by one inside the tapered channels with continuously-applied hydrodynamic forces. For behavioral analysis of the zebrafish larvae, their pectoral fin beats, eye saccades and body movements were quantified under exposure to ethanol with different concentrations. At the low ethanol concentration of 0.75%, fin beats and eye movements were increased, whereas significant drops in the fin, eye and body movements were observed at the high concentration of 3% ethanol. These results suggested that ethanol may cause impairment in the motor coordination and vision function of the zebrafish larvae. The larvae's heart rate plummeted after being treated with all doses of ethanol (0.75, 1.5, and 3 %), which showed that, up to 3% concentration, ethanol negatively affects the larvae's cardiac function. This study was expanded to the neuronal level where the brain-wide GCaMP (i.e. genetically encoded calcium indicators) activities in the nervous system were recorded during larva's exposure to ethanol. The dose-dependent effect of ethanol on the neural activities was also observed. At the low ethanol concentration, neuron responses initiated from the caudal hindbrain, then continued to grow into the cerebellum, ventral midbrain, and forebrain. As opposed to the results obtained for

weak behavioral activities at the high ethanol dosages, the forebrain neuronal activities were reported to be high and most intensely induced at that dosage.

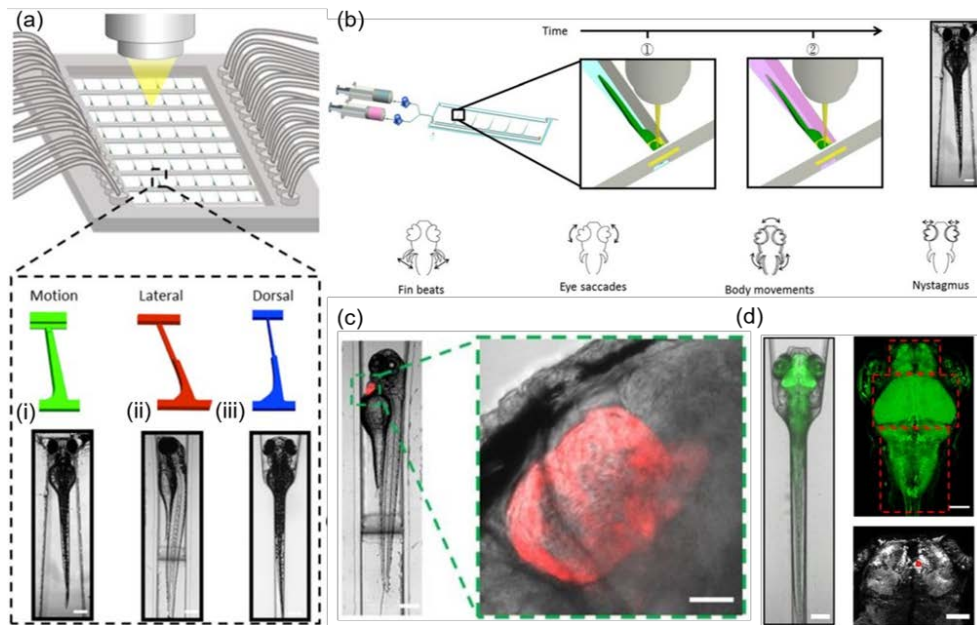


Figure 1-6. Microfluidic device for neural and behavioral screening of the zebrafish larvae activities [71]. (a) Scheme of the chip with real images of the immobilized fish in end-tapered channels of the (i) Motion, (ii) Lateral, and (iii) Dorsal chips. The larva is exposed to the chemical through the horizontal channel which is perpendicular to the trapping channel. Scale bar: 0.2 mm. (b) Behavioral responses of the larva trapped in the “Motion” chip for neural and movement monitoring. By maintaining a slow flow rate inside the channel, larva’s head was gently immobilized (top right) for florescence imaging (top left). Ethanol and E3 water switched at the specific periods to apply or release the stimulus (top left). Movement responses were classified into the fin beats, eye saccades, overall body movements, and eye nystagmus (bottom). Scale bar: 200 μm (top right). (c) Images of the larva trapped in the “Lateral” chip (left) where its cardiac physiology can be monitored and analyzed (right). Scale bar, 200 μm (left), 25 μm (right). (d) Brain function and neural imaging of the zebrafish larva trapped in the “Dorsal” chip. Scale bars: 200 μm (left image), 100 μm (top right image), 50 μm (bottom right image). Reprinted with permissions from the publishers of Ref 71.

S. Hong et al. [75] proposed a novel technique for zebrafish neural recording with a microfluidic-based electrophysiology platform (Fig. 1-7). They designed a multichannel platform made of PDMS with narrowing-end channels in which several larvae were trapped for monitoring. Electrophysiological recording of the brain activities was achieved using an array of readout electrodes positioned on top of the immobilized

larvae's heads and a reference electrode in front of their mouths. For chemical screening, they infused valproic acid (VPA) and topiramate (TOP) into the zebrafish media, followed by recording the electroencephalogram (EEG) activities of the immobilized larvae. In VPA treatment, all 9 treated mutants could successfully respond to the drug while only 7 of them showed a successful response after a successive treatment by TOP.

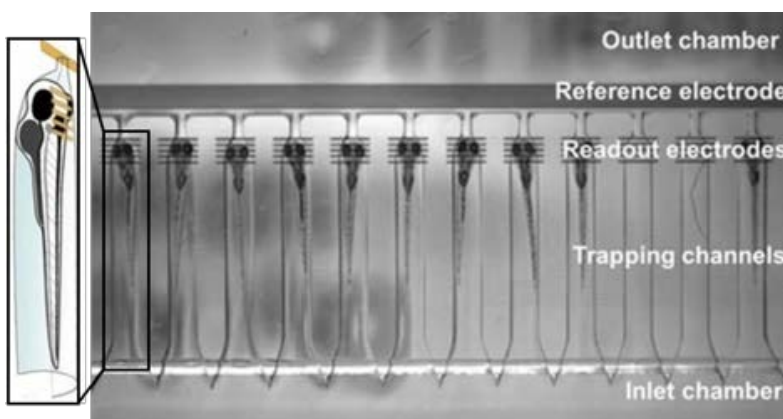


Figure 1-7 Real picture of multiple trapped zebrafish larvae in the electrophysiology microfluidic device [75]. Reprinted with permissions from the publishers of Ref 75.

Another conventional screening technique, which was also used in microfluidic-based studies, is scanning electron microscopy (SEM) which can capture a 3D-topographical image of the biological samples, more elaborated than common confocal imaging [76]. However, due to the intricate pre-experimental procedures including fixation, dehydration, and staining, SEM could not be employed for studying the model organisms. On the other hand, a novel imaging technique, called environmental SEM (ESEM) can address most of these issues because it can operate in a gaseous atmosphere under a low vacuum mode while there is no need for staining. ESEM can also provide a suitable environment to image tissue surfaces and various organs *in-vivo*. A. Jin et al. [76] proposed a proof-of-concept microfluidic device in which the

zebrafish larva can be immobilized (Fig. 1-8a) for ESEM imaging. The device consisted of the trapping arrays, microwells, and reservoirs for simultaneous immobilization of several larvae and ESEM imaging (Fig. 1-8b).

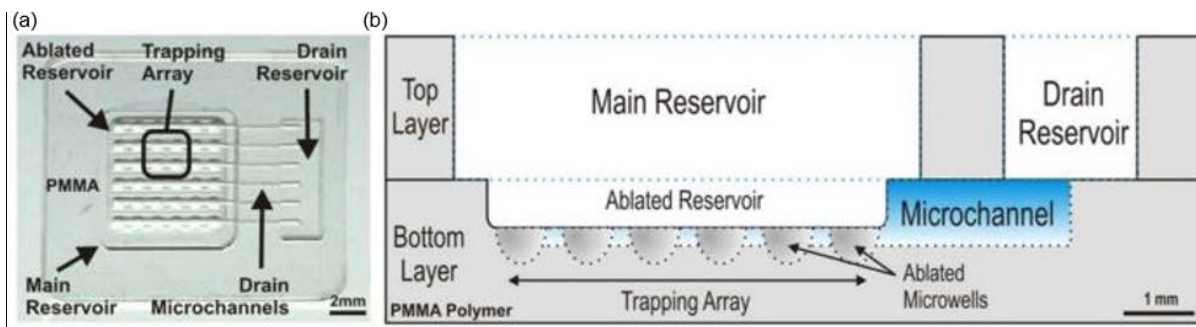


Figure 1-8. Microfluidic device for zebrafish larvae imaging. (a) Photograph of the microfluidic device in which the zebrafish larva can be immobilized for ESEM imaging [76]. (b) Cross-sectional side-view of the ESEM device illustrating its various features [76]. Reprinted with permissions from the publishers of Ref 76.

The introduced microfluidic technologies have provided us with powerful analytical systems to study the zebrafish larvae activities. Employing microfluidics, one can develop simple devices with high accuracy for applications in investigation of the zebrafish larvae behavior under various stimulation conditions.

1.4 BIOLOGICAL AND TECHNOLOGICAL GAPS: ZEBRAFISH LARVA

ELECTROTAXIS

Electrical signal is one of the important stimuli that evokes a movement behavior, dubbed electrotaxis, in different organisms [77]. Various studies have examined the effect of electrical signals on cells and organisms [78], [79] for a variety of biological applications such as movement controlling [56] and wound healing [80].

P. Rezai et al. [55], [56] showed that *C. elegans* display a directional movement towards the cathode pole (Fig. 1-9a) under exposure to the electrical stimulus in a

microfluidic channel (Fig. 1-9b). It was shown that *C. elegans* electrotaxis depends on the age and size of the worm while it is mediated by certain sensory neurons. In addition, multiple microfluidic platforms have been developed to assist either sort the worms electrotactically based on their age and mutation [58], [81]–[83] or assess the effects of various chemicals using electrotaxis as a behavioral readout tool [59], [60], [84]–[87].

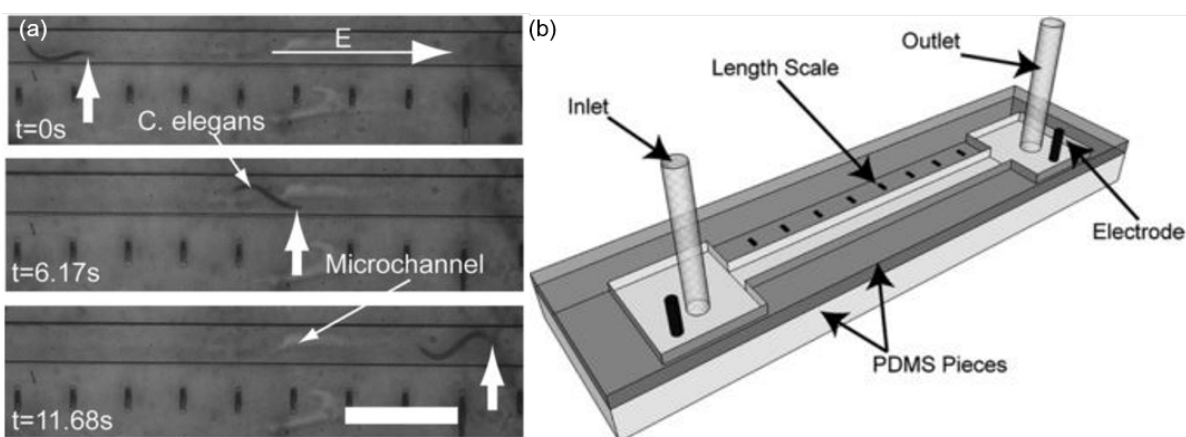


Figure 1-9. (a) Electrotaxis of *C. elegans* shown by the movement of a worm towards the cathode (at the right of the picture) under application of a 4 V.cm^{-1} electric field (E) inside a microchannel. (b) Schematic of the microchannel device used to study *C. elegans* electrotaxis [56]. Reprinted with permissions from the publishers of Ref 56.

B. Han et al. [88] demonstrated the electrotactic sorting of worms in a microfluidic device. Their device consisted of parallel arrays of micro-bump channels (Fig. 1-10a) optimized to allow a targeted size of worms to swim continuously. They were able to show that *C. elegans* can be sorted using their electrotaxis behavior and by developing optimal hexagonal structures of their environment based on their different body sizes. The possibility of sorting the adult worms in a mixed population was explored as well. P. Rezai et al. also designed two side-by-side microfluidic chambers [58], interconnected with small microchannels, and applied an electric field between the chambers (Fig. 1-

10b). A mixed population of *C. elegans* injected into one of the chambers were stimulated electrostatically to move towards the microchannels. Inside the microchannels, the electric field was elevated to a certain level that was intolerable to the older worms, while younger ones could pass through the microchannels and get sorted from the older worms. They demonstrated sorting of L3 or L4 stage worms from young adults or mutant worms from the wild type. N. Minc et al. [89] showed the orientation response of *Schizosaccharomyces pombe* (*S. pombe*), i.e. a fission yeast as a model organism, in response to an applied Direct Current electric field using the microfluidic device shown in Fig. 1-10c. The organisms were shown to orient perpendicular to the direction of the electric field. They also suggested the potential modulating role of intracellular pH in electrostatic response of *S.pombe*.

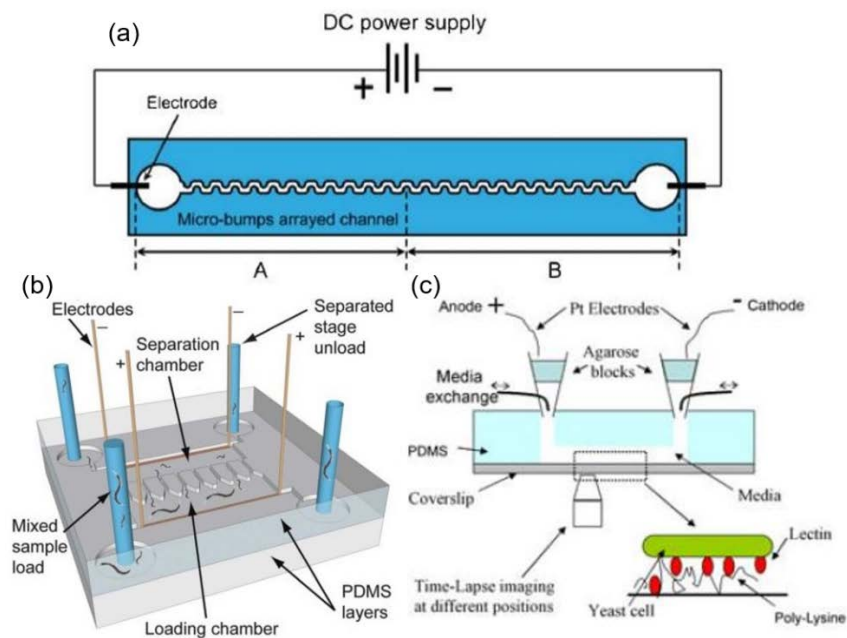


Figure 1-10. Schematics of different electric microfluidic devices for *C. elegans* sorting (a,b) [58], [82] and *S.pombe* electrostatics (c) [89]. Reprinted with permissions from the publishers of Ref 58, 82 and 89.

Furthermore, the electrical stimulation has been used to cure a variety of diseases such as bone injury [90] and neurological disorders [77]. Although the treatment mechanism is not well understood, one explanation can be the migration of newly-generated cells, which is resulted from the electric signal [91], to engage in tissue regeneration so as to heal the damage or to compensate for the cell losses [77].

Considering the importance of abovementioned studies, we have found that zebrafish electrotaxis has not been investigated in the literature thus far. Accordingly, there are several unanswered questions regarding zebrafish electrotaxis, some of which are listed below.

- Do zebrafish larvae respond to the electrical signal (i.e. electrotaxis)? If so, how would they exhibit electrotaxis?
- How sensitive are zebrafish to different amplitudes of the electrical signal and how do various amplitudes influence the electrotactic movement phenotypes?
- Are neuronal pathways involved in zebrafish electrotaxis? And can electrotaxis be used as a screening tool to study neuron and gene functions?
- Can electrical signal be utilized to induce specific zebrafish behaviors (e.g. visual stimuli have been used to evoke prey-capturing in the zebrafish)?

Furthermore, there are several technological gaps in studying zebrafish electrotaxis due to the difficulties associated with larva and signal manipulation as well as behavioral monitoring of the zebrafish. First challenge is establishing a suitable environment where a controllable, accurate, and on-demand electrical signal can be delivered to the zebrafish larvae. Second challenge is developing a platform on which

the zebrafish larva is free to move but in a controllable manner, in order to investigate the general zebrafish electrotaxis response. Third challenge is partially immobilizing the zebrafish larva so that any subtle electrotactic behaviors, such as the TBF or specific motor patterns, can be quantified.

1.5 RESEARCH GOALS AND OBJECTIVES

The goal of the thesis was to develop microfluidic devices inside which zebrafish electrotaxis could be investigated generally and phenotypically. We also intended to show the applications of our electrotaxis screening devices in neuronal and genetic studies. To achieve our goal, we defined the following objectives.

1. Smooth, Safe, and Convenient Loading of Zebrafish Larvae into Controllable Environments (e. g. microfluidic channels).

The challenge is to come up with a novel technique to load the larva inside the microfluidic device without any damage, for example, due to possible collision with the channel base and walls, during the loading process.

2. Controllable Trapping to Monitor and Quantify General and Phenotypic Movement Behaviors of the Zebrafish Larvae.

In order to assess the general (electrotactic) movement of the zebrafish inside our microfluidic device, the larva has to be laterally restricted so as to be able to exhibit only longitudinal orientation and movement. As such, this 1-dimensional movement under exposure to the electrical stimulus becomes easier to monitor and most importantly quantify. For screening and quantifying subtle movement phenotypes in

response to the electrical stimulus, the larva has to be partially immobilized within a screening region in a way that its tail is free to move while the larva is not able to exit the microscope field of view. As such, monitoring subtle movement patterns such as C- and J-bends becomes possible.

3. Controlled Application of Electrical Stimulus.

One of the challenges in electrotactic behavioral study of the zebrafish larvae is the application of electrical signal. Thus, our devices should possess suitable regions for precise, controllable, and simple application of the electrical signal in the form of electric current. Control over the initiation, termination, magnitude, and mode of the applied electric current are important experimental factors to be considered.

4. Screening and Quantifying Zebrafish Larvae Electrotaxis.

To screen and quantify zebrafish electrotaxis, our assay should be compatible with proper monitoring tools such as a microscope and camera. Moreover, the devices should consist of the appropriate and visually accessible screening sites to record the overall and subtle movement phenotypes of the zebrafish larvae.

5. Showing the Application of Microfluidic Electrotaxis Screening in Behavioral And Neuronal Studies.

We were interested to investigate the biological application of our electrotaxis assays. We intended to investigate if neuronal pathways are involved in zebrafish electrotaxis. We were also keen to utilize our device to explore the influence of particular zebrafish gene mutations on electrotaxis.

1.6 THESIS STRUCTURE

This thesis has been categorized into 5 chapters, starting with an introduction to the zebrafish model organism in the present chapter followed by a review of the conventional and microfluidic methods for behavioral screening. Second chapter reports on the methodologies and materials utilized to fabricate the devices and achieve our goal and objectives. Third chapter elaborates on our microfluidic device for studying general electrotaxis of the semi-confined (i.e. laterally confined) zebrafish larva under exposure to different electric currents. We also show the application of our device in dopamine system screening by exploring the effect of some selective and non-selective dopamine agonists on zebrafish electrotaxis. In the fourth chapter, a microfluidic device is proposed inside which the larva can be partially immobilized for subtle electrotaxis phenotyping. We also show the application of our electrotaxis screening device in studying knockout zebrafish models by testing electrotaxis of the Pannexin1 knockout zebrafish larvae. Finally, in chapter five, we provide a summary of the thesis and propose the future directions of our research. The appendix reports our research on zebrafish larva's response to water flow in a channel (i.e. rheotaxis) which was discovered during our electrotaxis studies.

1.7 CONTRIBUTIONS

Pouya Rezai conceived the idea of electrotaxis assays and helped with designing the devices, supervising the research and revising the thesis. Pouya Rezai and Georg Zoidl helped with results interpretation and manuscript writing. Amir Reza Peimani designed, fabricated, and tested the microfluidic devices, performed all data analyses,

and wrote the first drafts of the papers and the thesis. He also received reviewer comments and applied them to these documents. Asal Nady helped with device design and data analysis of the phenotypic electrotaxis assay. Janet Fleites Medina provided the wild type zebrafish samples constantly over the two years. Nickie Safarian generated and provided the knockout zebrafish samples. Georg Zoidl provided the chemicals and helped with zebrafish sample preparation. Below are the scholarly outcomes of this research.

1.7.1 Journal Papers

1. A.R. Peimani, G. Zoidl, and P. Rezai, “Zebrafish Larvae’s Electrotaxis and its Correlation with the Dopaminergic System Investigated in a Microfluidic Device”, *Submitted to Biomicrofluidics*, 2017.
2. A.R. Peimani, N. Safarian, G. Zoidl, and P. Rezai, “A Microfluidic Device to Study Subtle Phenotypes of Zebrafish Larvae Electrotaxis Using a Knockout Model”, *Under preparation for submission to Biomicrofluidics*, 2017.
3. A.R. Peimani, G. Zoidl, and P. Rezai, “A Microfluidic Device for Quantitative Investigation of Zebrafish Larvae’s Rheotaxis”, *Biomedical Microdevices*, **19**:99, 2017.
4. A. Nady, A.R. Peimani, G. Zoidl, and P. Rezai, “A microfluidic device for partial immobilization, chemical exposure and behavioural screening of zebrafish larvae,” *Lab Chip*, **17** (23), 4048–4058, 2017.

1.7.2 Book Chapters

Youssef, K., P. Bayat, A.R. Peimani, S. Dibaji, and P. Rezai, “Miniaturized Sensors and Actuators for Biological Studies on Small Model Organisms of Disease”, in *Environmental, Chemical and Medical Sensors*, S. Bhattacharya, Editor, *Springer*, 2017.

1.7.3 Conference Papers

1. A.R. Peimani, G. Zoidl, and P. Rezai, “Zebrafish Larva’s Cyclic Electrotaxis Behavior And Its Dependency On Dopamine Level Enabled By A Novel Microfluidic Assay”, in *21st MicroTAS*, Savannah, Georgia, USA. 1094-1095. Accepted on July 7, 2017.

2. A.R. Peimani, G. Zoidl, and P. Rezai, On-Demand Stimulation And Movement Analysis Of Zebrafish Larvae Inside Microchannels Using Electric And Fluidic Stimuli, in *26th CANCAM*, Victoria, Canada. Accepted on March, 2017.

3. Nady, A., A.R. Peimani, G. Zoidl, and P. Rezai, “A Microfluidic Device for Head Immobilization, Chemical Exposure, and Behavioral Screening of Zebrafish Larva”, in *20th MicroTAS*, Dublin, Ireland. 475-476. Accepted on June 24, 2016.

Chapter 2

Materials and Methods

2.1 ZEBRAFISH LARVAE GENERATION AND MAINTENANCE

Adult wild type Tupfel long fin strain (TL) and Panx1^(-/-) zebrafish (*Danio rerio*) were kept and raised at 28°C with a 14:10 hr light/dark cycle inside a recirculation system (Aquaneering, CA, USA). Fish were fed ad libitum with brine shrimps (Brine Shrimp Direct, Odgen, Utah, USA) twice-a-day. Eggs were collected from natural spawning and rinsed in the egg water containing 60 mg/ml of instant ocean sea salt (Instant Ocean, Blacksburg, VA, USA) and 0.1% methylene blue (M291-100 Fisher Scientific, CA). Embryos were maintained in the egg water inside an incubator (28°C). After hatching at 3 dpf, the larvae were collected and used for experiments at 5-7 dpf. The Panx1^(-/-) zebrafish were generated by transcription activator-like effector nucleases (TALEN) technology using the procedures outlined by Bedell et al. 2012 [92]. In this study, the larvae of the F3 generation were tested. These larvae have a 4pb frame shift mutation in the exon 4 of the panx1a gene generating a truncated channel protein with a premature stop codon at amino acid position 191. The procedures and functional characterization of the panx1^(-/-) fish are described in separate manuscripts [93], [94]. All experiments and procedures were performed according to the CACC guidelines of the Canadian Council for Animal Care (CCAC) after approval of the ACC protocol (GZ 2014-19 (R3)). The number of experiments including the zebrafish larvae were kept to the necessary minimum following guidelines approved by York University's Biosafety Committee (PR Biosafety Permit 02-19).

2.2 CHEMICAL PREPARATION AND LARVAE EXPOSURE

We have used three dopamine agonists to show the involvement of zebrafish's dopaminergic system in electrotaxis. Apomorphine hydro-chloride hemihydrate, SKF-38393 hydrochloride, and Quinpirole hydrochloride were purchased from Sigma-Aldrich (St. Louis, MO, USA). A standard protocol by T. D. Irons et al. [20] was followed to prepare various concentrations of these drugs for our studies. The drugs were first dissolved in deionized (DI) water to make 0.2 mL stock solutions of 0.5, 10, and 1 mM concentrations for the apomorphine, SKF 38-393 and Quinpirole, respectively. Then, the stock solutions were serially diluted in DI water to obtain three final apomorphine concentrations of 0.2, 1.8 and 50 μ M as well as 50 μ M SKF-38393 and 16.7 μ M Quinpirole hydrochloride (all used in studies by T. D. Irons et al. [20]). These concentrations were used for zebrafish larvae exposure and electrotaxis screening in our microfluidic device.

For exposure, individual 5-7 dpf zebrafish larvae were loaded into the wells of a 24-well plate. Animals were exposed to the specified apomorphine concentrations for a duration of 20 minutes. The exposure duration for SKF-38393 and Quinpirole hydrochloride were 140 min and 80 min, respectively. The exposure times were selected based on their peak effectiveness on the larvae behavior (reported in the literature [20]). Exposures were stacked 5 minutes apart to provide enough time for testing each larva in the device. Before each experiment, the selected larva was thoroughly washed in the E3 water in order to avoid any over-exposure effect of the drug on the electrotactic behavior. Procedures for electrotaxis screening are discussed separately for our two devices in Chapters 3 and 4.

2.3 MICROFLUIDIC DEVICE FABRICATION

The microfluidic devices were fabricated by replica molding of PDMS against a plastic master mold. The master molds were 3D designed in SolidWorks (SolidWorks Corp. MA, USA) and printed with an Objet260 Connex3 printer (Stratasys Ltd., MN, USA). To fabricate each device, PDMS base and curing agent (Sylgard 184 kit from Dow Corning, MI, USA) were mixed in a 10:1 ratio and de-bubbled for up to 30 minutes at room temperature. The de-bubbled PDMS pre-polymer was then casted on the master mold while the inlet and outlet tubes (Cole-Parmer Canada. QC, Canada) with an inner diameter of 1.6 mm were already PDMS glued to their respective reservoirs. Afterwards, the casted PDMS was cured at 60°C on a hot plate for 6 hours. Subsequently, the cured PDMS was peeled off the master mold, oxygen-plasma treated at 1 Torr pressure and 50 W power for 90 seconds (PDC-001-HP Harrick Plasma, USA) and bonded either to a flat glass slide or another PDMS layer (more details are provided in each following chapter). Using this method, the device could be fabricated with high reproducibility so our studies did not involve any device replicates and trials. Specific designs and operations of our devices will be elaborated in more details in the next chapters.

2.4 VIABILITY TEST

To examine whether the electric stimulation, loading technique, and device functionality harmed the zebrafish, we assessed the larvae's morphological abnormalities and survival following the procedures reported by Pardo-Martin et al. [95]. The stimulated larvae were recovered from the device through the tilted inlet tube by

using the withdrawal function of the syringe pump. This approach reduced the chances of damaging the larvae as they were being removed from the device for subsequent viability and morphological assessments. The retracted larvae along with a control group of zebrafish, which were not exposed to any electrical current in the microfluidic device, were then delivered to a fish tank and placed inside a 28°C incubator. The larvae were raised for four weeks while being fed twice a day with paramecia. For the survival assessment, we counted the number of days that the larvae remained alive under the controlled conditions. We used visual confirmation of the mortality in addition to the larvae's reaction to a gentle nudge. To evaluate morphological abnormalities, we visually monitored the fish inside the tank on a daily-basis during the 4-weeks period and counted any spinal bends (e.g., lordosis, kyphosis and scoliosis) as an abnormality.

2.5 STATISTICAL ANALYSIS

All of the statistical analyses were performed by using Microsoft Excel (Microsoft Corp., WA, USA). Results, such as electrotactic response rate of the zebrafish in exposure to the electric current, were reported as the average \pm SD (Standard Deviation). Two-tailed Student *t*-test with assumption of unequal variances was selected as the statistical method to identify any significant differences between two groups of data. Power analysis was performed to estimate the required sample sizes by maintaining the upper threshold of the significance level at 0.05 and the power at 80%. However, wherever the statistical difference was more significant, we report the most significant level at 0.01 or 0.001. The effect sizes of 0.5, 1.0, and 1.5 were assumed small, medium, and large, respectively.

A Microfluidic Device to Study Electrotaxis and Dopaminergic System of Zebrafish Larvae*

3.1 INTRODUCTION

As discussed in Chapter 1, in neurobehavioral studies, conducting quantitative analysis of the zebrafish larvae's behavior [45], such as movement [29], under exposure to different stimulations such as sound [47] and optical [49] signals has been a critical task. These studies have two major components in common including the application of an external stimulus to evoke the larvae's response followed by the investigation of their consequent body movements. As discussed in Chapter 1, to the best of today's knowledge, the inherent sensing and movement response of the zebrafish larva under electric signal stimulation and its underlying mechanisms have not been investigated.

Microfluidic technologies have provided us with simple and precise devices for application of the stimuli and behavioral investigation of freely-swimming organisms such as nematodes, flies and zebrafish larvae. For instance, our group and others [55], [56], [59], [61] have elaborately showed that, once exposed to a DC electric field, *C. elegans* tends to demonstrate the electrotaxis response towards the cathode pole. By testing of mutants, it has also been shown that the dopaminergic neuron signaling is

* This chapter has been submitted for publication: A.R. Peimani, G. Zoidl, and P. Rezai, "A Microfluidic Device to Study Electrotaxis and Dopaminergic System of Zebrafish Larvae", submitted to *Biomicrofluidics*.

involved in electrotaxis. These studies have inspired us to use microfluidics in order to investigate if the zebrafish larvae also demonstrate electrotaxis.

In this chapter, we introduce a versatile microfluidic device customized for on-demand electrical stimulation of the swimming zebrafish larvae and quantitative analysis of their electrotaxis movement inside a controllable microenvironment. Using this device and for the first time, we quantitatively demonstrate that the zebrafish larvae show electrotaxis towards the anode electrode under a DC electric stimulation. We observed that the electrotaxis response diminishes significantly at nighttime. As a biological application of our device in sensory-motor system studies, we examined whether reduced electrotaxis at night is correlated with the reduced dopamine receptor activity. We explore the effect of various non-selective and selective dopamine agonists on zebrafish electrotaxis at night. Our findings in this chapter shed light on electrotactic behavior of the zebrafish larvae, and demonstrate the usefulness of this screening method in studying the sensory-motor systems of the zebrafish larva. Our technique can be used for further investigation of zebrafish electrotaxis under exposure to chemical compounds for applications in drug discovery, toxicology, and disease pathology.

3.2 EXPERIMENTAL SECTION

3.2.1 Design of the Microfluidics Device

The microfluidic device (Fig. 3-1) used for electrotaxis screening of the zebrafish larvae consisted of a PDMS layer which was bonded to a glass slide as described in Chapter 2. The PDMS layer contained a 45°-tilted inlet tube, a 0.9mm-wide 43.2mm-

long larva loading channel, a U-shape channel gradually expanding in width from 0.9 mm to 1.6 mm, a 1.6mm-wide 63.3mm-long main screening channel, and a vertical outlet tube. All channels were 0.55 mm deep. The inlet and outlet reservoirs were extended by two side channels (0.1 mm wide, 0.2 mm deep and 26 mm long) to two electrode reservoirs at their anterior side. Introducing a simultaneous flow inside the side and tilted inlet channels during the animal loading precluded the larva from colliding with the base and the walls of the channel and resulted in a smooth delivery of the animals into the loading channel. The loading channel was implemented to visually confirm a larva entering the device; and the U-shape channel was used (i) to reduce the footprint of the device and (ii) to act as an electro-fluidic valve that prevented the larva from escaping the device during electrotactic movement towards the narrowing bend [58]. All the movement screening experiments were conducted in the main channel, using protocols discussed in the next section. Electric signals were applied to the channel via wire electrodes that were inserted into the side channel tubes.

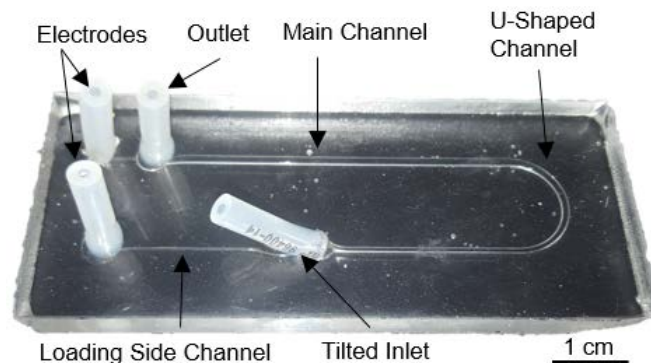


Figure 3-1. The microfluidic device consisted of inlet and outlet tubes, U-shaped channel, main channel and two side channels with tubes at the ends instrumented with two electrode wires. The length, width and height of the main channel were 63.3, 1.6 and 0.55 mm, respectively.

3.2.2 Experimental Setup and Procedure

The experimental setup shown in Fig. 3-2 consisted of the microfluidic device that was positioned on an inverted microscope (BIM-500FLD, Bioimager Inc., Canada) equipped with a camera (GS3-U3-23S6M-C, Point Grey Research Inc., Canada) for recording the animals' orientation responses in the main channel of the device.

Meanwhile, for further analysis of the immediate speed and motion pattern of the larvae (explained in the next section), a Samsung Galaxy S6 camera (Samsung Company, Suwon, South Korea) mounted vertically on top of the device was used. Two syringe pumps connected to the tilted inlet and side channel tubes were employed to load the larva into the device. A sourcemeter (Model 2410 Sourcemeter, Keithley, OH, USA) was utilized to apply the desirable electric currents (1-25 μA in continuous mode) across the channel via two wire electrodes that were connected from the sourcemeter outlets to the device's electrode reservoirs.

The day and night electrotaxis experiments were conducted at 11am-4pm and 8pm-11pm, respectively. To conduct an experiment, a single 5-7 dpf larva was pipetted into the device inlet tube. Flow rates of 10 $\text{ml}\cdot\text{min}^{-1}$ and 3 $\text{ml}\cdot\text{min}^{-1}$ in the inlet and side channel tubes were used to load the larva into the main channel (Fig. 3-3). Both syringe pumps were turned off once the loaded larva reached the main channel. The larva was given ~60 seconds to recover from any loading stress condition. The longitudinal orientation of the larva with respect to the two electrodes was first determined under the microscope (e.g. head towards the outlet or inlet). Afterwards, a continuous-mode electric current with a constant magnitude in a range of 1-25 μA was applied to the larva

in the direction of tail-to-head (e.g., anode at the tail) in order to explore zebrafish's reaction to the electric stimulus. The larva's electrotaxis was video-recorded at a speed of 60 frames per second (fps) for approximately 20 seconds of stimulation using the Samsung Galaxy S6 camera. Screening lasted until the larva stopped moving, caused either by the electric current or the channel's length limits. Subsequently, the tested larva was ejected through the outlet and the device was prepared for the next experiment with a fresh larva. Zebrafish larvae exposed to various concentrations of apomorphine, SKF-38393 and Quinpirole hydrochloride (see section 2.2 for details) and unexposed larvae (control group) were tested in our studies.



Figure 3-2. The experimental set-up consisted of the microfluidic device, two syringe pumps, direct current sourcemeter, microscope and two cameras, one on the microscope for close-up imaging and another on a stand for movement recording of the zebrafish larvae.

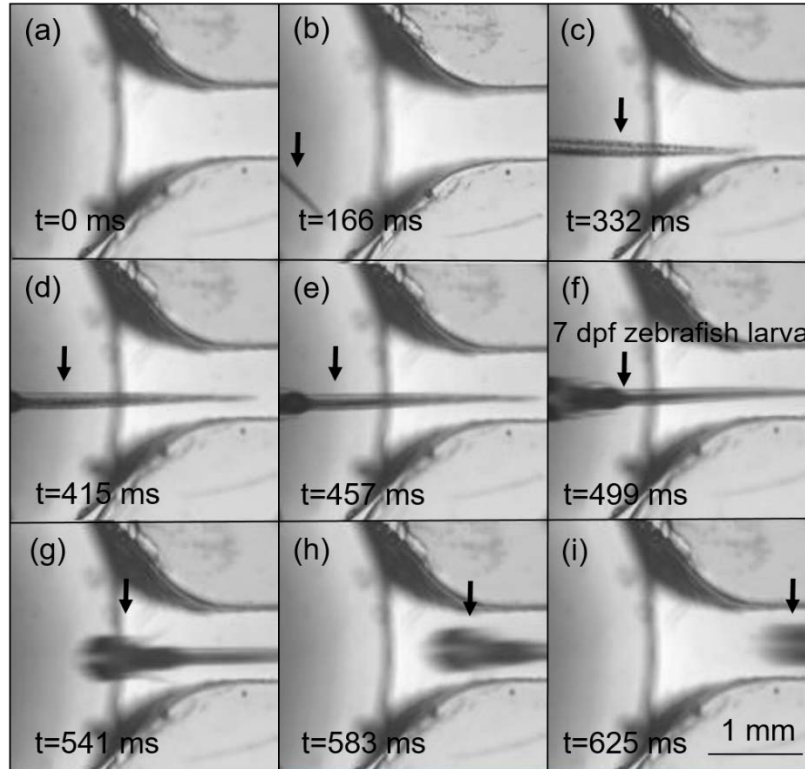


Figure 3-3. Bright-field images of a 7 dpf zebrafish larva being loaded into the device through the tilted inlet, shown in sequential images from a bottom view of the inlet reservoir under a microscope. Once the larva was loaded into the inlet reservoir, the flows in the side and main channels (from left to right) ensured smooth loading of the larva from the reservoir into the channel by keeping the zebrafish straight and clear from the channel walls. Scale bar: 1 mm.

3.2.3 Data Analysis

In our microfluidic device, zebrafish larvae's movement responses to the electric current stimulation were video-recorded by the microscope and cellphone cameras, as discussed in the previous section. ImageJ software [96] was used to convert the videos to a series of images and to analyze the images for quantifying the horizontal (X) and vertical (Y) positions of the larva along the channel axis and width, respectively. For this purpose, *Binary Process* function in ImageJ was used to convert each frame to a black and white image and to obtain XY coordinates of the center of mass of the fish in the

channel. These coordinates were also used to calculate the speed of the larvae as they moved along the channel in response to the electrical current stimulus.

3.3 RESULTS AND DISCUSSIONS

We first report an efficient technique to induce and quantitatively study zebrafish larvae's electrotaxis for the first time. As a significant advantage of this behavioural screening technique, the electric current stimulus used in our device can be easily and rapidly applied and manipulated inside the microfluidic environment [55]–[60]. After assessing zebrafish larvae's electrotaxis at various times in a day, we also show the application of this technique in investigating the involvement of D1- or D2-like dopamine receptors in modulating this sensory-motor response by treating the larvae with various doses of selective and non-selective dopamine agonists.

3.3.1 Electrotaxis of Zebrafish Larva in a Channel

Model organisms such as *C. elegans* have been shown to respond to an electric stimulus in a microchannel [56]. The electrotaxis behavior has been used for investigating the effect of various chemicals, such as neurotoxins, on *C. elegans* [59]. In this study, we questioned whether 5-7 dpf zebrafish larvae also respond to the electrical signal inside a channel. Accordingly, the microfluidic device shown in Fig. 3-1 was fabricated and used to study zebrafish larvae's electrotaxis. Individual animals were loaded into the channel and exposed to various electric currents along the channel axis in a manner that the anode electrode was positioned at the larva's tail (determined after some preliminary experiments). The fish's immediate response was captured under the

microscope. To assess the movement pattern and speed parameters, the larvae's response was video-recorded by a cellphone camera and quantitatively analyzed with the ImageJ software. Fig. 3-4a shows the sequential images of the electrostatic response (Fig. 3-4a-i and 3-4a-ii) and movement (Fig. 3-4a-iii and 3-4a-iv) of a 7 dpf zebrafish larva in the channel, under exposure to an electric current of 3 μA . It was observed that the zebrafish larvae had a tendency to move towards the anode electrode in a channel, which is opposite to electrotaxis in the hermaphrodite *C. elegans*.

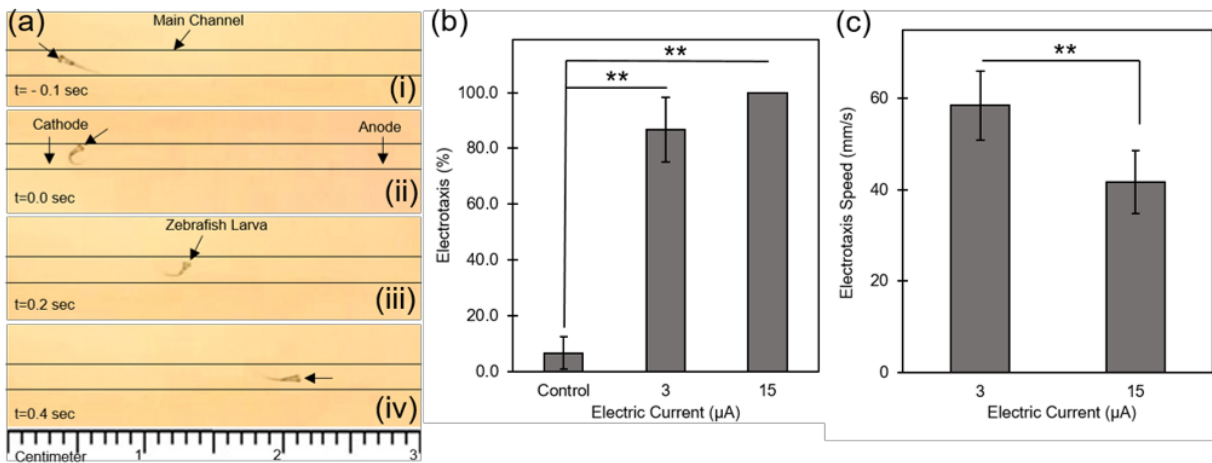


Figure 3-4. Electrotaxis of the 5-7 dpf zebrafish larvae in a microfluidic channel. (a) Electrotactic response of a 7 dpf zebrafish larva to a 3 μA electric current stimulus (i and ii) and its subsequent movement in the channel towards the anode (iii and iv) with a speed of 37.5 $\text{mm}\cdot\text{s}^{-1}$. (b) Electrotactic orientation of the 5-7 dpf zebrafish larvae ($N=30$ in three independent trials) stimulated with the electric currents of 3 μA and 15 μA . Results are compared to a control group of 30 animals, not exposed to any electric current, which shows statistically significant differences for both groups (: two-tailed t-test, $p\text{-value}<0.01$). The control group preferred staying in their original orientation, and less than 10% of the larvae demonstrated a rotation in the channel. Once the zebrafish were exposed to the electric current of 3 μA and 15 μA , more than 80% of them responded to the stimuli within 15 s by re-orientation towards the anode. Higher electric current resulted in a more robust electrotactic orientation (e.g., 100% for 15 μA) suggesting that the zebrafish larvae were sensitive to current magnitude, but there was no significant difference in the response between the two electrically-stimulated groups (two-tailed t-test: $p\text{-value}>0.05$). (c) Electrotactic speed of the 5-7 dpf zebrafish larvae ($N=15$ in three independent trials) in response to electric currents in the channel. Larvae responded to the 3 μA and 15 μA electric currents with movement speeds of $58.5\pm 19.0 \text{ mm}\cdot\text{s}^{-1}$ and $41.5\pm 13.1 \text{ mm}\cdot\text{s}^{-1}$ towards the anode, respectively. An increase in the electric current resulted in a significant (**: two-tailed t-test, $p\text{-value}<0.01$) decrease in the electrotactic speed. This observation can be attributed to a partial paralysis caused by the high electric current.**

We investigated a wide range of electric currents between 1 μA and 25 μA with 0.5 μA intervals to determine the current window within which electrotactic response could be reliably detected. This range was selected in a set of preliminary experiments because the zebrafish did not respond to electric currents under 1 μA while a severe paralysis and movement inability was observed at currents beyond 25 μA . Within the experimental current range of 1-25 μA , we were interested in minimizing the electric current magnitude to a level that electrotactic response could be evoked robustly.

Moreover, we sought to determine the maximum magnitude of electric current to which the zebrafish could respond without any significant paralysis and fatality. Our preliminary experiments revealed that the fish respond inconsistently to electric currents in the 1-2.5 μA range (data not shown). Starting from 3 μA , a robust electrotactic orientation response (>80% success rate) towards the anode was observed. After the orientation, the fish continued swimming towards the anode in the channel. We continued to increase the electric current from 3 to 15 μA and observed a similar directed response towards the anode. However, an immediate partial paralysis was observed in the fish exposed to electric currents beyond 10 μA , although most of the paralyzed fish could recover upon removing the electric stimulus. By increasing the electric current from 15 μA to 25 μA , although responding, the larvae were found completely paralyzed and sometimes dead right after the exposure due to the severe effect of electric stimulation. The majority of the fish lost their normal morphology, which was determined as a change in their eye position and a shivering effect during the exposure. The alive fish were also unable to swim for several minutes after the exposure. In a separate pilot study, no effect of the age on electrotaxis response of the

5-7 dpf zebrafish larvae was observed, which agreed with general locomotion of the larvae reported by R. Corwill et al. [45].

On the basis of the initial experiments, electric currents of 3 μA and 15 μA were selected for investigation of the electrotaxis response and speed of the 5-7 dpf zebrafish larvae. Out of a total number of 30 zebrafish tested per exposure condition, 86.7 \pm 11.5% and 100.0% responded immediately to 3 μA and 15 μA electric currents, respectively, by orienting towards the anode electrode (Fig. 3-4b). In comparison with the control group, which were loaded into the channel but not exposed to any electric current, the response to 3 μA and 15 μA signals were both statistically different (two-tailed t-test: p-value $<$ 0.01). Within the 3-15 μA window, the larvae exhibited sensitivity to the magnitude of electric current, as evident by a more robust response to the higher electric currents in Fig. 3-4b (in-between data not shown because of their similarity). However, the overall response of the fish to 15 μA was not statistically different from their response to 3 μA current (two-tailed t-test: p-value $>$ 0.05).

We also monitored and quantified the larvae's electrotactic movement speed (N=15) towards the anode in the channel right after their responses to 3 μA and 15 μA electric currents (Fig. 3-4c). The calculated electrotactic speeds for 3 μA and 15 μA currents were 58.5 \pm 19.0 mm.s $^{-1}$ and 41.5 \pm 13.1 mm.s $^{-1}$, respectively. The measured speeds were significantly different from each other (two-tailed t-test: p-value $<$ 0.01). The reduction in the electrotactic speed at higher current values can be explained as an effect of electric current on the body of the larvae and their partial paralysis during the movement towards the anode. The results above imply that although the larvae were

more responsive to the stronger electric currents, they were adversely influenced by these currents resulting in their slower moving speed in the channel.

We then investigated the reproducibility of electrotactic response in the zebrafish larvae. For this aim, we exposed N=30 fish to electric currents of 3 μ A and 15 μ A and allowed the larvae to recover from the electric stimulation for 5-10 minutes in the channel. Subsequently, we exposed the larvae to a reverse electric current of the same magnitude and observed that they displayed electrotactic behavior for the second time. This conveys that the 5-7 dpf zebrafish larvae's response to electric current is reproducible in a microchannel. We observed more than three times higher electrotaxis response of the larvae to electric currents of 10 μ A and higher.

To rule out the possible effect of electrokinetic flow in orienting the zebrafish, we exposed the dead larvae, which were morphologically intact, to the abovementioned electric currents in the channel. No movements were observed which revealed that there was no significant electrokinetic effect on the larvae during the electrotaxis experiments. Our calculations also showed that temperature elevation due to electric current is not significant in the channel. Therefore, we ruled out the possibility of any thermotaxis response. Based on the experiments above, we conclude the zebrafish larvae can sense the electric current magnitude and direction, and it is possible to speculate that they might share similar mechanisms like *C. elegans*. Our device provides a platform in which the mechanism of electrotaxis can be studied in the future.

3.3.2 Viability and Morphological State of Zebrafish Larvae after Electrotaxis in the Device

We were intrigued to find out if loading the larvae into the device and exposing them to various electric currents have any significant impact on their post-exposure health status. Morphology and survival were selected as the criteria to monitor short- and long-term effects of the aforementioned conditions on the zebrafish, respectively [95]. Four groups of larvae were tested, including a *Reference Control* group that was not exposed to the device or any electric current, a *Device Control* group that was loaded into the device but not exposed to any electric current, and two groups of larvae that were exposed to the electric currents of 3 μA and 15 μA inside the device. For survival assessment, the fish were removed from the device and their viability was monitored daily over a period of 30 days (Fig. 3-5a). For statistical comparison, we monitored 20 animals in three independent trials during the first 4-days of post-exposure [97]. It was observed that the larvae exposed to 15 μA were more likely to die (Fig. 3-5b). Their survival was significantly different from the *Reference Control* larvae (two-tailed t-test: $p\text{-value} < 0.05$). The survival rate of the *Device Control*, 3 μA exposure, and the *Reference Control* group were indistinguishable (two-tailed t-test: $p\text{-value} > 0.05$, Fig. 3-5b). For morphological assessment, the larvae were inspected for any physiological damages to their bodies each day (Fig. 3-5c).

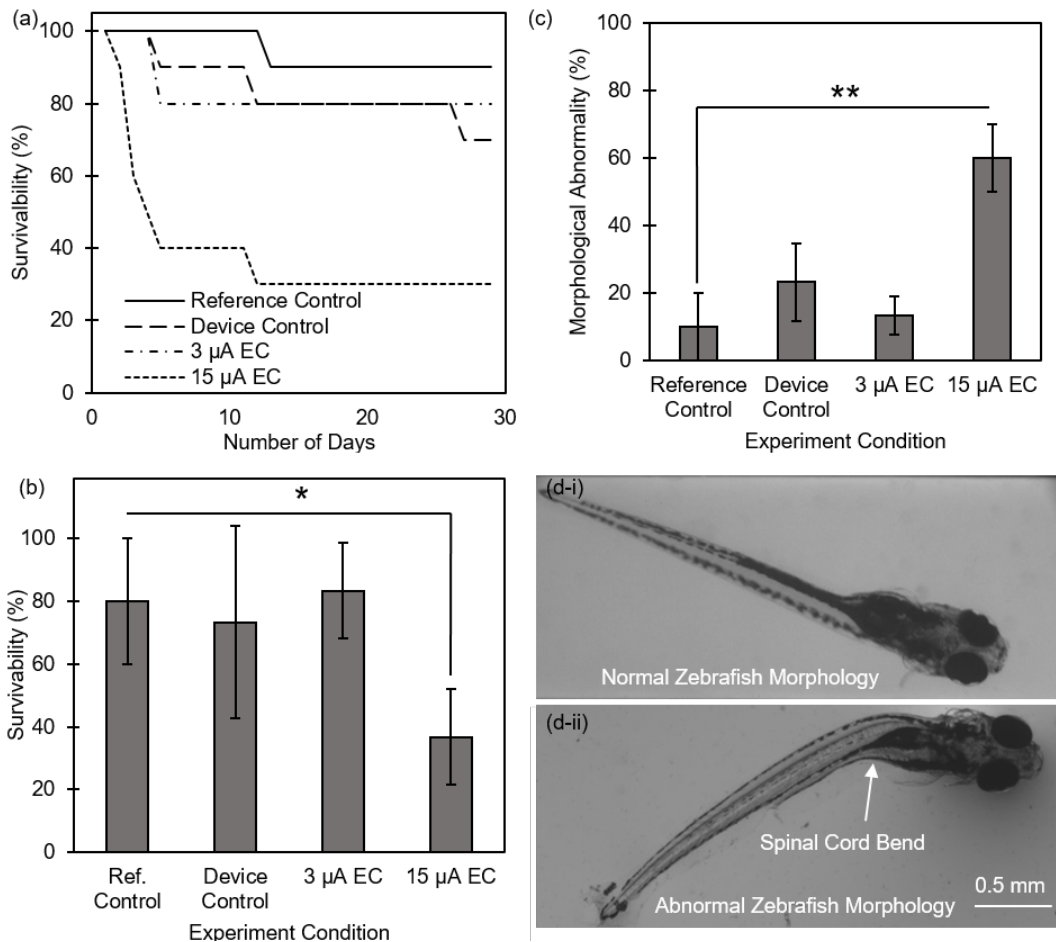


Figure 3-5. Survival and morphological abnormality of the 5-7 dpf zebrafish larvae tested in the microfluidic electrotaxis screening device, then monitored off-chip for 30 days ($N=10$ per condition). (a) Off-chip survival of zebrafish larvae, after exposure to 3 μ A and 15 μ A electric current (EC) in the device, compared to that of the fish not exposed to any EC in the device as Device Control group and the fish that were not exposed to the device or EC as Reference Control group. The Device Control zebrafish and the ones exposed to 3 μ A EC showed similar survival to the Reference Control group. The zebrafish exposed to 15 μ A EC were severely affected by the stimulus and demonstrated a significant fatality during the assay period. (b) Survival of 5-7 dpf zebrafish larvae during the first four days after the experiments ($N=20$ per condition). The larvae tested inside the device without any electrical exposure (Device Control) and the ones exposed to the 3 μ A electric current (EC) survived analogously to the Reference Control (two-tailed t-test: p -value >0.05). However, the 15 μ A EC application resulted in a larger number of fish deaths which was significantly different from the Reference Control (two-tailed t-test: p -value <0.05). This shows that the low EC of 3 μ A can be employed for further applications whereas the higher EC of 15 μ A is not viable for the larvae and brings about severe mortality. (c) Morphological abnormality of the above-mentioned zebrafish larvae during 4 weeks of observation after the experiments. The zebrafish exposed to the device and 3 μ A EC showed a small morphological abnormality effect ($<25\%$) and were mostly observed to be intact as the Reference Control fish (c-i). However, 60% of the larvae exposed to 15 μ A EC could not recover from the exposure and lost their normal morphology mostly with a spinal bending (c-ii) which was significantly different from the Reference Control (**: two-tailed t-test: p -value <0.01).

As shown in Fig. 3-5a, during the 30 days of post-experimental monitoring, the survival of *Reference Control* larvae was 90%. The zebrafish processed in the device and the ones exposed to 3 μ A electric current revealed almost similar survival during the assay, with 70% and 80% of them alive at the end of the 30-day period, respectively. The larvae exposed to 15 μ A current had a 30% survival rate after 30 days, which was different from the two control groups and the larvae exposed to 3 μ A current.

We also assessed the morphology of larvae during a 4-week period (Fig. 3-5c). Similar to the survival criterion, more than 70% of the fish passed through the device or exposed to 3 μ A current showed normal morphology when compared to the *Reference Control* group (two-tailed t-test: p-value<0.05) (Fig. 3-5d-i). In contrast, 70% of the larvae exposed to 15 μ A current experienced spinal bending abnormalities (Fig. 3-5d-ii), which was statistically different from the *Reference Control* group (two-tailed t-test: p-value<0.01).

In summary, the electrotaxis experiments, and survival and morphological abnormality assays of the 5-7 dpf zebrafish larvae let us conclude that electrical currents, ideally <10 μ A, should be used for future studies.

3.3.3 Time-of-Day Dependency of Electrotactic Behavior in Zebrafish Larvae

According to the literature, the circadian rhythms (i.e. readily day-night cycles) affect the biological and behavioral activities of the zebrafish [98]. For instance, it has been shown that the locomotion activities of the 5-7 dpf zebrafish larvae reduces significantly at nighttime [99]. Thus, we asked if the zebrafish larvae would show

behavioral changes in response to the electric current exposure at different times of the day. Electrical stimulation with 3 μ A electric current was conducted on the 5-7 dpf zebrafish larvae at night, i.e. 8-11 pm, and compared to the daytime responses at 11am-4pm and control groups of larvae not exposed to the electric current (Fig. 3-6).

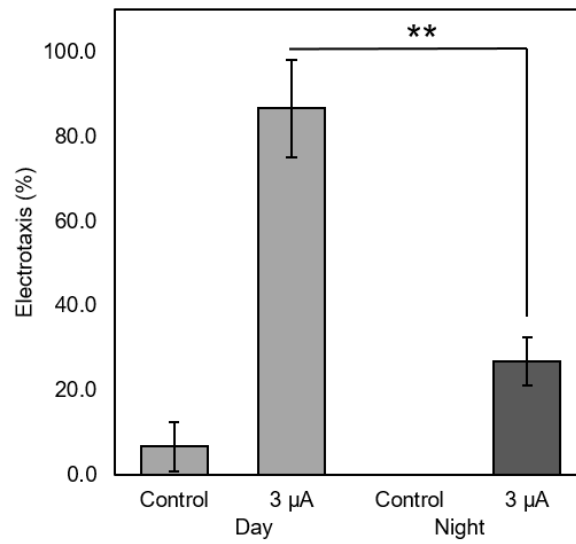


*Figure 3-6. Zebrafish larvae's electrotaxis (N=20 fish in three independent trials) stimulated by an electric current of 3 μ A during day (11am-4 pm) and night (8-11 pm) along with the control group of zebrafish not exposed to the current. The control groups showed an arbitrary movement with less than 10% reorientation or no movement at all at day and night, respectively. Exposure to electric current resulted in significant electrotaxis responses at different times, but there was a significant drop in the larvae's response at night (**: two-tailed t-test, p-value<0.01), revealing that the larvae are not amply sensitive to the electric current of 3 μ A at night.*

As shown in Fig. 3-6, the control groups showed an arbitrary movement with less than 10% reorientation or no movement at all at day and night, respectively. Zebrafish larvae's electrotaxis stimulated by 3 μ A electric current increased significantly at different times of the day. Interestingly at night, the response level was $26.8 \pm 5.8\%$, as compared to $86.7 \pm 11.5\%$ for the larvae tested during daytime. This drop-off in the night electrotactic response was significantly different from the day response level (two-tailed t-test, p-value<0.01). Our results correlated with the reduced level of general locomotion

activities observed in the zebrafish larvae at nighttime [99]. Apparently, this behavioral abnormality was provoked due to the circadian rhythm in the zebrafish larvae that could be studied quantitatively with our novel electrotaxis screening assay. We became interested in further understanding of the potential causes of such anomalous response, as discussed in the next section.

In addition, according to the literature [98], the day and night cycles for the zebrafish starts from 06:00 am and 20:00 pm, respectively. Due to the nature of the experiments which were done by a researcher inside the lab, performing experiments at 11pm to 9am was not very practical. That is why the night experiments were conducted before midnight. Moreover, performing electrotaxis assays before midnight provided statistically significant differences in day and night behaviors of the zebrafish larvae which were deemed sufficient for our research purposes. Nonetheless, we ran three independent trials (N=5 per trial) from 11:00 pm to 3:00 am as the middle of the night cycle to see how electrotaxis would be affected. As shown in Fig. 3-7, electrotaxis of the larvae at early (8:00pm-11:00pm) and late night were statistically similar (two-tailed t-test, $p\text{-value} > 0.05$) although a slight reduction in average response was observed at midnight. Furthermore, since the 8:00pm-11:00pm window was the first hours of the night cycle, we conducted three independent trials (N=5 per trial) from 6:00 am to 11:00 am as the first hours of the day cycle to see how analogous the results would be with the ones at the middle of the day. Interestingly, as shown in Fig. 3-7, the early and late day electrotaxis responses were again statistically similar (two-tailed t-test, $p\text{-value} > 0.05$).

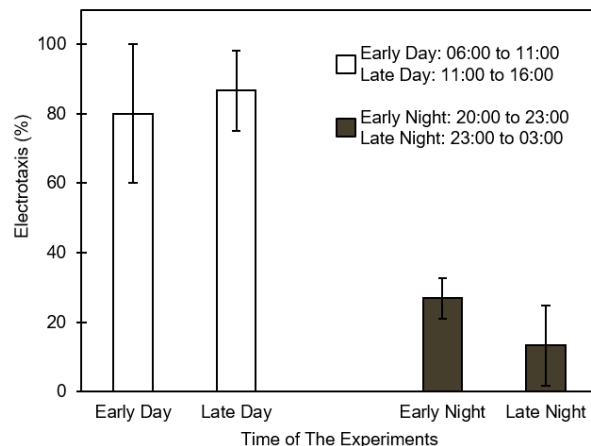
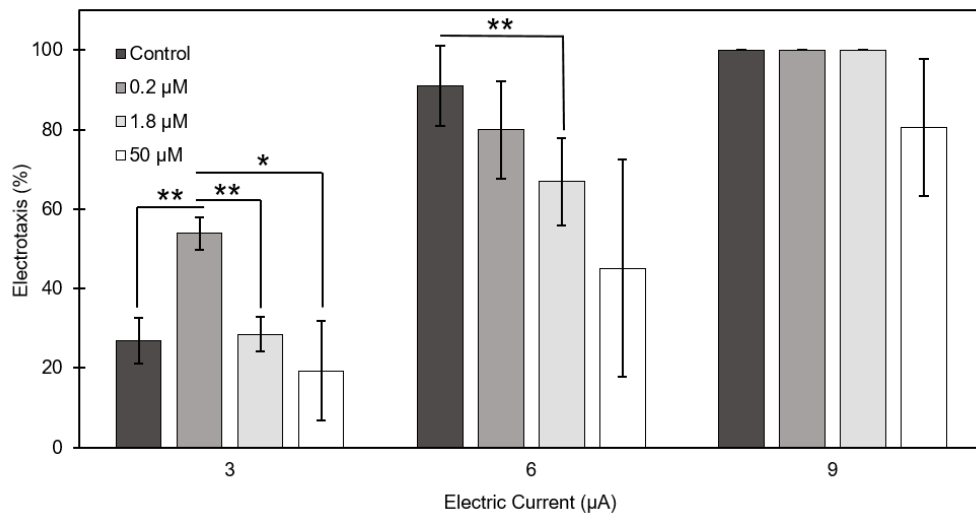


Figure 3-7. Effect of the time (i.e. early and late day and night) on electrotaxis of the zebrafish larvae ($N=15$ fish in three independent trials). Data shows that there is no difference between zebrafish electrotaxis within the early and late hours of the day or night (two-tailed t -test, p -value >0.05).

3.3.4 Microfluidic Electrotaxis as a Tool for Screening Dopaminergic Compounds

The observed attenuation of the electrotactic response at nighttime opened new lines of inquiry. Specifically, we wanted to evaluate the possibility to screen biological pathways involved in sensory-motor processes using the microfluidic electrotaxis assay. It is well understood that the motor behavior of zebrafish larva is mediated by the dopaminergic system [20]. For instance, it has been demonstrated that the activities of dopamine receptors alter in the zebrafish during the light-dark cycle [100]. It is also shown that mutation in the circadian gene *period1b* (*per1b*) [99] or exposure of the zebrafish larvae to the dopamine agonist apomorphine [20] can alter the dopamine level or receptor activities and result in significant changes in zebrafish's general locomotion behavior. For instance, exposing the zebrafish to 0.2 μM and 50 μM apomorphine in darkness resulted in a strong increase of larvae's average travel distance; and an intermediate exposure to 1.8 μM apomorphine significantly lowered that activity [20].

The above knowledge about involvement of the dopaminergic system in general locomotion and the results shown in Fig. 3-6 led us investigate whether the activities of the dopaminergic system regulate the electrotaxis behavior. Specifically, we asked if non-selective stimulation of the dopaminergic receptors could affect the electrotaxis response of zebrafish larvae at night. Accordingly, we exposed the 5-7 dpf zebrafish larvae to dopamine agonist apomorphine and investigated the electrotactic response at night in the microfluidic device. Dose dependency was tested with three different apomorphine concentrations of 0.2 μM , 1.8 μM and 50 μM , at three electric currents of 3, 6 and 9 μA , and including untreated controls (Fig. 3-7.).



*Figure 3-8. Effect of apomorphine at different concentrations on electrotaxis of 5-7 dpf zebrafish larvae at night. The larvae were treated with three apomorphine concentrations of 0.2, 1.8 and 50 μM , then tested in the microfluidic device at three electric current levels in three independent trials. Each drug concentration involved $N=30$ fish for 3 μA and 6 μA and $N=15$ fish for 9 μA electric currents. Results show that the low-dose apomorphine exposure of 0.2 μM significantly increases zebrafish's electrotaxis at nighttime (two-tailed t-test, *: $p\text{-value}<0.05$, **: $p\text{-value}<0.01$), but this effect can only be detected if a low electric current (e.g. 3 μA) is used. Increased dosage of apomorphine beyond 0.2 μM resulted in no electrotaxis difference from the control group, although statistically lower electrotaxis than 0.2 μM treatment was assessed. At the medium current, although there was a reducing trend in electrotaxis upon increase of apomorphine concentration, only the medium-dose exposure resulted in a significantly reduced response (two-tailed t-test, **: $p\text{-value}<0.01$). At the high-level current, effect of apomorphine on electrotaxis was benign because the electrotaxis response was fully saturated with the strong electric current.*

As shown in Fig. 3-8, only $26.8 \pm 5.8\%$ of the control larvae responded to a $3 \mu\text{A}$ electric current at night, while the larvae exposed to $0.2 \mu\text{M}$ apomorphine (low-dose: LD) exhibited an enhanced response of $53.9 \pm 4.2\%$. There was a significant difference (two-tailed t-test, $p\text{-value} < 0.01$) between the two groups which confirmed the positive effect of LD apomorphine on electrotaxis at night. This is consistent with the previous studies showing an enhanced level of general activities in the zebrafish larvae in a similar condition [20]. At $3 \mu\text{A}$ current level, exposing the larvae to medium-dose (MD) apomorphine resulted in an electrotaxis response of $28.5 \pm 4.3\%$ which was significantly lower than the LD response (two-tailed t-test, $p\text{-value} < 0.01$) but not the control group (two-tailed t-test, $p\text{-value} > 0.05$). This was also consistent with the results of T.D. Irons et al. [20]. At high dose (HD) apomorphine, electrotaxis response stayed at a low level of $19.3 \pm 12.6\%$ and did not increase as opposed to the high-level general activities of the zebrafish in a similar condition [20]. This may suggest that higher doses of the apomorphine fail to evoke the larvae's response to low electric current ($3 \mu\text{A}$) due to the possible saturation of the dopamine receptors after treatment [101], [102]. At the HD apomorphine, we also observed abnormal movement behaviors such as dizziness, drowsiness and confusion which might be due to any possible side effects of the higher dosage treatment.

At $6 \mu\text{A}$ and $9 \mu\text{A}$ electric currents, the electrotaxis response saturated due to the over-strength of the stimuli. This effect was also observed in the larvae that were exposed to the same-concentration apomorphine and tested at different current levels (i.e. $3\text{-}9 \mu\text{A}$). Their electrotactic response increased with the increase in electric current magnitude. At $6 \mu\text{A}$ current level, we noticed a gradual reduction in electrotaxis

response as the apomorphine concentration was increased. However, only the MD response was significantly lower than the control group (two-tailed t-test, p -value <0.05). The HD response was only marginally different from the control group with a p -value of 0.07. At 9 μ A electric current, the larvae stayed dominantly sensitive to the electrical stimulus and alteration of apomorphine dosage up to MD did not lead to any changes in electrotaxis. However, the HD apomorphine was again influential in disrupting electrotaxis, causing abnormal behavior, and plummeting the mean response rate in the larvae.

Overall, we showed that the dopaminergic system of zebrafish is most probably involved in electrotaxis, and a low electric current electrotaxis assay can be used to interrogate the effect of dopaminergic compounds on zebrafish larvae movement.

3.3.5 Electrotactic Speed, Place Preference, and Swimming Pattern of Zebrafish Larvae

It has recently been reported that apomorphine at different concentrations can influence the maximum speed and place preference of the zebrafish larvae [39]. Upon observing that exposure to 0.2 μ M apomorphine improves electrotaxis of the zebrafish at night at low current levels, we became interested to see whether the movement of the larvae in this condition is different from their untreated counterparts tested for electrotaxis during the daytime. To study this in detail, we quantified the movement speed and the absolute lateral position of the zebrafish larvae as they electrotactically moved along the main channel of the device. Two groups of larvae were tested at 3 μ A electric current, one group not exposed to any drug at daytime and one group exposed

to 0.2 μM of apomorphine at night. We observed no significant differences in the movement speed of the larvae that responded to the electric current in these two conditions (data not shown). However, assessment of the lateral positions, defined as larvae's center of masses in the channel, demonstrated differences as shown in Fig. 3-9.

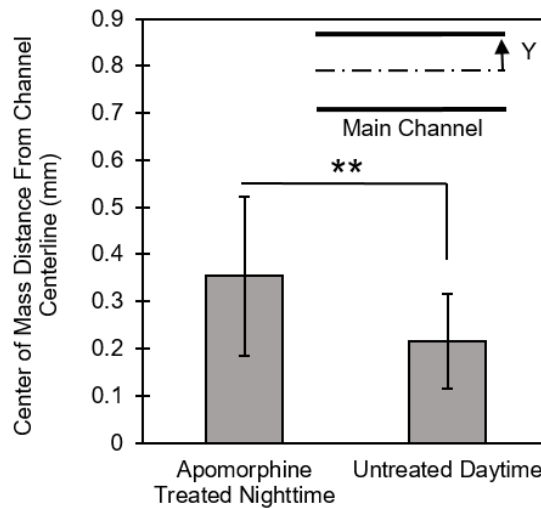


*Figure 3-9. Absolute lateral distance of larvae's center of mass from the centerline of the channel (dashed-line in the insert graph) during electrotaxis of the 5-7 dpf zebrafish larvae. Using a current of 3 μA , N=18 zebrafish were tested at daytime while N=21 larvae were exposed to a 0.2 μM dose of apomorphine and tested at night. The results were statistically different from each other (two-tailed t-test, **: p-value<0.01). This revealed that the apomorphine-treated zebrafish demonstrate preference to move closer to the channel wall by displaying stronger body strikes with more struggling swimming behavior, while the control zebrafish preferred to swim closer to the centerline of the channel with dominant forward swimming patterns.*

As shown in Fig. 3-9, the lateral distances of the two groups from the centerline of the channel were significantly different from each other (two-tailed t-test, p-value<0.01). The treated animals by apomorphine tested at night tended to stay closer to the wall of the channel while the movement of the untreated zebrafish at daytime was more smoothly at the centerline of the channel. Assessment of the movement patterns conveyed more struggling swimming for the treated larvae compared to the untreated

zebrafish that moved dominantly with forward swimming in the channel, as defined by O. Fajardo et al. [29]. The dominance of struggling swimming in the treated zebrafish resulted in more bouncing of the larvae in the channel and their overall positioning towards the wall of the device. Determining whether the body bend pattern differences were attributed to the time of the assay or the drug exposure requires further investigations in the future.

3.3.6 Role of D1- and D2-Dopamine Receptors in Zebrafish Larvae's Electrotaxis

After showing the possible involvement of the dopaminergic system in electrotaxis of the zebrafish larvae, we examined potential roles of specific dopamine receptors in regulating electrotaxis, as a first line to elucidate the underlying molecular and physiological mechanisms. Two widely-used selective dopamine agonists, SKF-38393 (for D1-like receptors) and Quinpirole (for D2-like receptors) were selected because of their prominent role in the dopamine signalling pathway. Treating the 5-7 dpf zebrafish larvae with 50 μ M of SKF-38393 and 16.7 μ M of Quinpirole have been shown to significantly affect the zebrafish movement activity at night [20]. Therefore, the larvae were tested at 3 μ A electric current after exposing them to the drugs above at night (see section 2.2 for exposure times). As shown in Fig. 3-9, for N=15 samples per condition, the electrotaxis responses were $13.3\pm 11.5\%$, $13.3\pm 11.5\%$, and $53.3\pm 11.5\%$ for control (not exposed), SKF-38393, and Quinpirole treatments, respectively. SKF-38393 appeared to be ineffective on electrotaxis (two-tailed t-test, p-value>0.05), while quinpirole significantly affected larvae's electrotaxis compared to the control group (two-tailed t-test, p-value<0.05). This finding suggests a significant involvement of the D2-

dopamine receptors in modulating zebrafish larvae's electrotaxis. Further investigations are required to prove the exact roles of dopamine receptors in electrotaxis. We propose that the microfluidic device introduced in this chapter will be instrumental to explore the molecular and physiological basis of electrotaxis, as well as the role of the dopaminergic pathway, including exploring a wider range of selective agonist drugs and concentrations, or using genetic approaches targeting the dopamine signalling pathway.

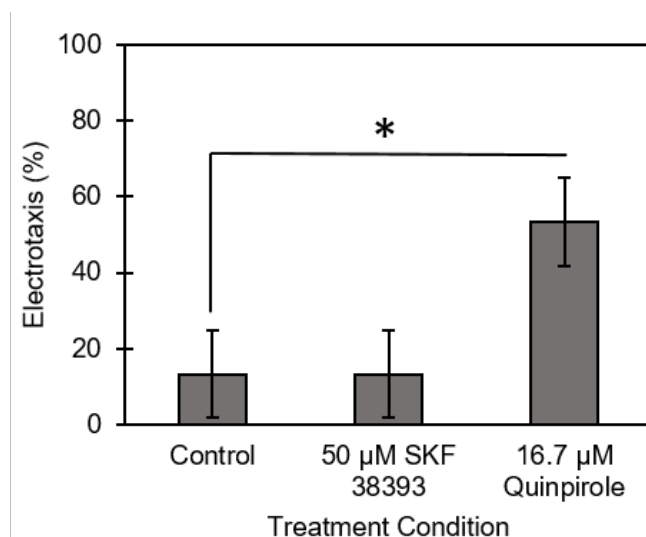


Figure 3-10. Electrotaxis of the zebrafish larvae treated with 50 μ M of SKF-38393 (D1-like receptors) and 16.7 μ M of Quinpirole (D2-like receptors) at night (N=15 in three independent trials for each condition). The results show no statistical difference between control and SKF-38393 treated larvae's electrotaxis (two-tailed t-test, p -value >0.05), while Quinpirole proves to significantly increase electrotaxis (two-tailed t-test, *: p -value <0.05).

3.4 CONCLUSION

In this chapter, we presented zebrafish larvae's behavioral response to the electric current (i.e. electrotaxis) in a channel for the first time, and demonstrated the application of our technique in screening the role of dopamine receptors in electrotaxis. The device and presented technique are simple to use for on-demand stimulation of movement and screening the effect of chemicals on the zebrafish larva as a model. The

tested zebrafish in our daytime assays responded robustly to a minimum electric current threshold of 3 μA by swimming towards the anode electrode. The response increased with the magnitude of the electric current up to 15 μA . However, the larvae exhibited slower electrotactic swimming speed, mortality and morphological abnormality at 15 μA . At currents in a range of 15-25 μA , we observed severe paralysis in the channel and elevated mortality after the assays.

Similar experiments with 3 μA electric current at nighttime revealed a significant drop in the electrotactic response. We benefited from the device and showed a possible link between zebrafish's electrotaxis and the dopamine receptors activities. Treating the larvae with a non-selective dopamine agonist, apomorphine, resulted in alteration of electrotactic response at night, proving the considerable involvement of the dopamine receptors in regulating this behavior. The effect of apomorphine on electrotaxis was more apparent at low-level electric currents. For instance, at 3 μA , low-dose apomorphine exposure significantly increased the response due to the enhancement of dopamine receptors activities; while higher doses failed to boost the behavior in the larvae potentially due to oversaturation effects [101], [102]. Moreover, higher electric currents (6 and 9 μA) resulted in more robust electrotaxis responses at night, with and without treatment of the larvae by different apomorphine dosages. This demonstrated the dominant role of electric current magnitude in zebrafish's electrotaxis and the importance of controlling this variable to achieve sensitive assays. Interestingly, for the apomorphine-exposed zebrafish that demonstrated enhanced electrotaxis at night, their movement pattern within the channel was dominated by struggling swimming and a center of mass trajectory that was closer to the wall of the channel; whereas the larvae

tested during the day with no drug exposure exhibited more forward swimming while moving closer to the centerline of the channel. Furthermore, performing assays with selective dopamine agonists SKF-38393 and Quinpirole revealed a dominant involvement of D2-dopamine receptors in electrotaxis.

All in all, our device provides an accurate, sensitive and versatile platform to evoke zebrafish's electrotactic movement behavior on-demand and investigate the effect of various drugs on it quantitatively. In addition, the biological basis of electrotaxis, which can be studied with this device, may lead to a better understanding of the pathways involved in sensory-motor processes of the zebrafish larvae.

Chapter 4

A Microfluidic Device to Study Subtle Phenotypes of Zebrafish Larvae Electrotaxis Using Wild-Type and Knockout Models*

4.1 INTRODUCTION

We demonstrated zebrafish electrotaxis inside a microfluidic device in the previous chapter. The larva was trapped in the main channel of our device in a semi-confined manner, i.e. it was only allowed to move and orient in the longitudinal direction. Once exposed to the electric signal, the zebrafish showed a preference to orient and swim towards the anode pole. However, due to their free movement alongside the channel axis, we were not able to quantify electrotaxis in further details including the tail-beat frequency (TBF) and response duration. Moreover, in our first device, we could not distinguish any subtle behavioral motions such as C- and J-bend patterns, which are believed to be majorly involved in well-established behaviors including the escape and prey-capturing. Being able to characterize and quantify the movement behaviors phenotypically will provide a better sensitivity and accuracy in biological assays involving the zebrafish larvae.

* This chapter is under preparation as a manuscript for submission to a Journal: A.R. Peimani, N. Safarian, G. Zoidl, and P. Rezai, "A Microfluidic Device to Study Subtle Phenotypes of Zebrafish Larvae Electrotaxis and Its Application in Gene Knockout Screening", *under preparation*.

To achieve phenotypic screening of the electrotactic movement, we propose a novel microfluidic device for on-demand electrical stimulation and electrotaxis assessment of individual 5-7 dpf semi-immobilized zebrafish larvae. This device can immobilize the larva's head up to the yolk region inside a funnel-like channel, while the tail is free to move in a downstream chamber. With this approach in animal handling, the TBF, response duration, and several subtle motor patterns of the larvae in response to various electric currents can be monitored and quantified.

In the previous chapter, we showed the application of our first microfluidic device in exploring the involvement of the dopaminergic system in regulating zebrafish electrotaxis. While we think the presented device in this chapter can also be used for dopaminergic system studies and drug screening [103], we sought to demonstrate the usage of our technique in studying the electrotaxis of knockout zebrafish using the semi-immobilized larval assay. For this purpose, we compared electrotaxis of the wild type (WT) zebrafish larvae with that of the Pannexin1 (Panx1) knockout (KO) larvae (i.e. a particular gene mutant) inside our device.

Panx1 protein membrane transcript is widely expressed in the brain [104], [105]. The cardinal role of Panx1 has previously been shown in the adult mice's physiological responses [106], nociception [107] and plasticity, i.e. sensing and responding to any kind of stimuli from the environment [108]. Furthermore, it was shown that once exposed to the electrical signal, the adenosine release of Panx1 depends on the electrical stimulus [104]. Thus, we asked whether Panx1 is involved in zebrafish's electrotaxis.

4.2 EXPERIMENTAL SECTION

4.2.1 Design and Fabrication of the Microfluidic Device

The microfluidic device (Fig. 4-1) used in this study was made of three separate PDMS layers which were plasma-bonded together (more details in Chapter 2). The top layer (main layer) consisted of a 45°-angled inlet tube, a loading channel, two side U-shaped channels, a funnel-like trapping region (TR), a screening pool, and an ejecting tube. The middle layer was a ~250 μm thin membrane sandwiched between the top and bottom layers. The bottom layer (valve layer) consisted of a L-shaped channel, called the valve actuation channel, which was designed exactly underneath the TR with a 1.5 mm horizontal margin from the screening pool.

The 45°-angled inlet tube was designed to help a smooth larva transition to the device. The loading channel of 0.9 mm width and 25.2 mm length was used for loading the larva from inlet to the TR. Two side U-shaped channels of 0.5 mm width with 20 mm offset from the loading channel centerline were connected to the inlet and ejecting tubes. These channels were implemented (i) to place the electrodes at their anterior ends for electric current application to the device; (ii) to maintain the electrical resistance of the device at ~35 MΩ, which is comparable to our previous device in Chapter 3 [109]; (iii) to provide a side flow to safely transfer the larva from the inlet to the loading channel by not allowing it to collide with the base and channel walls; and (iv) to save space for a cost- and size-effective design. The TR design mimicked the zebrafish's head from mouth to yolk region for an optimal immobilization and connected the loading channel to the screening pool with a gradual-narrowing width from 0.9 mm

to 0.25 mm. The screening pool of 6.5 mm width and 8.65 mm length was added for monitoring the tail oscillations and strikes, such as C-bends, when the larva was exposed to an electric current in the TR. As shown in Fig. 4-1, larva's tail tip-point was tracked automatically and two lower and upper thresholds, which were 0.25 mm away from the channel centerline, were defined to quantify the larva's motor behaviors (discussed later). After several design iterations, we added a crescent-shaped pillar inside the screening pool to preclude the middle PDMS membrane from collapsing. The pillar also prevented bubbles from getting trapped and aggregated at the pool corners. Otherwise, water flow could not reach the corners, leaving large bubbles in the pool which were disruptive to our experiments. The ejecting tube and channel of 0.9 mm width and 17.9 mm length were used to remove the larva after each experiment. The depth of all channels was 0.55 mm.

The main and valve layers were prepared as discussed in Chapter 2. The PDMS membrane was made by spreading 10:1 ratio PDMS pre-polymer on a transparent sheet and letting it completely cure overnight. To fabricate the device shown in Fig. 4-1, the valve (bottom) layer was bonded to the membrane at first (detailed procedure provided in Chapter 2). Then, the resulted layer was bonded to the main (top) layer in a way that the membrane was sandwiched between the other two layers. Due to reproducibility of this process, it was not needed to fabricate several devices to check for technical errors in our experiments. However, the errors associated with the operator and the experimental setup remain inevitable as in any assay.

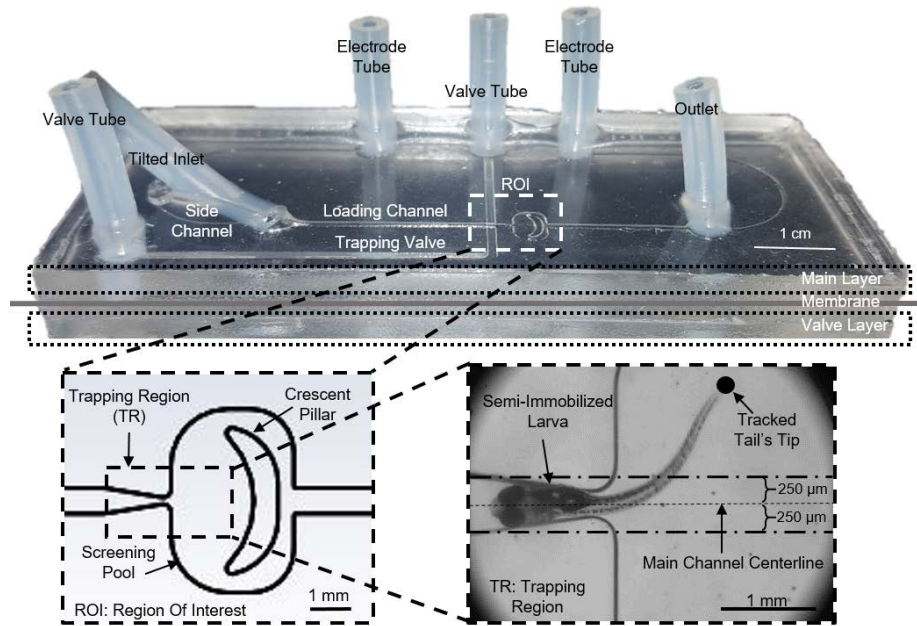


Figure 4-1. A microfluidic device for electrotaxis screening of the semi-immobilized zebrafish larva. The device (top image) consisted of three layers. Main (top) layer consisted of a tilted-inlet, side channel, loading channel, trapping region (TR), screening pool, outlet, and two electrode spots. The valve (bottom) layer consisted of a trapping valve channel and two tubes at the ends. The PDMS membrane (middle) layer was sandwiched between the other two layers. The region of interest (ROI) is magnified (bottom left) to show more details about the TR, pool, and crescent-like pillar, which aided fabricating and de-bubbling the device. The TR is also magnified (bottom right) to display how the larva is partially immobilized. Inside the TR, the tail tip-point is shown by a black circle which was tracked by a software. The main channel centerline and two lower and upper thresholds are also drawn manually which helped with calculating the TBF.

4.2.2 Experimental Setup

The experimental setup (Fig. 4-2) for electrotaxis assays on the 5-7 dpf semi-immobilized zebrafish larvae consisted of the microfluidic device, which was placed under an inverted microscope (BIM-500FLD, Bioimager Inc., Canada) equipped with a camera (GS3-U3-23S6M-C, Point Grey Research Inc., Canada) for behavioral recording. A sourcemeter (Model 2410 Sourcemeter, Keithley, OH, USA) was used to apply a Direct Current (DC) electric signal to the device. Two wire electrodes were connected from the sourcemeter outlets to the device electrode tubes. Two syringe

pumps (LEGATO 111 and 110, KD Scientific Inc., Holliston, MA, USA) were used for loading and positioning the zebrafish larva individually inside the device.

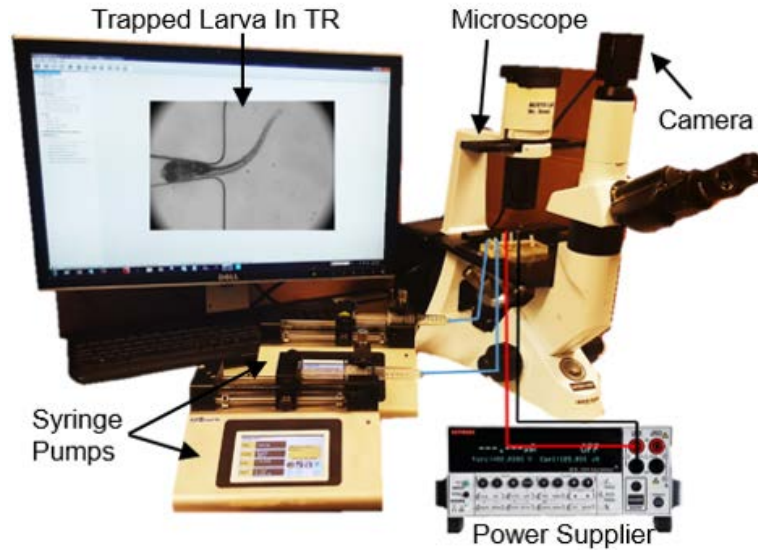


Figure 4-2. The experimental setup consisted of the microfluidic device, microscope, camera, two syringe pumps, sourcemeter, and computer to collect videos. The screen is showing a 7 dpf zebrafish larva trapped inside the TR.

4.2.3 Experimental Procedure

To conduct an experiment, a single 5-7 dpf zebrafish larva was pipetted into the device inlet. Flow rates of 2, 0.2, and 1 ml.min⁻¹ in the tilted inlet, side, and main channels were used to load the larva smoothly into the TR. The side channel assisted the loading by providing a side flow around the larva's body so that it will not collide with the channel base and walls. For every experiment, we assured that the larva is loaded with the appropriate orientation before reaching the main channel. We took advantage of the zebrafish rheotaxis behaviour [31], [110], i.e. turning and swimming against the water stream, to load the larva with its tail facing the screening pool. More details about zebrafish rheotaxis is provided in Appendix A of this thesis.

Once the zebrafish larva was positioned in the TR, the valve actuation channel was pressurized with air to stabilize the larva inside the TR (Fig. 4-1). By running air through the valve actuation channel, the PDMS membrane was inflated at an overlapping site of the valve and main channels, creating a physical barrier in front of the fish's head. Then, the larva was given 60 seconds to recover from any loading and handling burdens and to acclimate to the new environment. During this time, the larva started to randomly move its tail with no specific pattern, only trying to familiarize itself with the new situation.

The wire electrodes at the anterior ends of the U-shaped channels were then placed to apply an electric current to the device. A DC electric current in a range of 0.1-9 μA was applied for 15-20 seconds across the channel alongside the fish body axis with anode pole at its tail side (as explained in Chapter 3, section 3.2.2). The electrotaxis behavior of the semi-immobilized larva was video-recorded at a speed of 160 frames per second (fps) using the camera mounted on the microscope. Behavioral recording lasted until the larva stopped moving its tail or for a maximum duration of approximately 15-20 seconds post-stimulation.

After each experiment, the larva was removed through the outlet and the device was prepared for the next experiment with a new larva. The extracted larvae were sacrificed following the ACC Protocol GZ 2014-2019 (R3) and York University's Biosafety Permit PR 02-19. It should be noted that we had to completely wash, dry and re-wet the device once in approximately every 5-10 experiments to discard any disruptive bubbles trapped in the screening pool and channels.

Also, we assessed the survival rate of the zebrafish larvae in two groups. The control group of larvae were not passed through the device while the test group were loaded inside and ejected from the device. Both groups were monitored over a period of one month. We observed that the device did not have a fatal effect on the zebrafish survival in this period (data not shown).

4.2.4 Video and Image Analysis

The obtained videos of larvae's electrotaxis movement in the TR were semi-automatically analyzed offline using the Kinovea software (non-profit organization, France, www.kinovea.org), which is an open-source software for movement analysis of various objects. A frame-by-frame approach was taken in order to fully track the larva's tail tip-point inside the screening pool of the microfluidic device. Since we failed to capture a high-resolution image in some of the recorded frames in which the tail was moving fast and blurred, a semi-automatic method was applied. We let the software track the tail tip-point in most of the frames, but we had to selectively pick some of the frames to manually correct the tracking point position. For the blurred images, the closest point to the tip was manually selected. The raw tail movement data, which included valuable information such as the time duration of the response and the tail tip position in the pool, were collected in the .xml format. Calculations of the TBF, response duration, and motor patterns were performed using the Microsoft Excel (Microsoft Corp., WA, USA) as described in the next section.

4.2.5 Behavioral Phenotyping and Motor Pattern Characterization

Electrotaxis was characterized in terms of TBF, response duration, and various motor patterns (Fig. 1-3) of the semi-immobilized zebrafish larvae in our device. The response duration was measured from the beginning of tail motion until the larva ceased moving. Since no response latency was observed, the tail motion onset was defined as the time at which the electric current was applied. The TBF was defined based on a recently published article [41] where any tail flicks were excluded. We set a 0.25 mm threshold line, which was derived from our preliminary experimental observations, on both sides of the channel centerline as shown in Fig. 4-1. Every time that the tail tip passed over the threshold lines, we counted the movement as a half-strike cycle. Then, the TBF was calculated as the number of full cycles (two half-strike cycles) divided by the corresponding response duration. In order to rule out any possible errors in counting the cycles during TBF calculation, we randomly selected 10 videos and counted all of the considerable strikes visually. Our visual assessment showed the same TBF as our semi-automatic method above.

Inspection of the recorded videos of zebrafish electrotaxis resulted in identification of well-established subtle motor patterns [29], [39], [41], [111], [112]. We categorized the patterns into struggling or st, J-bend or J, no movement or nm, C-bend or C, routine swimming or rs, and flick or fl patterns. Detailed descriptions of each motor pattern were previously provided in Chapter 1 and shown in Fig. 1-3b. The fractional duration of each motor pattern was calculated based on the ratio of the time that a specific motor program lasted over the entire response duration and reported in a percentile format.

4.3 RESULTS AND DISCUSSIONS

4.3.1 Electrotaxis of Semi-Immobilized Zebrafish Larvae

We showed the electrotaxis movement of a semi-confined zebrafish larva towards the anode electrode in a channel in Chapter 3. However, we needed to partially immobilize the larva with its head fixed and tail freed to move so that any subtle electrotactic responses could be captured for more sensitive phenotypic assays. Here, the larva was loaded into the device as shown in Fig. 4-1, partially immobilized in the TR, and given 60 seconds to adopt to the new situation. Then, the larva was exposed to a range of 0.1-9 μA electric currents and its electrotactic response was video-recorded and analyzed for quantification of the TBF, response duration, and various motor patterns.

We were interested to assess how a semi-immobilized zebrafish larva exhibits electrotaxis which was defined as any reflexive tail oscillation due to application of the electric current. Once exposed to various electric currents, we observed that the 5-7 dpf WT zebrafish larvae began to respond by oscillating their tails in different patterns, revealing several motor phenotypes such as C- and J-bend, struggling, and routine swimming patterns. For instance, Fig. 4-3a shows the sequential images of a 7 dpf WT zebrafish larva revealing C-bend, struggling swimming, and no movement patterns when exposed to a 1 μA electric current. To characterize each motor pattern, we tracked the zebrafish tail tip-point and plotted its position versus time as shown in Fig. 4-3b. The TBF and response duration were determined using the data above with more details provided in section 4.2.5.

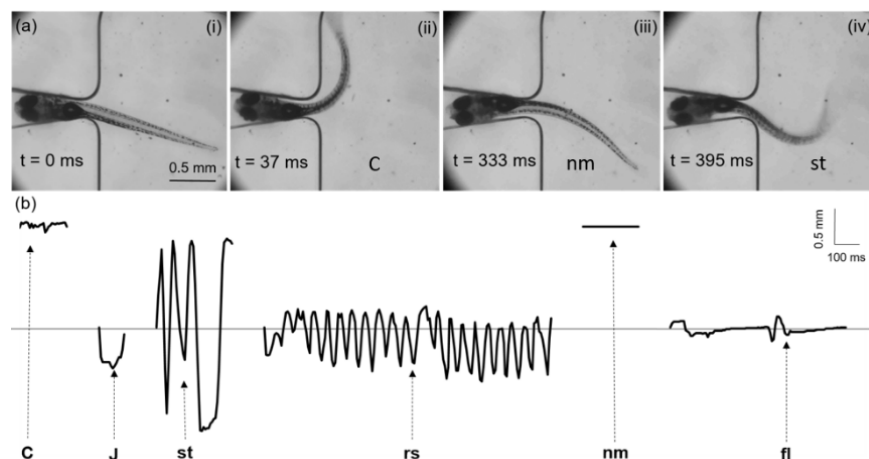


Figure 4-3. Electrotaxis of the semi-immobilized zebrafish larvae. (a) Microscope-based sequential images of a 7 dpf zebrafish larva exhibiting electrotaxis inside the microfluidic device. Once exposed to a $1 \mu\text{A}$ electric current (i), the zebrafish larva displayed different motor patterns such as C-bend (ii), no movement (iii), and struggling swimming (iv). (b) Different motor patterns were graphically recognized and characterized using the plot of tail tip position versus time during electrotaxis. The TBF and response duration were also determined using the data of this plot.

Furthermore, we conducted several preliminary trials with application of $0.1\text{-}1 \mu\text{A}$ electric currents (with $0.1 \mu\text{A}$ increments) on 15 larvae in total to find the minimum electrical threshold to which the larva can successfully respond. It was determined that the WT larva can robustly (i.e. $>80\%$ success rate) sense and respond to the electric currents as low as $0.5 \mu\text{A}$. By increasing the electric current to $1 \mu\text{A}$, the WT larvae showed electrotaxis similar to their response at the lower current of $0.5 \mu\text{A}$.

To show the application of our electrotaxis screening device in studying knockout models, we tested electrotaxis of the Panx1 KO larvae and compared it with the WT electrotaxis results. We observed that the KO larvae started to sense and respond robustly to electric current at $1 \mu\text{A}$, unlike the WT larvae that initiated a strong response at $0.5 \mu\text{A}$. This result might suggest an electrotactic threshold shift in the zebrafish larvae's response, hypothetically caused by the ablation of Panx1. It means that the KO larvae might fail to sense and perceive some environmental cues such as a weak

electrical signal. It should be noted that the WT and KO larvae displayed a robust electrotaxis under application of electric currents higher than 1 μA which were used in the following sections.

4.3.2 Electrotactic Tail-Beat Frequency (TBF) of Zebrafish Larvae

We assessed the overall electrotaxis response rate of the semi-immobilized zebrafish larvae at low electric currents in the previous section. Since the response rate saturated at a low current magnitude, this parameter could not be used for further investigation of electrotaxis at various current levels higher than the thresholds. Taking advantage of our device that enables phenotypic investigation, we carried out a more in-depth assay in which other electrotactic phenotypes were examined. We measured the TBF of the 5-7 dpf WT zebrafish larvae under exposure to various electric currents of 1, 3, 6, and 9 μA (Fig. 4-4). The lower threshold of 0.5 μA for the WT larvae was excluded since the TBF was statistically similar at 0.5 and 1 μA (data not shown). The electric currents of 3, 6, and 9 μA were selected based on our primary experimental observations where the larvae started to display distinct behaviors such as variations in the TBF, response duration, or motor patterns (discussed later). Also, the upper threshold of 9 μA was previously examined by us and proven not to have an immediate or long-term fatal effect on the larvae.

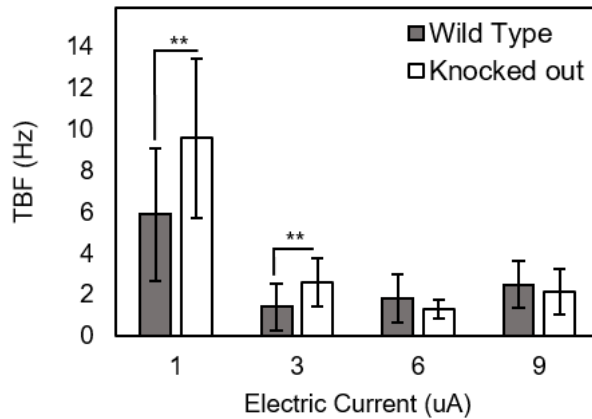


Figure 4-4. Electrotactic TBF of the WT and KO zebrafish larvae ($N = 20$ and 15 , respectively, per current in three independent trials) at different electric currents. The highest TBF was observed at the lowest electric current for both larvae types. Also, at the low currents of 1 and $3 \mu\text{A}$, the TBF of the WT larvae was statistically lower than the KO larvae ($p\text{-value} < 0.01$).

As shown in Fig. 4-4, the highest electrotactic TBF of the WT larvae was 5.9 ± 3.2 Hz at $1 \mu\text{A}$, which was significantly different from all other tested currents of 3 , 6 , and $9 \mu\text{A}$ ($p\text{-value} < 0.001$ for “ 3 and $6 \mu\text{A}$ ”, $p\text{-value} < 0.01$ for $9 \mu\text{A}$). By increasing the electric current to 3 , 6 , and $9 \mu\text{A}$, the TBF dropped significantly as compared to $1 \mu\text{A}$. However, the TBF at 3 , 6 , and $9 \mu\text{A}$ did not follow any specific behavioral trend in response to a varying current amplitude.

The results above may suggest that the zebrafish larvae are more sensitive to a very low electric current by revealing a higher TBF. The results might also reveal the potential effect of partial paralysis at the higher electric currents [56]. It has been shown that a weaker electrical signal leads to a lower nociception (i.e. responses to a harmful stimulus) in organisms such as rats [113]. Thus, likewise in the zebrafish as a novel model in nociception [114], one can hypothesize that a low electric current may cause a decreased nociception (i.e. a higher TBF), since the zebrafish nociceptive-like behaviors including the tail-beating movement alter under the stress-induced stimuli [113].

As an application of our device in studying knockout zebrafish models, we explored the electrotactic TBF of the KO zebrafish larvae as well. The highest TBF of the KO larvae was 9.6 ± 3.9 Hz at $1 \mu\text{A}$ (Fig. 4-4) and significantly distinct from the rest of the responses at higher currents ($p\text{-value} < 0.001$). This result for the KO zebrafish is following the similar behavioral trend of the WT larvae in response to electrical signal. Interestingly, it was observed that at low currents of 1 and $3 \mu\text{A}$, the KO larvae tended to respond with a higher TBF as compared to the WT larvae ($p\text{-value} < 0.01$ for both currents). In reference to studies on the involvement of pannexin hemichannels in mice's nociception [107] and the effect of Panx1 blocking on the rat's nociceptive behaviors [115], we hypothesized that Panx1 ablation might have caused a lower nociception (i.e. a higher electrotactic TBF) in the zebrafish at 1 and $3 \mu\text{A}$. However, further investigation needs to be implemented to examine this hypothesis. Our results in this section show the capability of our device in detecting the effect of gene mutations (such as the Panx1 knockout) on electrotaxis.

4.3.3 Electrotactic Response Duration of KO and WT Zebrafish Larvae

After assessing the zebrafish electrotactic TBF, we became interested in other screening capabilities of our device. Thus, we evaluated the electrotaxis response duration of the zebrafish larvae under exposure to different electric currents. Similar to the TBF, the response duration at 0.5 and $1 \mu\text{A}$ were not statistically different for the WT larvae (data not shown). Thus, we continued our experiments with the application of 1, 3, 6, and $9 \mu\text{A}$ electric currents, as shown in Fig. 4-5.

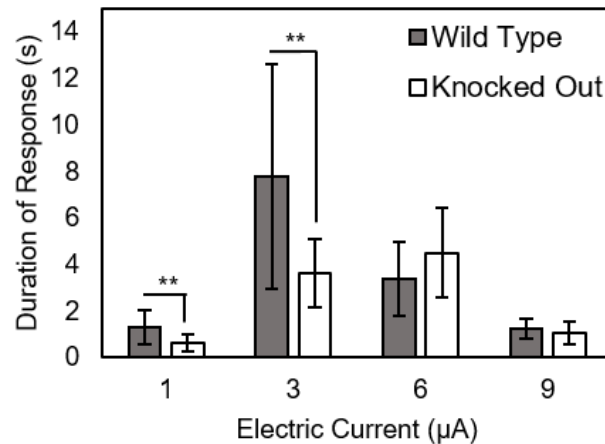


Figure 4-5. Electrotaxis response duration of the WT and KO zebrafish larvae ($N = 20$ and 15 , respectively, per current in three independent trials) at different electric currents. Shortest electrotaxis took place at the lowest and highest electric currents. At the low currents of 1 and $3 \mu\text{A}$, the *Panx1* loss seemed to have a regulating influence on larvae electrotaxis by statistically demonstrating a lower response duration in the KO larvae than the WT ones ($p\text{-value} < 0.01$).

As shown in Fig. 4-5, the response duration of the WT larvae was 7.8 ± 4.8 s at $3 \mu\text{A}$ which was the longest compared to the rest of the currents ($p\text{-value} < 0.001$ for “ 1 and $9 \mu\text{A}$ ”, $p\text{-value} < 0.01$ for $6 \mu\text{A}$) and 3.4 ± 1.6 s at $6 \mu\text{A}$ which was statistically longer than 1 and $9 \mu\text{A}$ ($p\text{-value} < 0.001$ for both). This implies that zebrafish electrotaxis lasted longer at 3 and $6 \mu\text{A}$, proposing an inverted U-shaped electrical-amplitude dependency of the response duration. This result shows that a weak electrical signal at $1 \mu\text{A}$ leads to an earlier end in response as compared to the intermediate currents of 3 and $6 \mu\text{A}$. Also, it contends that a stronger partial paralysis and elevated nociception in the larvae at the high current of $9 \mu\text{A}$ results in a significant reduction in electrotaxis response duration.

The response duration of the KO larvae was also assessed and compared with the WT larvae in our device. The response duration of the KO larvae at 1 and $9 \mu\text{A}$ were 0.6 ± 0.4 and 1.1 ± 0.5 s, respectively, which were statistically shorter than those at 3 and $6 \mu\text{A}$ ($p\text{-value} < 0.001$ for “ $3 \mu\text{A}$ vs 1 and $9 \mu\text{A}$ ” and “ $6 \mu\text{A}$ vs 1 and $9 \mu\text{A}$ ”). Again, the electrotaxis response duration of the KO larvae followed a similar behavioral trend as

observed for the WT larvae. That is, electrotaxis lasted longer at the medium currents of 3 and 6 μA , and shorter at the low and high currents of 1 and 9 μA . Moreover, at 1 and 3 μA , the KO larvae tended to display a shorter electrotaxis than the WT ones (p -value <0.01), while no statistical differences were measured at the higher currents of 6 and 9 μA (p -value >0.05). From this finding, we again concluded that the Panx1 ablation might have a strong influence on zebrafish electrotaxis that could be detected with our device.

4.3.4 Electrotactic Motor Patterns of Semi-Immobilized Zebrafish Larvae

After assessing the electrotactic TBF and response duration of the zebrafish larvae, we were intrigued to investigate the capability of our device in characterization of subtle electrotactic motor patterns. Since some motor patterns such as J- and C-bend are involved in specific zebrafish behaviors like the prey-capturing and escape, respectively, we also wondered if any of these behaviors could be triggered selectively and studied by the application of specific electrical signals in our device. Thus, we categorized the zebrafish electrotactic movements in our device into several well-established motor patterns as explained in sections 1.1 and 4.2.5. Fig. 4-6 quantitatively shows the percentile time duration of these electrotactic motor patterns for the WT and KO zebrafish under exposure to various electric currents.

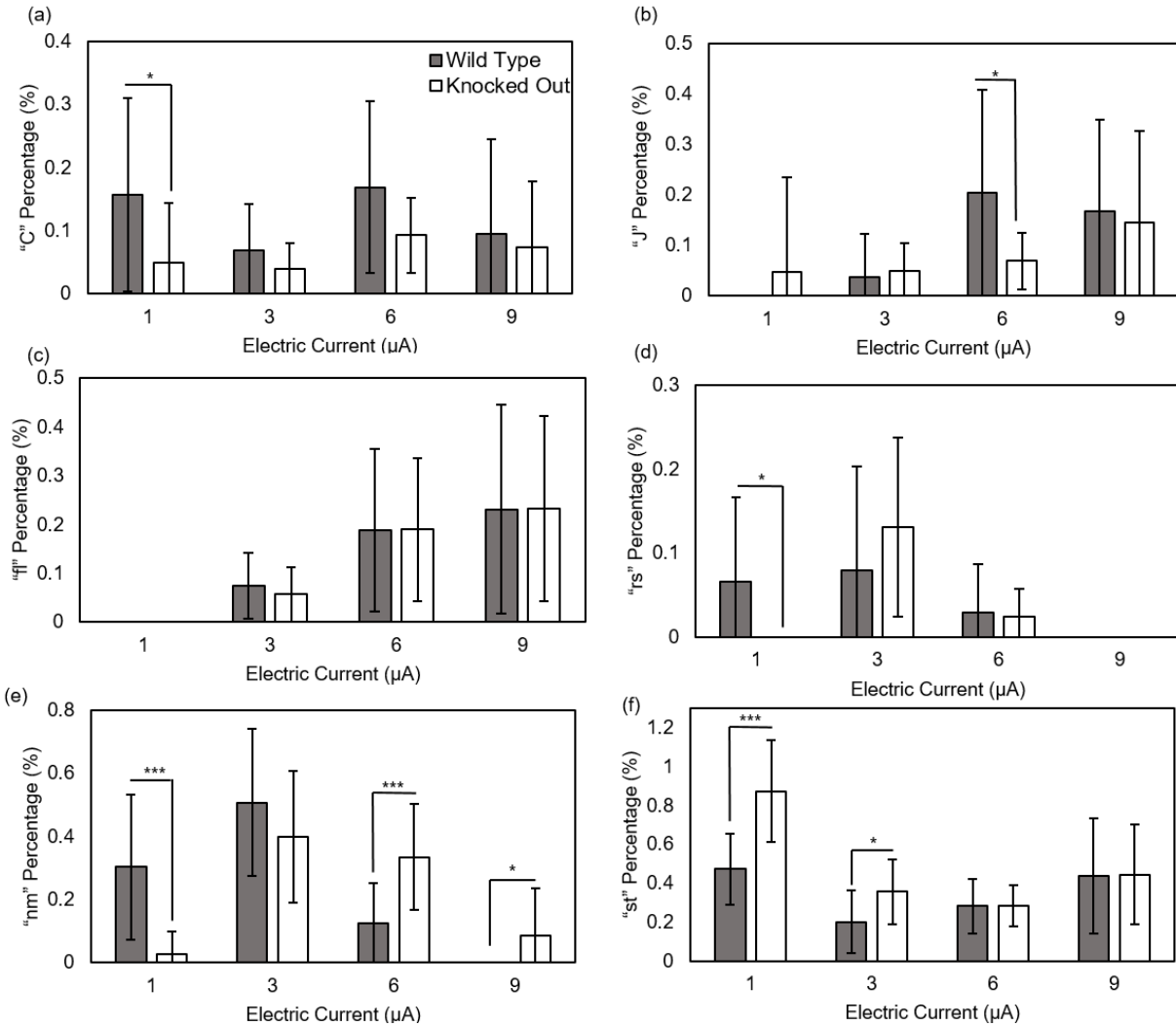


Figure 4-6. Quantitative analysis of the fractional duration of various electrotactic motor patterns of the WT and KO zebrafish larvae ($N = 20$ and 15 , respectively, per current in three independent trials). C-bend or C (a), J-bend or J (b), flick or fl (c), routine swimming or rs (d), no movement or nm (e), and struggling or st (f) are among the observed electrotactic motor patterns of the larvae.

As shown in Fig. 4-6a, no difference in C-bend pattern for the WT zebrafish larvae was measured at different currents ($p\text{-value} > 0.05$). This probably suggests that C-bend pattern is not regulated by the electrical signal. We observed no and low percentage of J-bend pattern (Fig. 4-6b) at the low currents of 1 and 3 μA , respectively. While at higher currents of 6 and 9 μA , the larvae tended to show statistically higher J-bends as compared to 1 and 3 μA currents ($p\text{-value} < 0.05$ for “3 μA vs 9 μA ”, p -

value <0.01 for "1 μA vs 6 μA and 9 μA " and "3 μA vs 6 μA "). The same behavioral trend was observed for the flick pattern (Fig. 4-6c). We measured zero and low percentage of flick patterns at 1 and 3 μA , respectively, and a higher percentage at 6 and 9 μA (p-value <0.001 for "1 μA vs 6 and 9 μA ", p-value <0.05 for "3 μA vs 6 and 9 μA ").

Our experiments showed that some motor patterns are modulated by the electrical signal which might be overridden by some other patterns at different current levels. For example, to compensate for the decreased J-bend and flick patterns at the low currents (1 and 3 μA), the larvae tended to display no movement, routine, and struggling swimming patterns (Fig. 4-6d) with a higher percentage. Also, at the high currents (6 and 9 μA), elevated flick pattern appeared to compensate for the immobile state of the zebrafish (i.e. no movement pattern, Fig. 4-6e). This finding might propose a side effect of stronger electrical signals on the electrotactic motor patterns due to the potential partial paralysis effect on the larvae. While the zebrafish are not revealing any high-performing behavioral patterns such as struggling and C-bend, they display continuous tail flicks and J-bend under a stronger stimulus rather than staying still or swimming routinely.

Furthermore, struggling pattern (Fig. 4-6f) exhibited a U-shaped behavior with high percentage at 1 and 9 μA and low percentage at 3 and 6 μA (p-value <0.001 for "1 μA vs all", p-value <0.05 for "6 μA vs 9 μA "). Our finding contends that struggling, which is believed to be a common motor pattern in the escape behavior [116], is modulated by application of different electric currents. At medium electrical signal levels, the behavior is moderate, while strongly induced at low and high levels.

As seen in Fig. 4-6b,c, we observed that J-bend and flick patterns are only triggered at high electric currents whereas lower currents can execute the high-performing behaviors. Moreover, as reported in the literature, each of the motor patterns can be evoked by specific stimuli and specific regions of the brain [117]. For example, the larva distinctly displays J-bend pattern during the prey capturing [30], [36]. It has also been shown that J-bend pattern can be evoked by the optical stimuli [29]. In line with the methods above, our device can be used as a tool to evoke and explore J-bend and flick patterns at high electric currents in the zebrafish larvae. At the lower electric currents, our device can be utilized for examining routine swimming and sluggishness in the larvae.

The behavioral trends in some of the observed patterns in the KO larvae were found to be relatively analogous to the WT larvae at different currents. For example, flick pattern remained intact in response to varying electric currents. This may hypothetically suggest that Panx1 is not considerably engaged in the fighting and aggressive behaviors, in which flick pattern is believed to be noticeably involved [118]. Further investigations must be carried out to back up this hypothesis.

Some behavioral distinctions were observed at the lowest current of 1 μ A between the WT and KO larvae. It was observed that the KO larvae tended to exhibit struggling pattern with a higher percentage, hypothetically as a compensation for low inactiveness and routine swimming percentages. Statistical comparison of the mentioned patterns showed significant differences between the KO and WT larvae (p-value<0.001 for "st and nm", p-value<0.05 for rs). C-bend pattern percentage in the KO

larvae, which was lower than the WT ones (p -value <0.05), appeared to be compensated by struggling pattern as well. This finding might suggest that the Panx1 loss leads to some behavioral alterations in the larva, such as more high-performing behaviors at the lowest current of 1 μ A.

Another intriguing difference between the WT and KO larvae responses was the J-bend pattern. Our results showed that the Panx1 ablation made the larvae reveal statistically similar J-bend patterns at different electric currents; while, in the WT larvae, it was shown that higher electric currents lead to a more frequent J-bend pattern. This finding may suggest the Panx1 role in prey tracking in which J-bend pattern is predominant in the zebrafish larvae. However, further investigation is needed in a more specific assay to prove this claim.

The results in this section support our claim that the semi-immobile electrotaxis assay can be used as a tool to interrogate various subtle movement behaviors in the zebrafish larvae and to investigate the functional role of various genes in electrotaxis.

4.4 CONCLUSIONS

To conclude, we have developed an accurate and sensitive device in which the subtle electrotaxis behavior of the WT and mutant zebrafish larvae can be quantitatively studied. The application of our device in studying a knockout zebrafish model was shown by testing the Panx1 KO larvae and comparing their behavior with the WT zebrafish. Our electrotaxis screening technique is suitable for on-demand movement stimulation and subtle behavioral monitoring of the larvae. We showed that the WT and

KO larvae are electrically sensitive to electric currents as low as 0.5 μA and 1 μA , respectively, at which the zebrafish robustly display electrotaxis.

A range of 1-9 μA electric currents were then tested to see how zebrafish electrotaxis is dependent on the electric current amplitude. We showed that the highest TBF is induced at the lowest electric current of 1 μA . At the currents of 3, 6, and 9 μA , the TBF was the same, suggesting that high currents can equally execute the TBF. Thus, we hypothesized that a possible partial paralysis at high currents might have occurred. Moreover, we found that longest zebrafish electrotaxis response duration is evoked at intermediate electric currents of 3 and 6 μA . We then hypothesized that partial paralysis and elevated nociception at high and low electric currents, respectively, might have led to a quicker termination to zebrafish electrotaxis (i.e. shorter response duration).

Furthermore, we took one further step in analyzing WT larvae electrotaxis by classifying their subtle electrotactic phenotypes into several recognizable motor patterns. We observed that struggling pattern, which is involved in the zebrafish escape behavior, reveals a U-shaped behavior under exposure to varying electric currents. J-bend pattern, as a dominantly-involved pattern in the prey-capturing behavior, was strongly displayed at the high electric currents of 6 and 9 μA . This result suggests that high electric current can be employed as a tool to simulate the prey-capturing behavior in the WT larvae. Some general behavioral trends were also evaluated during the electrotaxis screening. For example, it was shown that a weaker electrical signal can bring about sluggishness and induce routine swimming patterns; while a stronger electrical signal would lead to different patterns such as flick movement. Therefore, by

employing our device and technique, one can execute different motor patterns in the zebrafish larvae by only altering the electrical current strength.

Moreover, we showed the application of our device in screening the electrotaxis of a zebrafish larva knockout model. We explored electrotaxis of the KO zebrafish larvae and conducted a comparison with the WT larvae to see if *Panx1* would modulate electrotaxis. We showed that the electrotaxis onset in the KO larvae was at 1 μA electric current. Since the WT larvae started showing electrotaxis at 0.5 μA , it might suggest an electrotactic threshold in shifting the electrotaxis onset due to the *Panx1* ablation in the zebrafish larvae. Increasing the electric current amplitude resulted in the same behavioral trend as the WT larvae; however, the KO larvae exhibited more sensitivity at low currents of 1 and 3 μA by displaying a higher TBF. Also, at 1 and 3 μA electric currents, shorter electrotaxis was evaluated for the KO larvae as compared to the WT ones, which hypothetically suggests the effect of *Panx1* loss in shortening the zebrafish electrotaxis duration. Furthermore, analysis of the electrotactic motor patterns of the KO larvae showed that at low currents of 1 and 3 μA , struggling pattern is dominating. This contends that low currents might be useful to simulate the escape behavior of the KO zebrafish. J-bend pattern also altered in the KO larvae as compared to the WT ones. This finding suggests that *Panx1* might be involved in the larvae prey-capturing behavior.

All in all, our proposed framework provides a sensitive and precise platform in which zebrafish electrotaxis can be quantitatively evaluated. Also, our device can be utilized to examine and gain a better understanding of the biological and genetic pathways involved in zebrafish electrotaxis.

Thesis Summary and Prospects

5.1 THESIS SUMMARY

Zebrafish are the simplest vertebrate model organisms with high genomic homology with humans that are widely used in drug discovery, brain mapping, human disease modeling, and behavioral screening applications. Conventional techniques using petri dishes and agarose-based platforms have been used to study the zebrafish movement phenotypes. However, a few disadvantages that are associated with the current techniques are time-consuming and difficult manipulation procedures, irreversibility, morphological damages to the zebrafish, and difficulties in imaging and assessment of the complex movement phenotypes. Microfluidic technology has emerged as a powerful tool for neural and movement investigation of the zebrafish larvae by providing optimal platforms for precise manipulation, stimulation and behavioral monitoring.

We introduced a novel and simple microfluidic device for on-demand electrical stimulation of individual 5-7 dpf zebrafish larvae which were free to longitudinally move and orient inside a channel (i.e. semi-confined larva). The device consisted of a simple U-shaped channel with electrodes at its two ends to apply electric current across the main channel alongside the larva's body axis. Electrical resistance of the device was 30 M Ω . We demonstrated the effect of electric current in a range of 3-15 μ A in evoking a movement response in the larvae, called electrotaxis, for the first time. The zebrafish

revealed electrotaxis by orienting and swimming towards the anode pole of the applied electric current. Electrotaxis was then quantified in terms of orientation, movement speed, and lateral swimming position of the larvae in the channel. It was shown that the zebrafish larvae can robustly sense and respond to the currents as low as 3 μA . As we increased the electric current, zebrafish showed a higher electrotaxis rate and at 15 μA , the electrotaxis rate reached to 100%. However, due to the mortal and morphological damages to the larvae caused by higher currents, the zebrafish electrotactic speed significantly dropped at 15 μA .

Furthermore, we demonstrated that zebrafish electrotaxis significantly diminishes at nighttime (from higher than 80% during the day to under 25% at night). It was then hypothesized that this was related to the reduced level of activities in the zebrafish dopaminergic system. Thus, we examined our hypothesis by treating the zebrafish larvae with different doses (0.2-50 μM) of apomorphine, a non-selective dopamine agonist, at night. At low electric current levels, this resulted in an increased level of electrotaxis at the low dose apomorphine, while the medium and high doses of the drug resulted in a reduced electrotaxis again. We then took one further step to examine whether zebrafish electrotaxis is regulated by the D1- or D2-like dopamine receptors. We treated the larvae with two selective dopamine agonists of SKF 38393 (D1-like receptors) and Quinpirole (D2-like receptors). It was shown that unlike SKF 38393 (dose of 50 μM), Quinpirole (dose of 16.7 μM) can significantly enhance the electrotaxis response, potentially showing a significant involvement of the D2-like dopamine receptors in regulating zebrafish electrotaxis.

After investigating the general zebrafish electrotaxis movement and showing its correlation with the dopaminergic system, we utilized the microfluidic technology to analyze the zebrafish larvae's subtle electrotactic movement phenotypes. We designed another device in which the larva's head could be stabilized and partially immobilized inside a trapping region (TR), while the tail was free to move. *In-situ* electrical stimulation was achievable in our device by two electrodes at the anterior and posterior sides of the larva. We investigated electrotaxis of the wild type (WT) zebrafish larvae in terms of tail-beat frequency (TBF), response duration, and subtle motor patterns under exposure to electric currents in a range of 0.1-9 μA . We showed that the electrotactic TBF is highest at the low current of 1 μA . The larva also displayed longer electrotaxis at intermediate currents of 3 and 6 μA . Low TBF at the higher currents of 3-9 μA might be due to potential partial paralysis of the larvae at stronger electrical signals. The same reason might hold true for the shorter response at the highest current of 9 μA ; however, short electrotaxis at low current of 1 μA might be hypothetically due to the weak electrical signal causing a quicker termination of electrotaxis.

Moreover, we intended to show the application of our microfluidic-based electrotaxis screening technique in studying knockout zebrafish models. Pannexin1 (Panx1) protein membrane as one of the widely distributed transcripts in the brain has been proven to be involved in the mice's neuroplasticity (i.e. response to the environmental cues). Similarly, we took advantage of the Panx1 knockout (KO) zebrafish larvae to study electrotaxis inside our device. Similar experiments under similar conditions on the WT larvae were conducted on the KO zebrafish. Although the TBF and response duration results followed the same behavioral trends in the KO fish,

we showed that these responses differ significantly amongst the WT and KO larvae at low currents of 1 and 3 μA . It was proven that the KO larvae display electrotaxis with a significantly higher TBF than the WT ones. Our finding suggests the potential involvement of Panx1 in the zebrafish electrotaxis. Furthermore, by analyzing the electrotactic motor patterns of the KO and WT zebrafish, we noted the effect of Panx1 in zebrafish electrotaxis again. For example, in the KO larvae, higher struggling pattern at low currents of 1 and 3 μA and lower J-bend pattern at the higher current of 6 μA were observed. This finding conservatively suggested the role of Panx1 in the well-established prey-capturing and escape behaviors of the zebrafish. However, further investigation is needed to study how the Panx1 knockout is effective in evoking or moderating the mentioned behaviors.

In conclusion, our device and electrotaxis screening technique can be employed for examination of biological pathways engaged in zebrafish electrotaxis and for investigation of the effect of various chemicals and genes on electrotaxis.

5.2 THESIS PROSPECTS

In our research, we studied zebrafish larvae electrotaxis inside two distinct microfluidic devices. There are several complementary studies that can be conducted in the future. We have classified them into technological and biological research directions as discussed below.

5.2.1 Future Technological Research Direction

We designed our first device to partially confine the larva movement in the lateral direction and to allow it to move and orient longitudinally. We were able to accurately and sensitively evoke zebrafish electrotaxis and quantitatively explore the influence of various electrical stimulation levels. However, electrical resistance of our device was kept constant during all of our experiments. One can alter our device's electrical resistance to investigate the effects of current and voltage individually on zebrafish electrotaxis. Different resistances can be achieved by changing the larvae medium inside the device or by modifying the size of the channels. Moreover, to further investigate zebrafish electrotaxis, another factor that has not been considered in our device is the electrotactic orientation angle. By modifying the microfluidic environment in our first device (e.g. widening the main channel), orientation angle can be evaluated while an *in-situ* electrical stimulation is still applied.

Our second device was developed to observe and assess subtle zebrafish electrotaxis movements. The larva was partially immobilized by fixing its head and leaving the tail to freely oscillate. However, there are several opportunities which were not considered in studying zebrafish electrotaxis. First, one can investigate the neural activities of the zebrafish larvae evoked by the electrical stimuli since the larva is partially immobilized and its brain is visually accessible for imaging purposes. A simultaneous study of the behavioral and neural electrotactic responses is also achievable by designing an appropriate imaging setup and using our proposed device. Second, the channel depth of the device was designed to visually access the zebrafish

dorsal view. As shown by X. Lin et al. [71], by changing the depth of the main channel, one can have visual access to the zebrafish lateral view and monitor its cardiovascular system as well. Thus, zebrafish electrotaxis can be further investigated by assessing the heart beats and activities, although the tail motions might become inaccessible. Third, we planned to study individual zebrafish electrotaxis which naturally has a low throughput. With the knowledge developed in this thesis, one opportunity is parallelizing the trapping and screening regions of our device to fabricate a higher throughput device to investigate several zebrafish larvae at the same time. The *in-situ* electrical stimulation is still achievable in a higher throughput device.

5.2.2 Future Biological Research Directions

We have thus far explored the role of a few chemicals on zebrafish electrotaxis with a limited concentration range. One can be empowered with our devices to investigate how a broader range of drugs, including dopamine agonists and antagonists, at a wider dose range can influence zebrafish electrotaxis. Moreover, neurological pathways involved in zebrafish electrotaxis, which is not well understood, can be examined in more details. Furthermore, various gene mutant larvae can be experimented inside our devices and involvement of specific genes in regulating electrotaxis can be studied. For example, by ablating a specific gene, one can use our first device to study any general involvement of the gene in electrotaxis and our second device makes it possible to explore subtle behavioral responses to learn more about the gene's function phenotypically.

References:

- [1] J. C. Hendricks, A. Sehgal, and A. I. Pack, "The need for a simple animal model to understand sleep," *Prog. Neurobiol.*, vol. 61, no. 4, pp. 339–51, Jul. 2000.
- [2] L. Guarente and C. Kenyon, "Genetic pathways that regulate ageing in model organisms.," *Nature*, vol. 408, no. 6809, pp. 255–262, Nov. 2000.
- [3] T. J. Aitman, C. Boone, G. A. Churchill, M. O. Hengartner, T. F. C. Mackay, and D. L. Stemple, "The future of model organisms in human disease research," *Nat. Rev. Genet.*, vol. 12, no. 8, pp. 575–582, Jul. 2011.
- [4] T. Kaletta and M. O. Hengartner, "Finding function in novel targets: *C. elegans* as a model organism.," *Nat. Rev. Drug Discov.*, vol. 5, no. 5, pp. 387–98, 2006.
- [5] J. Bilen and N. M. Bonini, "*Drosophila* as a model for human neurodegenerative disease.," *Annu. Rev. Genet.*, vol. 39, pp. 153–71, 2005.
- [6] A. Seth, D. L. Stemple, and I. Barroso, "The emerging use of zebrafish to model metabolic disease.," *Dis. Model. Mech.*, vol. 6, no. 5, pp. 1080–8, 2013.
- [7] M. de Bono and A. Villu Maricq, "Neuronal Substrates of Complex Behaviors In *C. elegans*," *Annu. Rev. Neurosci.*, vol. 28, no. 1, pp. 451–501, Jul. 2005.
- [8] H. Manev and N. Dimitrijevic, "*Drosophila* model for in vivo pharmacological analgesia research," *Eur. J. Pharmacol.*, vol. 491, no. 2–3, pp. 207–208, May 2004.
- [9] Z. Lele and P. H. Krone, "The Zebrafish As A Model System In Developmental,

- Toxicological And Transgenic Research,” *Biotechnol. Adv.*, vol. 14, no. 1, pp. 57–72, 1996.
- [10] S. A. Patten, J. A. Parker, X.-Y. Wen, and P. Drapeau, “Simple animal models for amyotrophic lateral sclerosis drug discovery,” *Expert Opin. Drug Discov.*, vol. 11, no. 8, pp. 797–804, Aug. 2016.
- [11] E. Bier and W. McGinnis, “Model Organisms in the Study of Development and Disease,” in *Oxford Monographs On Medical Genetics*, 2004, pp. 25–45.
- [12] L. I. Zon and R. T. Peterson, “In vivo drug discovery in the zebrafish,” *Nat. Rev. Drug Discov.*, vol. 4, no. 1, pp. 35–44, 2005.
- [13] J. R. Fetcho and K. S. Liu, “Zebrafish as a Model System for Studying Neuronal Circuits and Behavior,” *Ann. N. Y. Acad. Sci.*, vol. 26539, pp. 333–345, 1998.
- [14] G. J. Lieschke and P. D. Currie, “Animal models of human disease: zebrafish swim into view,” *Nat. Rev. Genet.*, vol. 8, no. 5, pp. 353–367, 2007.
- [15] O. Bandmann and E. A. Burton, “Genetic zebrafish models of neurodegenerative diseases,” *Neurobiol. Dis.*, vol. 40, no. 1, pp. 58–65, 2010.
- [16] T. W. Dunn, Y. Mu, S. Narayan, O. Randlett, E. A. Naumann, C. T. Yang, A. F. Schier, J. Freeman, F. Engert, and M. B. Ahrens, “Brain-wide mapping of neural activity controlling zebrafish exploratory locomotion,” *Elife*, vol. 5, p. e12741, 2016.
- [17] S. L. Renninger and M. B. Orger, “Two-photon imaging of neural population activity in zebrafish,” *Methods*, vol. 62, no. 3, pp. 255–267, 2013.

- [18] F. Ahmad, L. P. J. J. Noldus, R. a J. Tegelenbosch, and M. K. Richardson, "Zebrafish embryos and larvae in behavioural assays," *Behaviour*, vol. 149, pp. 1241–1281, 2012.
- [19] M. A. Wolman, R. A. Jain, L. Liss, and M. Granato, "Chemical modulation of memory formation in larval zebrafish.," *Proc. Natl. Acad. Sci. U. S. A.*, vol. 108, no. 37, pp. 15468–73, 2011.
- [20] T. D. Irons, P. E. Kelly, D. L. Hunter, R. C. MacPhail, and S. Padilla, "Acute administration of dopaminergic drugs has differential effects on locomotion in larval zebrafish," *Pharmacol. Biochem. Behav.*, vol. 103, no. 4, pp. 792–813, 2013.
- [21] K. Howe and A. Et, "The zebrafish reference genome sequence and its relationship to the human genome.," *Nature*, vol. 496, no. 7446, pp. 498–503, 2013.
- [22] F. M. Richards, W. K. Alderton, G. M. Kimber, Z. Liu, I. Strang, W. S. Redfern, J. P. Valentin, M. J. Winter, and T. H. Hutchinson, "Validation of the use of zebrafish larvae in visual safety assessment," *J. Pharmacol. Toxicol. Methods*, vol. 58, no. 1, pp. 50–58, 2008.
- [23] C. B. Kimmel, W. W. Ballard, S. R. Kimmel, B. Ullmann, and T. F. Schilling, "Stages of embryonic development of the zebrafish," *Dev Dyn*, vol. 203, no. 3, pp. 253–310, 1995.
- [24] V. Surendra, U. Raj Sharma, and D. Goli, "Behavioral Studies of Different Drugs Using Zebrafish as a Model," *Int. J. Pharmagenes.*, vol. 2, no. 1, pp. 75–82, 2011.

- [25] R. Portugues and F. Engert, "The neural basis of visual behaviors in the larval zebrafish," *Curr. Opin. Neurobiol.*, vol. 19, no. 6, pp. 644–647, 2009.
- [26] J. Schweitzer, H. Löhr, A. Filippi, and W. Driever, "Dopaminergic and noradrenergic circuit development in zebrafish," *Dev. Neurobiol.*, vol. 72, no. 3, pp. 256–268, 2012.
- [27] F. a Issa, G. O'Brien, P. Kettunen, A. Sagasti, D. L. Glanzman, and D. M. Papazian, "Neural circuit activity in freely behaving zebrafish (*Danio rerio*).," *J. Exp. Biol.*, vol. 214, no. Pt 6, pp. 1028–1038, 2011.
- [28] R. Portugues, C. E. Feierstein, F. Engert, and M. B. Orger, "Whole-brain activity maps reveal stereotyped, distributed networks for visuomotor behavior," *Neuron*, vol. 81, no. 6, pp. 1328–1343, 2014.
- [29] O. Fajardo, P. Zhu, and R. W. Friedrich, "Control of a specific motor program by a small brain area in zebrafish," *Front. Neural Circuits*, vol. 7, no. April, p. 67, 2013.
- [30] I. H. Bianco, A. R. Kampff, and F. Engert, "Prey Capture Behavior Evoked by Simple Visual Stimuli in Larval Zebrafish," *Front. Syst. Neurosci.*, vol. 5, no. December, pp. 1–13, 2011.
- [31] R. Olive, S. Wolf, A. Dubreuil, V. Bormuth, G. Debrégeas, and R. Candelier, "Rheotaxis of Larval Zebrafish: Behavioral Study of a Multi-Sensory Process.," *Front. Syst. Neurosci.*, vol. 10, no. February, p. 14, 2016.
- [32] K. H. Huang, M. B. Ahrens, T. W. Dunn, and F. Engert, "Spinal projection neurons control turning behaviors in zebrafish," *Curr. Biol.*, vol. 23, no. 16, pp. 1566–1573, 2013.

- [33] E. A. Osipova, V. V Pavlova, V. A. Nepomnyashchikh, and V. V Krylov, "Influence of magnetic field on zebrafish activity and orientation in a plus maze," vol. 122, pp. 80–86, 2016.
- [34] A. Takebe, T. Furutani, T. Wada, M. Koinuma, Y. Kubo, K. Okano, and T. Okano, "Zebrafish respond to the geomagnetic field by bimodal and group-dependent orientation," *Sci. Rep.*, vol. 2, p. 727, 2012.
- [35] H. A. Burgess, M. Granato, H. A. Burgess, and M. Granato, "Modulation of locomotor activity in larval zebrafish during light adaptation," *J. Exp. Biol.*, vol. 210, no. 14, pp. 2526–2539, 2007.
- [36] A. Muto and K. Kawakami, "Prey capture in zebrafish larvae serves as a model to study cognitive functions," *Front. Neural Circuits*, vol. 7, no. June, pp. 1–5, 2013.
- [37] P. Mcclenahan, M. Troup, and E. K. Scott, "Fin-Tail Coordination during Escape and Predatory Behavior in Larval Zebrafish," *PLoS One*, vol. 7, no. 2, p. e32295, 2012.
- [38] A. V. Kalueff and J. M. Cachat, Eds., *Zebrafish Models in Neurobehavioral Research*, Illustrate. Humana Press, 2010.
- [39] F. Ek, M. Malo, M. Å. Andersson, C. Wedding, J. Kronborg, P. Svensson, S. Waters, P. Petersson, and R. Olsson, "Behavioral Analysis of Dopaminergic Activation in Zebrafish and Rats Reveals Similar Phenotypes," *ACS Chem. Neurosci.*, vol. 7, pp. 633–646, 2016.
- [40] M. H. Green, R. K. Ho, and M. E. Hale, "Movement and function of the pectoral fins of the larval zebrafish (*Danio rerio*) during slow swimming.," *J. Exp. Biol.*, vol.

- 214, no. Pt 18, pp. 3111–3123, 2011.
- [41] T. Bartolini, V. Mwaffo, S. Butail, and M. Porfiri, “Effect of acute ethanol administration on zebrafish tail-beat motion,” *Alcohol*, vol. 49, pp. 721–725, 2015.
- [42] D. M. O’Malley, Y. H. Kao, and J. R. Fetcho, “Imaging the functional organization of zebrafish hindbrain segments during escape behaviors,” *Neuron*, vol. 17, no. 6, pp. 1145–1155, 1996.
- [43] A. Suli, G. M. Watson, E. W. Rubel, and D. W. Raible, “Rheotaxis in larval zebrafish is mediated by lateral line mechanosensory hair cells,” *PLoS One*, vol. 7, no. 2, pp. 1–6, 2012.
- [44] T. D. Irons, R. C. MacPhail, D. L. Hunter, and S. Padilla, “Acute neuroactive drug exposures alter locomotor activity in larval zebrafish,” *Neurotoxicol. Teratol.*, vol. 32, no. 1, pp. 84–90, 2010.
- [45] R. M. Colwill and R. Creton, “Locomotor behaviors in zebrafish (*Danio rerio*) larvae,” *Behav. Processes*, vol. 86, no. 2, pp. 222–229, 2011.
- [46] A. M. Stewart, O. Braubach, J. Spitsbergen, R. Gerlai, and A. V Kalueff, “Zebrafish models for translational neuroscience research: from tank to bedside,” *Trends Neurosci.*, vol. 37, no. 5, pp. 264–278, 2014.
- [47] Z. Lu and A. A. Desmidt, “Early development of hearing in zebrafish,” *JARO - J. Assoc. Res. Otolaryngol.*, vol. 14, no. 4, pp. 509–521, 2013.
- [48] Y. Mu, X. quan Li, B. Zhang, and J. lin Du, “Visual Input Modulates Audiomotor Function via Hypothalamic Dopaminergic Neurons through a Cooperative Mechanism,” *Neuron*, vol. 75, no. 4, pp. 688–699, 2012.

- [49] B. D. Monesson-Olson, J. Browning-Kamins, R. Aziz-Bose, F. Kreines, and J. G. Trapani, "Optical stimulation of zebrafish hair cells expressing channelrhodopsin-2," *PLoS One*, vol. 9, no. 5, pp. 1–8, 2014.
- [50] P. Pais-Roldán, A. P. Singh, H. Schulz, and X. Yu, "High magnetic field induced otolith fusion in the zebrafish larvae," *Sci. Rep.*, vol. 6, p. 24151, 2016.
- [51] R. Creton, "Automated analysis of behavior in zebrafish larvae," *Behav. Brain Res.*, vol. 203, no. 1, pp. 127–136, 2009.
- [52] A. Kaufmann, M. Mickoleit, M. Weber, and J. Huisken, "Multilayer mounting enables long-term imaging of zebrafish development in a light sheet microscope," *Development*, vol. 139, no. 17, pp. 3242–3247, 2012.
- [53] G. M. Whitesides, "The origins and the future of microfluidics.," *Nature*, vol. 442, no. 7101, pp. 368–73, 2006.
- [54] X. J. Li and Y. Zhou, *Microfluidic devices for biomedical applications*. 2013.
- [55] P. Rezai, A. Siddiqui, P. R. Selvaganapathy, and B. P. Gupta, "Behavior of *Caenorhabditis elegans* in alternating electric field and its application to their localization and control," *Appl. Phys. Lett.*, vol. 96, no. 15, p. 153702, Apr. 2010.
- [56] P. Rezai, A. Siddiqui, R. Selvaganapathy, and B. P. Gupta, "Electrotaxis of *Caenorhabditis elegans* in a microfluidic environment," *Lab Chip*, vol. 10, pp. 220–226, 2010.
- [57] P. Rezai, S. Salam, P. R. Selvaganapathy, and B. P. P. Gupta, "Effect of pulse direct current signals on electrotactic movement of nematodes *Caenorhabditis elegans* and *Caenorhabditis briggsae*," *Biomicrofluidics*, vol. 5, no. 4, p. 44116,

Dec. 2011.

- [58] P. Rezai, S. Salam, P. R. Selvaganapathy, and B. P. Gupta, "Electrical sorting of *Caenorhabditis elegans*," *Lab Chip*, vol. 12, no. 10, p. 1831, 2012.
- [59] S. Salam, A. Ansari, S. Amon, P. Rezai, P. R. Selvaganapathy, R. K. Mishra, and B. P. Gupta, "A microfluidic phenotype analysis system reveals function of sensory and dopaminergic neuron signaling in *C. elegans* electrotactic swimming behavior," *Worm*, vol. 2, no. September, p. e24558, Apr. 2013.
- [60] J. Tong, P. Rezai, S. Salam, P. R. Selvaganapathy, and B. P. Gupta, "Microfluidic-based electrotaxis for on-demand quantitative analysis of *Caenorhabditis elegans*' locomotion," *J. Vis. Exp.*, no. 75, p. e50226, May 2013.
- [61] R. Ardeshiri, B. Mulcahy, M. Zhen, and P. Rezai, "A hybrid microfluidic device for on-demand orientation and multidirectional imaging of *C. elegans* organs and neurons," *Biomicrofluidics*, vol. 10, no. 6, p. 64111, Nov. 2016.
- [62] B. Gupta and P. Rezai, "Microfluidic Approaches for Manipulating, Imaging, and Screening *C. elegans*," *Micromachines*, vol. 7, no. 7, p. 123, Jul. 2016.
- [63] R. Ghaemi, P. Rezai, B. G. Iyengar, and P. R. Selvaganapathy, "Microfluidic devices for imaging neurological response of *Drosophila melanogaster* larva to auditory stimulus," *Lab Chip*, vol. 15, no. 4, pp. 1116–22, 2014.
- [64] J. C. K. Leung, R. W. Taylor-Kamall, A. J. Hilliker, and P. Rezai, "Agar-polydimethylsiloxane devices for quantitative investigation of oviposition behaviour of adult *Drosophila melanogaster*," *Biomicrofluidics*, vol. 9, no. 3, p. 34112, May 2015.

- [65] R. Ardeshiri, L. Hosseini, N. Amini, and P. Rezai, "Cardiac screening of intact *Drosophila melanogaster* larvae under exposure to aqueous and gaseous toxins in a microfluidic device," *RSC Adv.*, vol. 6, pp. 65714–65724, 2016.
- [66] J. C. K. Leung, A. J. Hilliker, and P. Rezai, "An integrated hybrid microfluidic device for oviposition-based chemical screening of adult *Drosophila melanogaster*," *Lab Chip*, vol. 16, pp. 709–19, 2014.
- [67] M. Erickstad, L. A. Hale, S. H. Chalasani, and A. Groisman, "A microfluidic system for studying the behavior of zebrafish larvae under acute hypoxia," *Lab Chip*, vol. 15, pp. 857–866, 2015.
- [68] X. Lin, S. Wang, X. Yu, Z. Liu, F. Wang, W. T. Li, S. H. Cheng, Q. Dai, and P. Shi, "High-throughput mapping of brain-wide activity in awake and drug-responsive vertebrates," *Lab Chip*, vol. 15, no. 3, pp. 680–689, 2015.
- [69] F. Yang, C. Gao, P. Wang, G.-J. Zhang, and Z. Chen, "Fish-on-a-Chip: Microfluidics for Zebrafish Research," *Lab Chip*, vol. 7, pp. 1106–25, 2016.
- [70] R. Candelier, M. Sriti Murmu, S. Alejo Romano, A. Jouary, G. Debréguas, and G. Sumbre, "A microfluidic device to study neuronal and motor responses to acute chemical stimuli in zebrafish," *Sci. Rep.*, vol. 5, p. 12196, Jul. 2015.
- [71] X. Lin, V. W. T. Li, S. Chen, C.-Y. Chan, S.-H. Cheng, and P. Shi, "Autonomous system for cross-organ investigation of ethanol-induced acute response in behaving larval zebrafish," *Biomicrofluidics*, vol. 10, no. 2, p. 24123, 2016.
- [72] S. Mondal, S. Ahlawat, and S. P. Koushika, "Simple Microfluidic Devices for in vivo Imaging of *C.elegans*, *Drosophila*, and Zebrafish," *J. Vis. Exp.*, vol. 2025, no.

- 67, pp. 1–9, 2012.
- [73] H. Hwang and H. Lu, “Microfluidic tools for developmental studies of small model organisms--nematodes, fruit flies, and zebrafish.,” *Biotechnol. J.*, vol. 8, no. 2, pp. 192–205, 2013.
- [74] M. M. Crane, K. Chung, J. Stirman, and H. Lu, “Microfluidics-enabled phenotyping, imaging, and screening of multicellular organisms.,” *Lab Chip*, vol. 10, no. 12, pp. 1509–1517, 2010.
- [75] S. Hong, P. Lee, S. C. Baraban, and L. P. Lee, “A Novel Long-term, Multi-Channel and Non-invasive Electrophysiology Platform for Zebrafish,” *Sci. Rep.*, vol. 6, no. January, p. 28248, 2016.
- [76] A. Jin, Z. Feng, J. Skommer, C. J. Hall, P. S. Crosier, M. Cialkowski, and D. Wlodkowic, “Microfluidic Device for a Rapid Immobilization of Zebrafish Larvae in Environmental Scanning Electron Microscopy,” *Cytom. Part A*, vol. 87A, no. 2014, pp. 190–194, 2015.
- [77] A. Jahanshahi, L.-M. Schönfeld, E. Lemmens, S. Hendrix, Y. Temel, A. Jahanshahi, L. Schönfeld, Y. Temel, E. Lemmens, and S Hendrix, “In Vitro and In Vivo Neuronal Electrotaxis,” *Mol Neurobiol*, vol. 49, pp. 1005–1016, 2014.
- [78] J. Li and F. Lin, “Microfluidic devices for studying chemotaxis and electrotaxis,” *Trends Cell Biol.*, vol. 21, no. 8, pp. 489–497, 2011.
- [79] L. Li, Y. H. El-Hayek, B. Liu, Y. Chen, E. Gomez, X. Wu, K. Ning, L. Li, N. Chang, L. Zhang, Z. Wang, X. Hu, and Q. Wan, “Direct-Current Electrical Field Guides Neuronal Stem/Progenitor Cell Migration,” *Stem Cells*, vol. 26, no. 8, pp. 2193–

2200, Aug. 2008.

- [80] M. Hook and J. Grau, "An animal model of functional electrical stimulation: evidence that the central nervous system modulates the consequences of training," *Spinal Cord*, vol. 45, no. 11, pp. 702–712, 2007.
- [81] X. Manière, F. Lebois, I. Matic, B. Ladoux, J. M. Di Meglio, and P. Hersen, "Running worms: *C. elegans* self-sorting by electrotaxis," *PLoS One*, vol. 6, no. 2, 2011.
- [82] B. Han, D. Kim, U. H. Ko, J. H. Shin, U. Hyun Ko, and J. H. Shin, "A sorting strategy for *C. elegans* based on size-dependent motility and electrotaxis in a micro-structured channel," *Lab Chip*, vol. 12, no. 20, pp. 4128–34, Oct. 2012.
- [83] X. Wang, R. Hu, A. Ge, L. Hu, S. Wang, X. Feng, W. Du, and B.-F. Liu, "Highly efficient microfluidic sorting device for synchronizing developmental stages of *C. elegans* based on deflecting electrotaxis," *Lab Chip*, vol. 15, no. 11, pp. 2513–2521, 2015.
- [84] M. M. Shanmugam, "Galvanotaxis of *Caenorhabditis elegans*: current understanding and its application in improving research," *Biol. Eng. Med.*, vol. 2, no. 1, pp. 1–5, 2017.
- [85] P. Rezai, S. Salam, P. R. Selvaganapathy, and B. P. Gupta, "Transport , Localization and Separation of *Caenorhabditis Elegans* Using Electrotaxis for Movement Based Behavioral Assays in Drug Discovery," *Main*, no. October, pp. 2010–2012, 2010.
- [86] D. Liu, B. Gupta, and P. R. Selvaganapathy, "An automated microfluidic system

- for screening *Caenorhabditis elegans* behaviors using electrotaxis,” *Biomicrofluidics*, vol. 10, no. 1, p. e014117, 2016.
- [87] H.-S. Chuang, W.-J. Kuo, C.-L. Lee, I.-H. Chu, and C.-S. Chen, “Exercise in an electrotactic flow chamber ameliorates age-related degeneration in *Caenorhabditis elegans*,” *Sci. Rep.*, vol. 6, no. April, p. 28064, 2016.
- [88] B. Han, D. Kim, U. Hyun Ko, and J. H. Shin, “A sorting strategy for *C. elegans* based on size-dependent motility and electrotaxis in a micro-structured channel,” *Lab Chip*, vol. 12, no. 20, p. 4128, Sep. 2012.
- [89] N. Minc and F. Chang, “Electrical control of cell polarization in the fission yeast *Schizosaccharomyces pombe*,” *Curr. Biol.*, vol. 20, no. 8, pp. 710–6, Apr. 2010.
- [90] S. Matsuyama, M. Moriuchi, M. A. Suico, S. Yano, S. Morino-Koga, T. Shuto, K. Yamanaka, T. Kondo, E. Araki, and H. Kai, “Mild electrical stimulation increases stress resistance and suppresses fat accumulation via activation of LKB1-AMPK signaling pathway in *C. elegans*,” *PLoS One*, vol. 9, no. 12, pp. 1–23, 2014.
- [91] Y. Sun, H. Do, J. Gao, R. Zhao, M. Zhao, and A. Mogilner, “Keratocyte fragments and cells utilize competing pathways to move in opposite directions in an electric field,” *Curr. Biol.*, vol. 23, no. 7, pp. 569–574, 2013.
- [92] V. M. Bedell, Y. Wang, J. M. Campbell, T. L. Poshusta, C. G. Starker, R. G. Krug II, W. Tan, S. G. Penheiter, A. C. Ma, A. Y. H. Leung, S. C. Fahrenkrug, D. F. Carlson, D. F. Voytas, K. J. Clark, J. J. Essner, and S. C. Ekker, “In vivo genome editing using a high-efficiency TALEN system,” *Nature*, vol. 491, no. 7422, pp. 114–118, Sep. 2012.

- [93] N. Safaraian, E. Hernandez-Gomez, S. Al-Rass, C. Zoidl, X.-Y. Wen, and G. Zoidl, "The phenotype of *Panx1a* knock out zebrafish reveals a novel role in sensory-motor gating," *Submitted*, 2017.
- [94] V. Cenedese, W. Graaff, M. Poovayya, T. Csikós, G. Zoidl, and M. Kamermans, "Pannexin1 is critically involved in feedback from horizontal cells to cones," *Front. Mol. Neurosci.*, p. In Press, 2017.
- [95] C. Pardo-Martin, T.-Y. Chang, B. K. Koo, C. L. Gilleland, S. C. Wasserman, and M. F. Yanik, "High-throughput in vivo vertebrate screening.," *Nat. Methods*, vol. 7, no. 8, pp. 634–6, 2010.
- [96] C. A. Schneider, W. S. Rasband, and K. W. Eliceiri, "NIH Image to ImageJ: 25 years of image analysis," *Nat. Methods*, vol. 9, no. 7, pp. 671–675, 2012.
- [97] T. Chang, P. Shi, J. D. Steinmeyer, I. Chatnuntaweck, K. T. Love, P. M. Eimon, D. G. Anderson, and M. Fatih, "Organ-targeted high-throughput in vivo biologics screen identifies materials for RNA delivery," *Integr Biol*, vol. 6, no. 10, pp. 926–934, 2014.
- [98] M. W. Hurd, J. Debruyne, M. Straume, G. M. Cahill, M. W. Hurd, J. Debruyne, M. Straume, and G. M. Cahill, "Circadian rhythms of locomotor activity in zebrafish," *Physiol. Behav.*, vol. 65, no. 3, pp. 465–472, 1998.
- [99] J. Huang, Z. Zhong, M. Wang, X. Chen, Y. Tan, S. Zhang, W. He, X. He, G. Huang, H. Lu, P. Wu, Y. Che, Y.-L. Yan, X. H. Postlethwait, W. Chen, and X. H. Wang, "Circadian Modulation of Dopamine Levels and Dopaminergic Neuron Development Contributes to Attention Deficiency and Hyperactive Behavior," *J.*

Neurosci., vol. 35, no. 6, pp. 2572–2587, 2015.

- [100] V. P. Connaughton, B. Wetzell, L. S. Arneson, V. Delucia, and A. L. Riley, “Elevated dopamine concentration in light-adapted zebrafish retinas is correlated with increased dopamine synthesis and metabolism,” *J. Neurochem.*, vol. 135, no. 1, pp. 101–108, 2015.
- [101] N. Svante, C. Yuan-Hwa, and H. Christer, “Saturation of striatal D2 dopamine receptors by clozapine,” *Int. J. Neuropsychopharmacol.*, vol. 5, pp. 11–16, 2002.
- [102] S. Jauhar, M. Veronese, M. Rogdaki, M. Bloomfield, S. Natesan, F. Turkheimer, S. Kapur, and O. Howes, “Regulation of dopaminergic function: an [18F]-DOPA PET apomorphine challenge study in humans,” *Transl. Psychiatry*, vol. 7, p. e1027, 2017.
- [103] A. Nady, A. R. Peimani, G. Zoidl, and P. Rezai, “A microfluidic device for partial immobilization, chemical exposure and behavioural screening of zebrafish larvae,” *Lab Chip*, vol. 17, no. 23, pp. 4048–4058, Nov. 2017.
- [104] V. Kovalzon, L. Moiseenko, A. Ambaryan, S. Kurtenbach, V. Shestopalov, and Y. Panchin, “Sleep-wakefulness cycle and behavior in pannexin1 knockout mice,” *Behav. Brain Res.*, vol. 318, pp. 24–27, 2017.
- [105] S. Penuela, R. Gehi, and D. W. Laird, “The biochemistry and function of pannexin channels,” *Biochim. Biophys. Acta*, vol. 1828, no. 1, pp. 15–22, 2013.
- [106] S. Kurtenbach, P. Whyte-Fagundes, L. Gelis, S. Kurtenbach, Ã. Brazil, C. Zoidl, H. Hatt, V. I. Shestopalov, and G. Zoidl, “Investigation of olfactory function in a Panx1 knock out mouse model,” *Front. Cell. Neurosci.*, vol. 8, p. 266, Sep. 2014.

- [107] C. Zhang, K. F. Medzihradzsky, E. E. Sánchez, A. I. Basbaum, and D. Julius, “Lys49 myotoxin from the Brazilian lancehead pit viper elicits pain through regulated ATP release,” *Proc. Natl. Acad. Sci. U. S. A.*, vol. 114, no. 12, pp. E2524–E2532, Mar. 2017.
- [108] N. Prochnow, A. Abdulazim, S. Kurtenbach, V. Wildförster, G. Dvorianchikova, J. Hanske, E. Petrasch-Parwez, V. I. Shestopalov, R. Dermietzel, D. Manahan-Vaughan, G. Zoidl, and S. Barnes, “Pannexin1 Stabilizes Synaptic Plasticity and Is Needed for Learning,” *PLoS One*, vol. 7, no. 12, p. e51767, 2012.
- [109] A. R. Peimani, G. Zoidl, and P. Rezai, “A Microfluidic Device to Study Electrotaxis and Dopaminergic System of Zebrafish Larvae,” *Submitt. to Biomicrofluidics*, 2017.
- [110] J. Olszewski, M. Haehnel, M. Taguchi, and J. C. Liao, “Zebrafish larvae exhibit rheotaxis and can escape a continuous suction source using their lateral line,” *PLoS One*, vol. 7, no. 5, p. e36661, 2012.
- [111] Q. Yang, P. Sun, S. Chen, H. Li, and F. Chen, “Behavioral methods for the functional assessment of hair cells in zebrafish,” *Front. Med.*, vol. 2, no. 11, pp. 178–190, 2017.
- [112] N. S. Sankrithi and D. M. O. Malley, “Activation of a multisensory, multifunctional nucleus in the zebrafish midbrain during diverse locomotor,” *NSC*, vol. 166, no. 3, pp. 970–993, 2010.
- [113] C. Maximino, “Modulation of nociceptive-like behavior in zebrafish (*Danio rerio*) by environmental stressors,” *Psychol. Neurosci.*, vol. 41, no. 1, pp. 149–155, 2011.

- [114] “A novel zebrafish-based model of nociception,” *Physiol. Behav.*, vol. 174, pp. 83–88, May 2017.
- [115] D. Bravo, P. Ibarra, J. Retamal, T. Pelissier, C. Laurido, A. Hernandez, and L. Constandil, “Pannexin 1: A novel participant in neuropathic pain signaling in the rat spinal cord,” *Pain*, vol. 155, pp. 2108–2115, 2014.
- [116] K. S. Liu, J. R. Fetcho, S. Brook, and N. York, “Laser Ablations Reveal Functional Relationships of Segmental Hindbrain Neurons in Zebrafish,” vol. 23, pp. 325–335, 1999.
- [117] M. Wolman and M. Granato, “Behavioral genetics in larval zebrafish: Learning from the young,” *Dev. Neurobiol.*, vol. 72, no. 3, pp. 366–372, Mar. 2012.
- [118] R. F. Oliveira, J. F. Silva, and J. M. Simoes, “Fighting zebrafish: characterization of aggressive behavior and winner-loser effects,” *Zebrafish*, vol. 8, no. 2, pp. 73–81, 2011.
- [119] R. T. P. Calum A. MacRae, “Zebrafish as tools for drug discovery,” *Nat. Rev. DRUG Discov.*, vol. 14, pp. 721–731, 2015.
- [120] S. Basu and C. Sachidanandan, “Zebrafish : A Multifaceted Tool for Chemical Biologists,” *Chem. Rev.*, vol. 113, p. 7952–7980, 2013.
- [121] S. D. Pelkowski, M. Kapoor, H. a. Richendrfel, X. Wang, R. M. Colwill, and R. Creton, “A novel high-throughput imaging system for automated analyses of avoidance behavior in zebrafish larvae,” *Behav. Brain Res.*, vol. 223, no. 1, pp. 135–144, 2011.
- [122] S. a Budick and D. M. O’Malley, “Locomotor repertoire of the larval zebrafish:

- swimming, turning and prey capture.," *J. Exp. Biol.*, vol. 203, no. Pt 17, pp. 2565–79, 2000.
- [123] R. M. Colwill and R. Creton, "Imaging escape and avoidance behavior in zebrafish larvae.," *Rev. Neurosci.*, vol. 22, no. 1, pp. 63–73, 2011.
- [124] S. I. Higashijima, "Transgenic zebrafish expressing fluorescent proteins in central nervous system neurons," *Dev. Growth Differ.*, vol. 50, no. 6, pp. 407–413, 2008.
- [125] D. L. McLean and J. R. Fetcho, "Ontogeny and innervation patterns of dopaminergic, noradrenergic, and serotonergic neurons in larval zebrafish," *J. Comp. Neurol.*, vol. 480, no. 1, pp. 38–56, 2004.
- [126] G. P. Arnold, "Rheotropism in fishes.," *Biol. Rev. Camb. Philos. Soc.*, vol. 49, no. 4, pp. 515–576, 1974.
- [127] M. J. Mchenry, K. E. Feitl, J. A. Strother, W. J. Van Trump, and W. J. Van Trump, "Larval zebrafish rapidly sense the water flow of a predator's strike.," *Biol. Lett.*, vol. 5, no. 4, pp. 477–9, 2009.
- [128] D. De Paiva, D. Forsin, R. Armando, D. Cunha, A. Rosa, and D. F. Baptista, "Analysis of Individual Versus Group Behavior of Zebrafish: a Model Using pH Sublethal Effects," *Bull Env. Contam Toxicol*, vol. 88, pp. 1009–1013, 2012.
- [129] A. R. Peimani, G. Zoidl, and P. Rezai, "Zebrafish Larva's Cyclic Electrotaxis Behavior And Its Dependency On Dopamine Level Enabled By A Novel Microfluidic Assay," in *The 21th International Conference on Miniaturized Systems for Chemistry and Life Sciences (MicroTAS)*, 2017, p. In press.
- [130] H. A. Swain, C. Sigstad, and F. M. Scalzo, "Effects of dizocilpine (MK-801) on

circling behavior, swimming activity, and place preference in zebrafish (*Danio rerio*)," *Neurotoxicol. Teratol.*, vol. 26, no. 6 SPEC. ISS., pp. 725–729, 2004.

A. A Microfluidic Device for Quantitative Investigation of Zebrafish Larvae's Rheotaxis*

A.1. INTRODUCTION

Zebrafish is an emerging model organism in biological studies for various applications such as drug discovery [119], neural circuit investigations [27], and behavioral assays [38]. Zebrafish larva's high genetic homology to humans, small size, transparency, and rapid embryonic development are among the most important advantages of zebrafish as a model organism [120]. Moreover, at larval stage, their behavioral functionalities such as escape [110], avoidance [121], turning [31], [32], [43], and overall locomotor behaviors [122], [123] are fully evolved [124], [125], providing a platform in which the biological pathways involved in sensing environmental cues and responding to them can be investigated.

One of the most common and important behaviors among many of the aquatic species is rheotaxis. It is defined as animals' ability to sense the fluid flow surrounding their bodies and to respond to it spontaneously by turning and swimming against the stream [31]. Zebrafish larvae have been shown to demonstrate rheotaxis for avoiding the predators attack, holding their position during a flow strike, and migrating upstream

* This appendix was accepted for publication: A.R. Peimani, G. Zoidl, and P. Rezai, "A Microfluidic Device for Quantitative Investigation of Zebrafish Larvae's Rheotaxis", *Biomedical Microdevices*, vol. 19, p. 99, 2017.

in the rivers and oceans [31], [43], [110], [126], [127]. Using relatively complicated experimental setups to control the stimulating flow, it has been shown that zebrafish larvae utilize several sensory systems such as the lateral line, visual and vestibular systems to respond to the mechanical stimulation exerted by the water current [31], [43].

Existing rheotaxis screening setups can be divided into two major configurations based on their flow stimulation modalities, i.e. (i) using a fluid suction source-point to generate a radially inward flow in a tank [31], [110] and (ii) exposing the larvae to streamlined flow along the axis of a chamber [43], [127]. Some challenges associated with these setups are the large fluid velocity variations between the tested larvae depending on their radial location on the platform, lack of control over flow direction with respect to larvae's initial orientation, and involvement of multiple stimuli such as flow and visual cues (e.g. flow generation source). Moreover, current studies have mostly focused on group response investigations while the behavior of individual zebrafish larva differs from their group-based responses [128]. Technologies to address the above-mentioned challenges are needed in order to enable systematic investigation of individual larva's rheotaxis and its biological basis.

Microfluidic platforms have enhanced our ability to perform controlled, quantitative and high throughput biological assays on model organisms including the zebrafish larvae [62], [69]. These technologies have been employed to investigate the effects of many stimuli such as chemical [70], [103], mechanical [18], electrical [109], [129] and optical [49] stimulations on the zebrafish larvae. Here, we have employed

microfluidics to develop a simple, effective, and efficient device to study individual zebrafish larvae's rheotaxis. Our device provides several advantages over the conventional methods by allowing placement of a single semi-confined larva along the axis of a channel, application of a streamlined and repeatable flow with a constant average velocity and direction axially towards the larva in the channel, and quantification of their rheotactic response in a simple manner. Altogether, this technology can be used in the future to interrogate the biological pathways involved in rheotaxis of zebrafish larvae and other aquatic species with improved control over stimulus and accuracy in behavioral quantification.

A.2. MICROFLUIDIC DEVICE

Our experimental setup consisted of a microfluidic device (Fig. A1), two syringe pumps (LEGATO 111 and 110, KD Scientific Inc., Holliston, MA, USA), and an inverted microscope (BIM-500FLD, Bioimager Inc., Canada) with a camera (GS3-U3-23S6M-C, Point Grey Research Inc., Canada) that was connected to a computer. The microfluidic device was used to study the rheotaxis of zebrafish larvae. The syringe pumps were used to apply the desired water flow rates for loading and flow stimulation of the larvae. The microscope and camera were used for recording the larvae's rheotactic behavior in the device.

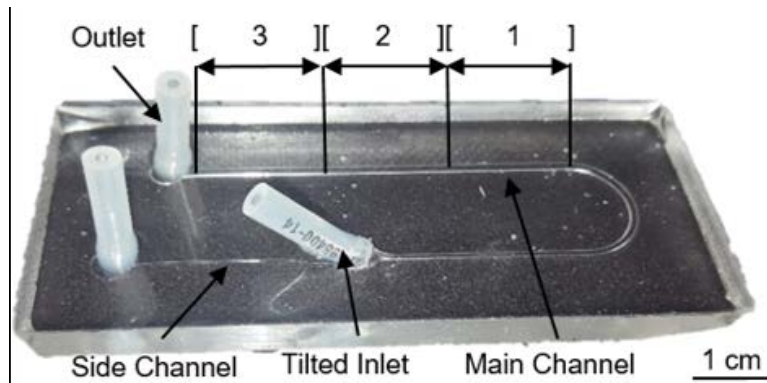


Figure A. 1. The microfluidic device used to study the rheotaxis of 5-7 days post fertilization (dpf) zebrafish larvae. It consisted of a tilted inlet tube for loading the larva, a U-shaped expanding channel for retaining the larva in the device, and a main channel for rheotaxis studies. Water flow in the side channel helped conveniently loading the zebrafish larva into the main channel with length, width, and height of 63.3 mm, 1.6 mm, and 0.55 mm, respectively. The main channel was divided into three sections 1, 2, and 3, representing the spatial locations at which the larvae responded to the flow at different flow velocities. The setup included two syringe pumps, a microscope connected to a camera, and the microfluidic device.

To fabricate the device in Fig. A1, de-bubbled 10 to 1 ratio base to reagent polydimethylsiloxane or PDMS pre-polymer (Sylgard 184 kit from Dow Corning, MI, USA) was casted on a 3D-printed master mold with a negative replica design of the device. Subsequently, PDMS was cured at room temperature for 24hr, peeled off the master and oxygen-plasma bonded to a flat glass slide. The device consisted of a 45° angle inlet tube for smooth and convenient loading of larvae; a side channel (0.1 mm wide, 0.2 mm deep, and 26 mm long) to assist the loading process by precluding the larvae from colliding with the base and walls of the channel; a main channel (1.6 mm wide, 0.55 mm deep, and 63.3 mm long) for zebrafish rheotaxis assays; and a U-shaped channel narrowing from 1.6 mm to 0.9 mm that acted as a fluidic valve to keep the larva inside the device. To assess larvae's sensitivity to flow, we tracked the location of the rheotactic response by dividing the main channel into three equal-length sections 1 (initial position), 2 (mid-channel), and 3 (posterior) as shown in Fig. A1.

A.3. EXPERIMENTAL PROCEDURE AND RHEOTAXIS QUANTIFICATION

Zebrafish larvae at 5-7 dpf were transferred individually into the main channel of the device using the two syringe pumps set to flow rates of 10 and 3 ml.min⁻¹ at the angled and side channels, respectively. The syringe pumps were turned off once the larva reached section 1 of the main channel. Larvae were allowed to recover from the loading process for 60 seconds. After the exploration phase and when larvae turned towards the outlet tube, rheotaxis was evoked by flow velocity in the range of 9.5-38 mm.sec⁻¹ injected from the angled inlet set to flow rates of 0.5-2 ml.min⁻¹. These velocities encompassed conditions evoking rheotaxis before the larvae were hydrodynamically carried out of the device. The response of each larva was monitored and video recorded for 30 seconds. A response was defined as a full 180° rotation and reorientation in the channel against the flow. Videos were analyzed for determination of the rheotaxis rate and location in the main channel (i.e. within sections 1, 2, and 3 in Fig. A1). Finally, larvae were ejected through the outlet and the device was reused for experimental repeats.

A.4. RESULTS AND DISCUSSIONS

The conventional techniques used to study a group of larvae's rheotaxis inside open platforms are not able to elucidate the effect of the flow velocity and direction accurately, due to the complexity of controlling the fluid flow and larvae's intricate responses to various flow conditions. For instance, it has been shown that rheotaxis occurs with a peak rate when the water stream is directed coaxially towards the tail of the zebrafish larvae parallel to their body axis [110]. However, a number of questions

remain unaddressed such as whether and how individual zebrafish larva respond to flow in enclosed and semi-confined environments with no flow source visual cues. Thus, we intended to answer these questions with a simple microfluidic device that was used to quantitatively study the rheotaxis response frequency and place preference, a parameter used in chemical screening assays on zebrafish behaviour [39], [130].

A.4.1 Rheotaxis of Zebrafish Larva in a Channel

To provide a simple assay to study the coaxial rheotactic behavior of 5-7 dpf zebrafish larvae in an enclosed semi-confined environment, we developed the microfluidic device shown in Fig. A1. A semi-confined larva could be positioned along the main channel in this device and be stimulated with a streamlined, controllable and constant-velocity water flow. The larvae were loaded individually into the main channel and positioned at section 1 of the channel (Fig. A1) with their heads facing the outlet. A 60 seconds recovery time with no flow in the device was provided so that the larvae became habituated to the device environment. During the recovery phase, the larvae were able to explore the device environment by conveniently turning in the main channel. Afterwards, they were stimulated by different tail-to-head flows and their positive rheotactic response (i.e. complete 180° orientation against the flow direction) was investigated at different locations in the channel. Control groups of larvae that were not exposed to any flow after loading into the device were also tested. For instance, once a larva was exposed to a 19 mm.sec⁻¹ flow, it exhibited positive rheotaxis within 1.3 seconds of stimulation as shown in Fig. A2.

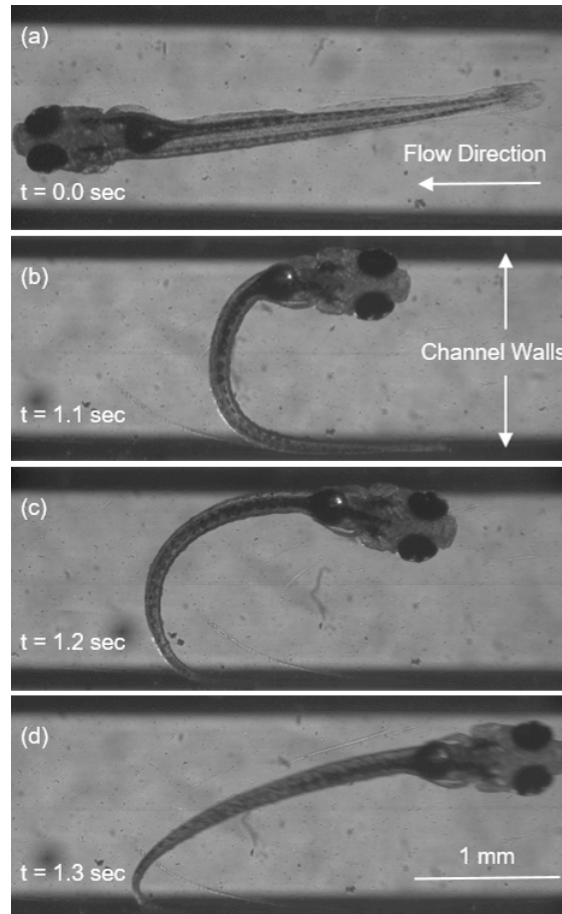


Figure A. 2. Bright field images of a 7 dpf zebrafish larva (a) before, (b-c) during, and (d) after rheotactic orientation upon stimulation by a water flow velocity of $19 \text{ mm}\cdot\text{sec}^{-1}$ in section 1 of the device. The direction of the flow is from right to the left of the pictures (tail-to-head). It is observed that the larva tends to display rheotaxis by swimming against the flow within 1.3 seconds.

The U-bend design and the large length of the main channel in comparison with its small cross-section in our device enabled us to exclude any visual cues in the assay, stimulate the larvae with unidirectional flows, and apply the flow at a constant rate along the axis of the zebrafish in order to evoke and study a complete positive rheotaxis. Furthermore, the larvae were assayed individually, avoiding any potential group-based influence on their rheotaxis behavior. These experimental modalities are not achievable with conventional rheotaxis screening setups.

A.4.2 Effect of Flow Velocity on Rheotaxis of Zebrafish Larva in a Channel

It has been shown that the zebrafish larvae can sense the flow immediately within 15 ms of stimulation [127]; however, we were interested in investigating the coaxial rheotactic response thoroughly from the sensing moment to full reorientation against the flow direction in a semi-confined channel. Moreover, we asked if the magnitude of the flow velocity affects zebrafish coaxial rheotaxis in a channel. Accordingly, we tested the effect of coaxial flow velocity in the range of 9.5-38 mm.sec⁻¹ on the rheotactic response of 5-7 dpf zebrafish larvae as shown in Fig. A3. Any flow velocity lower than 9.5 mm.sec⁻¹ appeared not to evoke a robust positive rheotactic response. Suli et al. [43] hypothesized that this decrease in rheotaxis might be due to the undeveloped hair cells in zebrafish larvae's superficial neuromasts. Velocities higher than 38 mm.sec⁻¹ also failed to induce a robust rheotaxis in the channel, following the same behavioral observations in the literature that rheotaxis only occurs within a range of flow velocities [110]. One possible explanation can be the dominant role of fluid shear that leads to ejection of the larva from the main channel before it demonstrates a positive rheotaxis response (data not shown).

As shown in Fig. A3, out of the 34 larvae tested at each flow velocity, 69±10.3%, 68.4±9.4% and 32.5±8.0% were able to show a positive rheotactic response at 9.5, 19, and 38 mm.sec⁻¹ velocities, respectively. The control animals that were not exposed to any flow preferred to stay in their initial orientation along the channel while exploring the surrounding environment and showing only a random turning of 19.40±10.1%. This low rate of movement indicated that the responses to other stimuli (e.g. visual cues) were kept at a minimum and relatively constant range in our device.

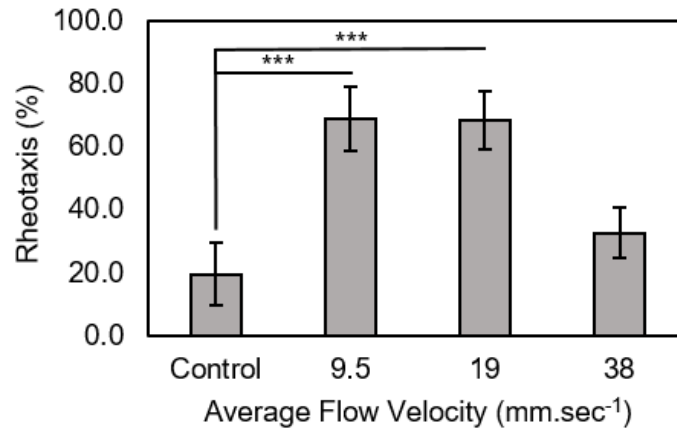


*Figure A. 3. Positive rheotaxis of zebrafish larvae (N=34 larvae per condition) inside an enclosed channel in response to average flow velocities of 9.5, 19, and 38 mm.sec⁻¹. The control group was not exposed to any flow in the device and the reported response is for any arbitrary re-orientation. The results show no desire in the larvae for rotation and their preference to remain in the initially loaded orientation without any flow in the channel; however, once the flow velocities of 9.5 and 19 mm.sec⁻¹ were applied, the rheotactic behavior increased significantly (***: two-tailed t-test, p-value<0.001). At 38 mm.sec⁻¹, the zebrafish larvae demonstrated a low rheotactic response which was not different from the random movement of control larvae (two-tailed t-test, p-value>0.05).*

Flow velocities of 9.5 and 19 mm.sec⁻¹ were effective and sufficiently strong to induce similar rheotactic responses that were statistically different from the random turning of the control larvae (two-tailed t-test, p-value<0.001). However, at the higher flow velocity of 38 mm.sec⁻¹, there was a significant drop in rheotactic response while no statistical difference was measured comparing to the control group (two-tailed t-test, p-value>0.05). The reason for the low rheotactic response at 38 mm.sec⁻¹ is that the flow velocity was sufficiently strong to eject the larva from the channel before it could reveal a positive rheotaxis.

Although the literature has shown that increasing the flow velocity results in linear enhancement of rheotaxis in a non-confined platform [31], [43], [110], our findings demonstrate that the rheotaxis response of zebrafish larvae first plateaus and then

diminishes at high flow velocities in an enclosed channel. These differences may stem from variations in the type of assays (internal versus external flows), ranges of flow velocities tested, channel confinement to ensure coaxial exposure to flow, and the fact that we investigated a thorough rheotactic reorientation in the channel as opposed to the instantaneous turning against and adjustment along the flow direction. For instance, Olive et al. [31] examined the rheotaxis of zebrafish larvae at a velocity range of ~230-685 mm.sec⁻¹, while we studied the coaxial rheotaxis at much lower flow rates and demonstrated larvae's sensitivity to approximately 25 times slower velocities.

A.4.3 Effect of Flow Velocity on Rheotaxis Location in the Channel

Based on our observations, we became interested in investigating if different flow velocities in a coaxial rheotaxis assay would influence the larvae's response location in the channel. Moreover, since the rheotaxis response was similarly high at 9.5 and 19 mm.sec⁻¹, we hypothesized that the flow sensitivity of the larva could also be delineated in more detail by tracking the response location. For this, we determined the number of responses occurred in sections 1, 2, and 3 of the channel (Fig. A1b) for the responding zebrafish larvae at flow velocities reported in the previous section. The results are shown in Fig. A4.

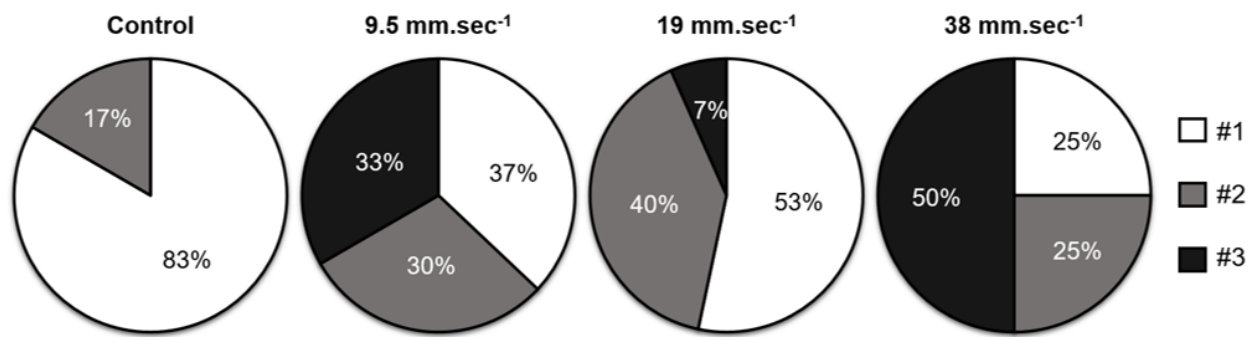


Figure A. 4. Spatial distribution of rheotactic response of zebrafish larvae ($N=14$ larvae per condition) along the three sections of the main channel (1: initial anterior, 2: mid-channel, and 3: posterior location). The control larvae tended to randomly reorient mostly within section 1 of the device where they were initially loaded. At the lowest flow velocity of $9.5 \text{ mm}\cdot\text{sec}^{-1}$, the spatial distribution of response was uniform across the three sections, whereas at $19 \text{ mm}\cdot\text{sec}^{-1}$, a large portion of responses took place at section 1 immediately upon exposure to flow. This contends that the larvae become more sensitive to the flow once exposed to a medium flow velocity of $19 \text{ mm}\cdot\text{sec}^{-1}$ compared to $9.5 \text{ mm}\cdot\text{sec}^{-1}$. The response to $38 \text{ mm}\cdot\text{sec}^{-1}$ mostly occurred in section 3, which implies that the larvae failed to overcome the flow strength and were carried out of the device before they could appropriately respond.

It is shown in Fig. A4 that for the control group of larvae, an arbitrary orientation at no flow was observed mostly in section 1 (initial loading position) of the channel with a response distribution of 83%, 17%, and 0% in sections 1, 2, and 3, respectively. When the larvae were exposed to the lowest flow velocity of $9.5 \text{ mm}\cdot\text{sec}^{-1}$, their rheotactic response was evenly distributed among the three sections (response in 1: 37%, 2: 30% and 3: 33%). However, application of a medium-level flow velocity of $19 \text{ mm}\cdot\text{sec}^{-1}$ led to responses mainly in sections 1 and 2 of the channel with a considerable drop at section 3 (response in 1: 53%, 2: 40% and 3: 7%). This demonstrated that the zebrafish larvae became more sensitive to the medium flow velocity and showed an early response in the channel despite having a similar rheotaxis rate to low-level flow (Fig. A3). At $38 \text{ mm}\cdot\text{sec}^{-1}$, most of the rheotaxis took place in section 3 showing that the larvae were predominately carried away by the flow without being able to successfully display rheotaxis in a timely manner (response in 1: 25%, 2: 25% and 3: 50%). This outcome

also suggests that high flow velocity can postpone the rheotactic reaction by taking the larva away from its initial position alongside the channel, although the flow sensation was most often immediate. To expand our study in the future, we will extend the length of the channel and investigate the effect of the channel width on zebrafish larvae rheotaxis.

A.4.4 Viability of Zebrafish Larvae after Rheotaxis Assay in the Channel

To assess if the zebrafish larvae could survive after microfluidic-based rheotaxis and if the device had any negative effect on the larvae, we assessed larvae's health status after exposure to the device and flow stimulation. The assay included a set of flow-exposed larvae at the highest velocity of $38 \text{ mm}\cdot\text{sec}^{-1}$ compared to the zebrafish that were kept intact in water throughout the experiment (N=15 per condition). After four days of post-experimental observation, more than 70% of the larvae in both groups survived the assay with no statistical significant discerning between them (two tailed t-test, $p\text{-value}>0.05$). This implied that neither the device nor the utilized flow velocities cause any detrimental effect on the larvae.

A.5. CONCLUSIONS

We have developed a microfluidic device in which the coaxial rheotactic behavior of individual zebrafish larvae could be quantitatively examined in a simple, controllable, precise, and repeatable manner. The design of the channel enabled us to expose the larvae to constant-velocity and directionally consistent flows while eliminating the possibility of visual responses as opposed to the conventional rheotaxis screening setups. The results suggested that the larva fails to effectively display the rheotaxis

within the channel to the high velocity of $38 \text{ mm}\cdot\text{sec}^{-1}$. Whereas, the larva showed higher rate of the coaxial rheotaxis to the lower flow velocities of 9.5 and $19 \text{ mm}\cdot\text{sec}^{-1}$. The locations of the rheotaxis occurrence along the channel was uniformly distributed between the three sections at the low velocity of $9.5 \text{ mm}\cdot\text{sec}^{-1}$. However, at the higher velocities of 19 and $38 \text{ mm}\cdot\text{sec}^{-1}$, the larvae tended to display rheotaxis at the initial loading position and further downstream of the channel, respectively. This finding states that despite the similar high rheotaxis rates, the larva reveals more sensitivity by responding to the velocity of $19 \text{ mm}\cdot\text{sec}^{-1}$ right away, unlike $9.5 \text{ mm}\cdot\text{sec}^{-1}$.

Here, the larva was experimented individually, ruling out any possibility of behavioral alterations of the larvae in a group. In the future, researches can benefit from our device to explore the regulation, time dependency and the effectiveness of the flow velocity in the zebrafish's rheotactic behavior. Although our device is designed for single larva studies, it is also amenable to high throughput investigations simply by parallelizing the screening microchannel into tens of side-by-side units. Thin walls between channels can provide flow isolation while allowing the larvae to see each other to resemble group-based assays. Furthermore, investigating this reflexive behavior can also open a window for examination of potential inductive neurons of lateral line system or other sensory systems of the zebrafish larvae involved in coaxial rheotaxis.